

Acoustics Australia



Airfoil tonal noise
Pile driving noise
Vibrations of bubbles and balloons
Music, order and complexity
Helmholtz attenuators for pipes
Vibration of a double-leaf plate
Electric vehicles: too quiet?
Future generation road vehicles



SignalCalc ACE QUATTRO

ACE-QUATTRO has:

- Standard FFT, Synthetic 1/3 Octave standard,
- Quality Control, Point & Direction,
- Sound Power, Sound Intensity,
- Acoustic Intensity, Human Vibration,
- Sound Quality, Demodulation,
- Disk Record & Playback Analysis,
- Frequency Domain Compensation,
- Real Time Octave Analysis, Event Capture,
- 4-32 Inputs (Abacus), 2-8 Outputs + Tachy,
- ActiveX command & control macro programs,
- Single to Multi-Plane Balancing ...and more



BSWA TECH

MEASUREMENT MICROPHONES.

microphones & accessories for Australian & NZ.

High quality, calibrated electret prepolarized microphones to class 1 & 2 & preamplifiers.

Some of the Accessories available:

- IEPE power sources, - portable sound level calibrators,
- USB powered 2 channel measurement soundcard
- a 12 speaker dodecahedral sound source,
- compact light weight 2 channel power amplifiers,
- a self contained Tapping Machine sound source for foot fall measurements.
- impedance tubes providing 125 Hz to 3200 Hz range,
- Outdoor noise monitoring, terminal and software
- Small Reverberation chamber,
- Artificial Ear, Mouth & Head

For Good Measure !
use the bag of tricks from
Kingdom Pty Ltd.

For Hi Performance

- FRF / TRF / Modal Output /
- Power Spectrum, Time & Frequency
- Advanced Print to Word / Power Point

Rotating

- Balancing
- Rotor Dynamics & vibration

Structural

- MIMO
- Stepped Sine

Environmental

- Shock Response Spectrum
- Drope Test

Production Test

- Quality Control, Pass Fail Limits

Remote Communication

- Command & Control by ActiveX

Excitation & Control

- Vibration & Acoustic Control of
- Electro Dynamic, Long Stroke, Hydraulic and power driven shakers with
- Random Vibration
- Random Acoustic
- Sine
- Shock
- SRS
- Transient
- Mixed Mode

TOOLS FOR SUCCESS
NEW IEPE accelerometers and impulse hammers for all your modal testing needs!

Modal sensors features include:

- Small size
- Extremely lightweight
- High sensitivity
- Ultra low noise
- Broad frequency response
- Triaxial measurements

DYTRAN INSTRUMENTS, INC.

TEDS Available

5900 series impulse hammers
Broad ranges available

 3263MS Low noise triaxial	 3097A Ultra low noise	 3225M23/24 High output	 3224A1 0.2 grams, 10 mV/g
---	---	--	---

AAS9100 Certified · ISO 9001:2000 Certified · A2LA Accredited to ISO 17025

For more information phone: **02 9975 3272**
or visit: **www.kingdom.com.au**



Acoustics Australia



EDITORIAL COMMITTEE:

Nicole Kessissoglou ,
Marion Burgess, Tracy Gowen

BUSINESS MANAGER: Leigh Wallbank

Acoustics Australia General Business

(subscriptions, extra copies, back
issues, advertising, etc.)

Mrs Leigh Wallbank
P O Box 70
OYSTER BAY NSW 2225
Tel (02) 9528 4362
Fax (02) 9589 0547
wallbank@zipworld.com.au

Acoustics Australia All Editorial Matters

(articles, reports, news, book reviews, new products, etc)

The Editor, Acoustics Australia
c/o Nicole Kessissoglou
School of Mechanical and
Manufacturing Engineering
University of New South Wales
Sydney 2052 Australia
+61 401 070 843 (mobile)
AcousticsAustralia@acoustics.asn.au
www.acoustics.asn.au

Australian Acoustical Society Enquiries see page 234

Acoustics Australia is published by the
Australian Acoustical Society
(A.B.N. 28 000 712 658)

ISSN 0814-6039

Responsibility for the contents of
articles and advertisements rests upon
the contributors and not the Australian
Acoustical Society. Articles are copyright,
by the Australian Acoustical Society.
All articles, but not Technical Notes or
contributions to Acoustics Forum, are
sent to referees for peer review before
acceptance. Acoustics Australia is
abstracted and indexed in Inspec, Ingenta,
Compendix and Acoustics Archives
databases, Science Citation Index
Expanded and in Journal Citation Reports/
Science Edition.

Printed by
Cliff Lewis Printing
91-93 Parraweena Rd,
CARINGBAH NSW 2229
Tel (02) 9525 6588
Fax (02) 9524 8712
email: matt@clp.com.au
ISSN 0814-6039

Vol. 40, No. 3

December 2012

LETTERS

- Response to:** S. Cooper, "Wind farm noise - an ethical dilemma for the Australian Acoustical Society?", *Acoustics Australia* **40**(2), 139-142 (2012)
Renzo Tonin **Page 167**
- Response to:** S. Cooper, "Wind farm noise - an ethical dilemma for the Australian Acoustical Society?", *Acoustics Australia* **40**(2), 139-142 (2012)
Timothy Marks, Christophe Delaire, Justin Adcock and Daniel Griffin **Page 168**
- Response to:** S. Cooper, "Wind farm noise - an ethical dilemma for the Australian Acoustical Society?", *Acoustics Australia* **40**(2), 139-142 (2012)
Kym Burgemeister **Page 169**
- Australian Standards**
Marion Burgess **Page 171**

PAPERS

- Reduction of flow induced airfoil tonal noise using leading edge sinusoidal modifications**
Kristy Hansen, Richard Kelso and Con Doolan **Page 172**
- Modelling of pile driving noise by means of wavenumber integration**
Tristan Lippert and Stephan Lippert **Page 178**
- The vibrations of bubbles and balloons**
Kirsty A. Kuo and Hugh E.M. Hunt **Page 183**
- The sound of music: Order from complexity**
Neville H. Fletcher **Page 188**
- Design of Helmholtz Resonators in one and two degrees of freedom for noise attenuation in pipelines**
S. Mekid and M. Farooqui **Page 194**
- Vibration field of a double-leaf plate with random parameter functions**
Hyuck Chung **Page 203**

TECHNICAL NOTES

- Adding noise to quiet electric and hybrid vehicles: An electric issue**
Ulf Sandberg **Page 211**
- Acoustical impacts of future generation road vehicles**
Matthew Stead, Adrian White and Deb James **Page 221**

REGULAR ITEMS

News	225
New Products	226
Meeting Reports	226
Future Conferences	228
Diary	230
Sustaining Members	232
Advertiser Index	234

Cover design: Helena Brusic

More than just calibration...

Brüel & Kjær provides that extra level of service

Brüel & Kjær offers:

- Accredited Calibration and Repair Services
- Microphone, Accelerometer and Instrumentation Calibration
- Calibration available for Third Party Products
- Easy to use booking system – no lengthy delays



Accredited
Lab No 1301

Call Brüel & Kjær's
Service Centre today on
02 9889 8888
www.bksv.com.au



SERVICE AND CALIBRATION

HEAD OFFICE, SERVICE AND CALIBRATION CENTRE
Suite 2, 6-10 Talavera Road * PO Box 349 * North Ryde * NSW 2113
Telephone 02 9889 8888 * 02 9889 8866
e-mail: bk@spectris.com.au * www.bksv.com.au

Brüel & Kjær



cliff lewis printing

*Specialists in Scientific
Printing and Publishing*

MORE THAN JUST PRINTING

- Art and Design
- Branding Design
- Stationery
- Binding & Finishing
- Promotional Material

t (02) 9525 6588 f (02) 9524 8712
e printing@clp.com.au

www.clp.com.au

91-93 Parraweena Road, Taren Point, NSW 2229

Matrix Resilient Wall Ties and Floor Mounts

The Matrix range of resilient acoustic wall ties and floor mounts are a structural connection that reduces airborne and impact noise passing through masonry and stud walls. They are suitable when discontinuous construction is required in separating walls and any specialised room that requires high acoustic isolation.



MB01 - Resilient masonry wall tie for cavity width 40mm - 100mm.



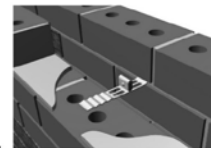
SB06 - Resilient masonry wall tie for joining stud walls.



SB08 - Universal resilient masonry wall tie for stud or stud to stud cavity 20mm to 100mm.



SB03 - Resilient stud wall tie for attaching top plate or underside of slab or masonry wall.



SB10 and MB10 HD wide cavity acoustic wall mount in 2mm x 38 mm Gal or SS for 200mm to 450+ cavities.



FM01 - Resilient floor mount -reduces impact vibration passing through floors.



MB04 - Resilient masonry wall tie for attaching a pre-built masonry or stud wall.



MB08 - Universal resilient masonry wall tie for cavities 20mm - 100mm.

Matrix Industries Pty Ltd

144 Oxley Island Road, Oxley Island, NSW 2430
Phone: +61 2 6553 2577 Fax: +61 2 6553 2585
www.matrixindustries.com.au

MESSAGE FROM THE PRESIDENT



I wish to welcome all members of the AAS with this final issue of Acoustics Australia for 2012. Well what a way to end the year and my tenure as President.

A large number of our members have just attended Acoustics 2012 Fremantle: Acoustics, Development and the Environment. The WA division conference set new records for our annual Society conference, with

more than 280 delegates attending and over 124 papers published. I would like to congratulate the Organising and Scientific Committee, plenary guests and keynote speakers, authors, reviewers, event sponsors, exhibitors, partners and members in attendance who made this event such a success

Prior to and during these annual conferences, the Federal Councillors attend their face to face meetings to conduct the official business of running the society, in accordance with our articles of association and registered companies requirements. On behalf of the society I thank the councillors for the preparation, time and effort in attending to their duties. It is worthy to highlight several significant outcomes from the recent Fremantle meetings and these were highlighted during the Conference Dinner and are noted below:

- Fellows of the Society. The federal committee reviewed and unanimously approved three nominations for member elevation to the grade of fellow of the AAS. The AAS welcomes the following new fellows of the society:
 - Emeritus Professor Bob Randall
 - Dr Renzo Tonin
 - Russell Brown

Bob Randall was present for his award at the conference dinner. It was an honour to read his citation and award his certificate to him.

- Website Upgrade. The upgrade of our website is progressing with defined scope, and number of options and preliminary quotes reviewed and discussed. The aim is that we shall have a new fully integrated and functional website operational by 1 July 2013 for the benefit of all members and to assist in streamlining a number of Federal general secretary, registrar, and web manager workload. I appreciate the feedback received by the subcommittee (Peter Heinze, Matthew Stead, Terry McMinn and Richard Booker).
- AAS Research Grants. The AAS has agreed to investigate and proceed with funding of major research projects with matching and or linkage funding from other research grant providers, e.g. ARC, based on their current importance and benefit for the Acoustical Society members and the Australian Community. This committee is headed by Matthew Stead with bipartisan input from a federal councillor representative from each division. The committee is currently addressing the system and

framework for processing applications and determining project priorities. The work will commence with a member survey for assistance in prioritising projects with research project bids requested during May-June 2013.

- The success of the AAS website online issue of AA journal back issues is increasing with some 24,000 requests per month. The quality and variety of the journal articles and technical notes is acknowledged by its members and the hard work of the AA journal team.
- The AAS increased its total membership in 2011-2012 by 10.4% with 41 new MAAS members.

The AAS received a large number of submissions for the AAS Education Grant and the council appreciates the efforts by the applicants. The council thanks Charles Don and John Davy for being our judges for these submissions. The following three recommended awards were concurred by the Federal Council:

- Dr Danielle Moreau – *Characterising noise and annoyance in homes affected by wind turbine noise.*
Danielle was present at the conference and was notified of her award at the conference dinner.
- Dr Cate Madill – *Acoustic and High-speed Analysis of Radio broadcasters*
- Dr Iftekhar Ahmad – *Acoustic signal analysis for beehive health monitoring*

The President's Prize for the AAS2012 conference best paper was awarded to Dr Paul Dylejko for his paper titled *Optimisation of an inertial mechanism within a uni-axial vibration isolator to suppress internal resonance.* Thanks to both John MacPherson and Alec Duncan from the WA Division conference organising committee for reviewing all papers.

There were three submissions for the CSR award for Excellence in Acoustics in 2012. Whilst all entries were of a high calibre, none satisfied all of the criteria of the competition guidelines as set out on the AAS home page. As a result, it was CSR Bradford's recommendation that no prize be offered for 2012.

ACOUSTICS 2013 Victor Harbor: Science, technology and Amenity, the 2013 conference of the Australian Acoustical Society, is well into its initial stages of planning and will be held in Victor Harbor, South Australia from 17 to 19 November 2013.

Now that I step down to Vice President's role and Norm Broner steps back into the President's role, I would to thank the support of all federal councillors, the general secretary, Acoustics Australia team and other members who assist the society and trust they will also assist Norm as he progresses in this role and into 2014 also as Congress President for the InterNoise 2014 Congress to be held in Melbourne.

Along with the Federal Councillors, I take this opportunity to wish everyone a safe and enjoyable break over Christmas and New Year period and best wishes for 2013.

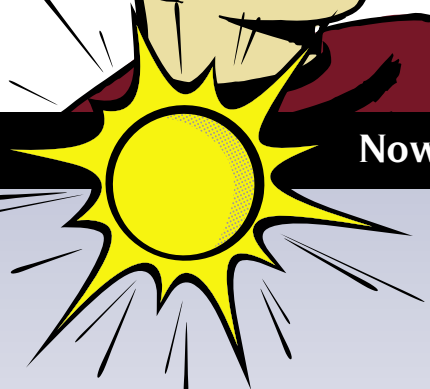
Peter Heinze



SAVTek Sales+Rentals

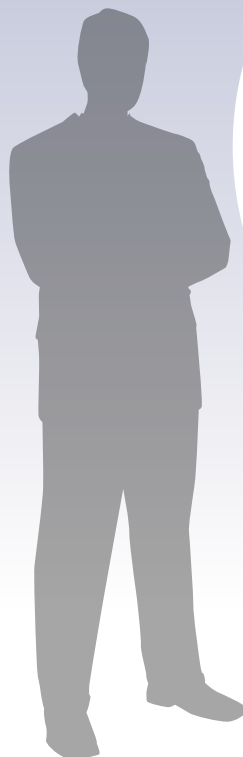


Now selling and renting a wide range of equipment including:



SK2 Audio and Spectral Logger by SINUS

- Long term noise and vibration monitoring now available utilising all the power of the SoundBook and SAMURAI
- Solar powered for remote deployment
- 1 to 4 channels of noise and/or vibration
- Statistical levels, level recorder, fractional Octaves, FFT (up to 25601 lines), wave file
- Weather and video data all synchronised
- Daily summary reports sent by 3G. Interrogation of files and audio via 3G.



LETTER TO THE EDITOR

Renzo Tonin, Renzo Tonin & Associates (NSW) Pty Ltd, Surry Hills, NSW 2010

RTonin@renzotonin.com.au

Response to article by S. Cooper, "Wind farm noise - an ethical dilemma for the Australian Acoustical Society?", *Acoustics Australia* 40(2), 139-142 (2012)

I wish to respond to Mr Steven Cooper's technical note "*Wind farm noise – An ethical dilemma for the Australian Acoustical Society?*" published in *Acoustics Australia*, Vol. 40, No. 2 (2012).

The author in his opening paragraph refers to a series of papers and technical notes published in the April 2012 edition of *Acoustics Australia*, Vol. 40, No. 1 (2012). He refers to some of those articles "*supporting wind farms*" and is critical that they do not "*discuss the acoustic impact of the wind farms*".

Firstly, in reading the articles referred to, I am unable to find any that are "*supporting wind farms*". The articles are technical papers describing various aspects of wind farm noise, some of which document the relevant authors' findings in respect of their work relating to the measurement of noise at wind farm sites or a review of work by others. My own paper in that series of articles, for example, is simply a summary of wind farm noise sources and noise propagation algorithms. There is no evidence put forward by Mr Cooper that the authors of those articles are associated in some way with wind farm operators. Some may have a proper business relationship as client and consultant (as referred to in clause 4 of the AAS Code of Ethics appended to by Mr Cooper's technical note), however this does not of itself make the authors of those articles persons who are "*supporting wind farms*".

My understanding of the AAS Code of Ethics (in clause 1) is that members of the AAS must act independently and without bias one way or the other. Just because some of the authors of the articles referred to above have clients who are wind farm operators does not make them supportive of the industry or biased. I am aware that Mr Cooper has many clients in NSW who are in the hotel industry and gives evidence in the NSW Land & Environment Court as an impartial expert. This does not make Mr Cooper a person who supports hotels or is biased toward hotel development.

Secondly, in Mr Cooper's opening paragraph he states that "*the articles did not identify the basis of the criteria or the acoustic impact of wind farms even when they complied with the nominated criteria*". A discussion then follows regarding how aircraft noise impacts are addressed in Australia, in my opinion meandering from the main point.

Nevertheless, the main point I believe Mr Cooper is trying to make is that, according to him, there is no connection between the criteria that is adopted in environmental noise impact studies and the affectation (including health impacts) of people who live in close proximity to wind turbines.

The first thing that can be said is that members of AAS who are contracted by clients to prepare environmental noise impact assessments of wind farms (at least in the state of NSW where I practice) must do so in accordance with the

NSW Director General's Requirements. The Director General determines how the EIS should be prepared and what standards should be followed. There may be similar requirements in the other States. The Director General has already made a decision about what standards are to be applied taking into account the interests of the local community and the interests of the wider community, noise impacts, economic opportunities and so on. Therefore, if the Director General's Requirements, for example, state that the South Australian Wind Farm Guidelines is the relevant standard to be applied in respect of the project, this must be complied with.

If a member of the AAS has serious concerns about any directions given by the Director General then the appropriate forum for that discussion is a formal objection to the proposal. The fact that one member of the AAS has prepared an EIS in accordance with the Director General's Requirements and another member of the AAS is opposed to that standard being applied does not make the former member a person who is "*supporting wind farms*". In other words, just because a member of the AAS contracts to the wind farm industry does not make that member someone who "*supports*" the wind farm industry. Furthermore, just because a member of the AAS follows directions given by the Director General does not put that member in conflict with the AAS Code of Ethics notwithstanding that Mr Cooper may disagree with the content of the South Australian Wind Farm Guidelines or any other wind farm guideline for that matter.

The second thing that can be said about the "*connection*" issue raised above is that there is in fact technical literature which Mr Cooper may not be aware of relating to noise dose-response studies, one conducted in Sweden and one in the Netherlands (see [1, 2]).

On page 140 of Mr Cooper's technical note, he refers to "*anti-wind farm' and 'pro-wind farm' acousticians who are Members of the Society*". I sincerely hope that there is no such dichotomisation in the AAS, that we are all professionals and work without bias as to whether or not a wind farm is constructed. It would then follow that there cannot be any "*dilemma*" for any member to abide by the Code of Ethics and to sincerely and honestly, and for technical reasons alone, support or oppose the construction of any particular wind farm project.

On the 4th December 2012, Mr Cooper was interviewed by Alan Jones on the Sydney radio station 2GB wherein Mr Jones made the following statements (to which Mr Cooper did not disagree):

- Wind farm noise impact studies don't assess the noise to tell you what the impact will be;

- There is a lack of scientific evidence to prove wind farms do not create health impacts;
- There is no scientific evidence of health studies;
- The appropriate scientific studies have not been undertaken;
- The precautionary principle says we should stop building wind farms;
- We are making this up as we go along;
- The World Health Organisation noise limits apply to the city and are entirely inappropriate for rural areas;
- Wind farm operators should guarantee there are no adverse noise effects, no adverse health effects, no offensive noise and no sleep disturbance.

I certainly don't agree with Alan Jones's assessment as summarised above and I hold that view for technical reasons not for emotive ones.

In conclusion, it is a serious concern to me that Mr Cooper thinks that members of the AAS can be labelled as "pro" or "anti" anything. Members should have a technical opinion based on technical reasons for supporting or opposing a particular development. Furthermore, just because they may oppose a particular development, that should not then make

them opposed to all like developments because, as we all know, every case depends on its merits. In addition, the fact that members oppose a particular development should not then brand them as "pro" or "anti".

Yours faithfully,

Dr Renzo Tonin, FAAS

REFERENCES

- [1] E. Pedersen and K. Persson Waye, "Perception and annoyance due to wind turbine noise – a dose-response relationship", *Journal of the Acoustical Society of America* **116**(6), 3460-3470 (2004)
- [2] E. Pedersen, F. van den Berg, R. Bakker and J. Bouma, "Response to noise from modern wind farms in The Netherlands", *Journal of the Acoustical Society of America* **126**(2), 634-643 (2009)

LETTER TO THE EDITOR

Marshall Day Acoustics, Melbourne VIC 3066
melbourne@marshallday.com.au

Response to article by S. Cooper, "Wind farm noise - an ethical dilemma for the Australian Acoustical Society?", *Acoustics Australia* **40**(2), 139-142 (2012)

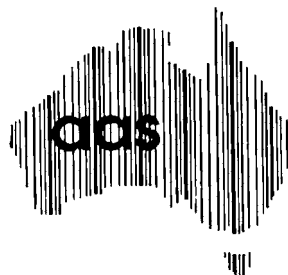
In light of recent allegations of ethical misconduct directed at Australian Acoustical Society (AAS) members working on Australian wind farm projects, the question posed by the technical note would seem timely. Whilst an open discussion of this point is worthwhile, unsubstantiated statements such as "...it would seem to be more than 10% of the population are seriously affected" are not helpful contributions to a debate that already suffers from significant misrepresentations.

In contrast to some other sources of noise, including aircraft noise as raised in the technical note, wind farm noise assessment in all Australian jurisdictions has clearly defined limits applicable to operational noise, including in rural areas. A key point of all these policies is that they are not designed to prevent annoyance in all cases but to strike a balance between the potential advantages of wind energy developments in Australia with the potential adverse noise impacts on local communities. We consider it essential that any discussion of appropriate ethical standards should therefore have due regard to this key balancing objective which underpins all noise assessment work. Such discussions should therefore address matters such as planning and energy policy and therefore

require the input of experts outside of the acoustics profession.

It would seem appropriate for the AAS to formally respond on this matter, and provide clarification to its membership on the matter of ethical conduct in environmental noise assessment, recognising the factors raised above.

Timothy Marks (MAAS)
Christophe Delaire (MAAS)
Justin Adcock
Daniel Griffin



LETTER TO THE EDITOR

Kym Burgemeister, Arup, Melbourne, VIC 3000
kym.burg@arup.com

Response to article by S. Cooper, "Wind farm noise - an ethical dilemma for the Australian Acoustical Society?", *Acoustics Australia* 40(2), 139-142 (2012)

I was disappointed to read Stephen Cooper's technical note asking if the acoustical engineers and consultants preparing wind farm noise assessments in Australia are acting in accordance with the Australian Acoustical Society's Code of Ethics. It is apparent that Mr Cooper believes that many of the acoustical engineers and consultants who undertake these assessments are acting unethically on the basis that they are relying on ill-informed standards and guidelines and not challenging those guidelines or looking beyond them.

I have been fortunate enough to have recently been engaged by several government agencies to undertake an independent review of the standards and guidelines relating to the assessment of wind farm noise. Since I have never previously consulted to either the wind farm developers or the wind farm opponent groups I was able to approach this work from a 'neutral' position. The study has allowed me to develop an over-arching and contemporary view of the practice of wind farm noise assessment in Australia – a view which leads me to largely reject Mr Cooper's accusations.

I agree that there is genuine community concern regarding the potential for adverse effects associated with noise from wind farm developments, and a great deal of publicity regarding wind farm noise, particularly in the popular media. Nevertheless, much of the publicity is inaccurate and ill-informed, and articles such as Mr Cooper's technical note will, at best, only serve to reinforce the public perception that there is still significant disagreement amongst 'acoustic experts' regarding the best ways to measure, predict and assess wind farm noise - there is not. At worst, it will be adopted as a 'key reference' by wind farm development opponents.

In his note, Mr Cooper contrasts the lack of informed consideration of the 'acoustic impact of wind farms' against the apparently more robust acoustic and socio-acoustic studies which informed the 'aircraft noise debate' following the opening of the third runway at Kingsford Smith Airport in Sydney. He then provides an account of his own contribution to the prediction of aircraft noise, in particular, the identification of several 'errors' in the common prediction methodology. The implication is that consultants are making similar errors in their prediction and assessment of wind farm noise, particularly by simply adopting international standards, with no 'localisation' to Australian conditions.

It is fair to say that the assessment methodology and choice of assessment criteria for wind farms is not perfect. But, as discussed in Isaac Asimov's enlightening and entertaining essay *The Relativity of Wrong*^[1], it is important not to assume that 'that which isn't perfectly and completely right, is totally and equally wrong'. In practice, most of us are able to accept that there are no criteria, or guidelines, or assessment

techniques that are ever perfect. They are always the result of compromise and an attempt to *balance* the impact of noise on the amenity of the community against the wider benefits that the noise source provides. It therefore must be accepted that noise criteria, whether they are for industrial noise, noise from pubs, or barking dogs, or even wind farms, could always result in some adverse impact, particularly on people who have heightened sensitivity to noise.

My view is that consultants in Australia are doing their best to provide a reasonable and fair assessment of noise from wind farms. Much of this is based on reliable research and technical work that has been, and continues to be undertaken overseas by Geoff Leventhall, Andrew Bullmore, Dick Bowdler and other prominent acoustic engineers [2-7], research that appears to have been overlooked by Mr Cooper.

There are also many consultants and engineers in Australia and New Zealand who are undertaking excellent research, people like Tom Evans, Jon Cooper, Christophe Delaire and Colin Tickell amongst others in Australia, and Michael Smith and Stephen Chiles in New Zealand. These engineers are exploring new techniques to measure and assess noise from wind farms in a fair and equitable way [8-10], for example, by exploring 'bin analysis' of measured background and wind farm noise level [11] rather than the cumbersome 'regression' analysis which is usually adopted.

Furthermore, the continuing research into the potential health effects of wind farm noise is not being ignored; rather, the New Zealand Standard is based on a *reasonable* interpretation of the current research, and the New Zealand standards technical committee and other experts continue to review work such as that by Møller and Pedersen [12] and from DELTA [13, 14].

Mr Cooper has also published a peer review of the acoustic assessment undertaken for the Flyers Creek Wind Farm [15] which demonstrates several fundamental misunderstandings and inaccuracies which are also worthwhile examining.

With regard to low-frequency noise, Mr Cooper notes that a significant number of papers report low-frequency noise impacting on residents where the wind farm '*give[s] rise to frequencies below that of the human ear*' (sic).

His measurements of wind farm indoor and outdoor noise levels at residences near the Capital wind farm are claimed to show an impact from low-frequency noise from the wind turbines. However, only noise levels measured both with the wind farm operating in windy conditions and without the wind turbines operating, in calm conditions, are presented. The necessary case of the wind farm *not* operating in windy conditions is not shown, and would be likely to show low frequency noise due to increased environmental noise

generation. It is accepted that this type of measurement is difficult, or impossible to do without the participation of the wind farm operator – nevertheless, such a significant omission makes the subsequent analysis meaningless.

For example, it seems irrational to suggest that ‘*typically when the wind farm was generating an electrical output [that] the background level increased, and when the wind farm reduced generating electrical output the background reduced*’ infers that the wind farm is solely responsible for the background noise, while ignoring the fact that high ambient wind conditions, which is a necessary condition for the wind turbine to operate, also generates significant noise.

With regards to the internal noise level measurements undertaken inside nearby properties, Cooper’s report states that ‘*no noise associated with the turbines could be detected inside the dwelling because the sound pressure levels recorded in those bands are below the nominal threshold of hearing*’.

There are further anomalies; data in Appendix G of the Flyer’s Creek review showing a so-called ‘Pulse Time Analysis’ analyses the measured wind farm sound level using *fast response exponential averaging at 50ms*. Yet 125 ms is commonly accepted as a time constant representing that of human hearing, and the measurements shown in Appendix G does not appear to be exponentially averaged. While the figure title suggests a 24.4 Hz high-pass filter was applied, the measured levels only roll-off below around 5 Hz. Similarly, the results shown in Appendix H do not appear to have been high-pass filtered as suggested in the text.

Finally, he concludes that the measured Capital wind farm sound levels exceed various low frequency noise criteria. This includes the suggestion that Norm Broner has proposed a low-frequency noise limit of the dB(A) level + 30 dB ‘*where the C-weighted value is above 30 dB(A)*’ (sic). Actually, Dr Broner recommends a ‘desirable’ outdoor L_{eq} limit of 60 dBC, with a maximum limit of 65 dB(C) for night-time operation [16]. In any case, the wind farm sound levels Mr. Cooper measured near the Capital wind farm are below the internationally recognised guidance limits of 85 dB(G) and 65 dB(C) [14, 17].

In order to constructively contribute to the wind farm noise discussion, it is helpful to examine some of those key aspects of wind farm noise measurement and assessment that would benefit most from additional research in order to *improve* the way that wind farms are measured and assessed.

Firstly, I agree with Mr Cooper that there is value in undertaking psycho-acoustic studies of the impact and annoyance of noise from operating wind farms – this was recommended by the Senate Enquiry into the Social and Economic Impact of Rural Wind Farms [18]. This would help to inform the science. This should particularly look at understanding the influence of amplitude modulation on the audibility and subjective response of wind turbine noise. The measurement of background and wind farm noise also requires improvement; the current regression techniques are quite cumbersome and not particularly transparent. While filtering by day, night, season, wind direction or atmospheric stability (or some combination of these) usually helps, perhaps alternative ‘bin’ type analysis (proposed to be adopted in the 3rd revision of IEC 61400-11) might prove more appropriate.

The proposed *Good practice guide to wind turbine noise assessment* currently being developed by the UK IoA is likely help to inform the procedure.

The application of penalties for so-called ‘Special Audible Characteristics’ (or SACs) to measured noise levels requires further refinement – should penalties be applied to individual 10 minute measurements (and included in the regression, as implied in NZS 6808), or applied in bulk to the regression curve should a particular threshold of occurrence be exceeded?

We require better definition about when it might be appropriate to suggest or apply a more conservative limit (such as the High Amenity limit in NZS 6808-2010), and when the base limit is reasonable.

We should consider some standardisation of the structure of assessment studies and compliance reports, so that the community can be assured of some minimum level of information.

So, taking guidance from Dr. Asimov who concludes that ‘theories are not so much wrong, as incomplete’, until the outcomes of the research are available, I see no ‘unethical behaviour’ in using existing theory and the tools that are currently available to assess noise from wind farms.

Yours sincerely,



Dr Kym Burgemeister

REFERENCES

- [1] I. Asimov, *The Relativity of Wrong*, 1988. Full text available at http://hermiene.net/essays-trans/relativity_of_wrong.html
- [2] G. Leventhall, A. Bullmore, M. Jiggins, M. Hayes, A. McKenzie, R. Bowdler and R. Davis, “Prediction and assessment of wind turbine noise, Agreement about the relevant factors for noise assessment from wind energy projects”, *Acoustics Bulletin* **34**(2), 35-37, March/April (2009)
- [3] Hayes McKenzie Partnership Ltd, *Analysis of how noise impacts are considered in the determination of wind farm planning applications*. Report 2293/R1, Research Contract 01.08.09.01/492A (Analysis), UK Department of Energy and Climate Change, April 2011
- [4] UK Institute of Acoustics, *Good practice guide to wind turbine noise assessment, Working Group terms of reference* <http://www.ioa.org.uk/pdf/ioa-good-practice-guide-terms-of-reference-v-09-12-11-version-5.pdf> (last accessed November 2012)
- [5] A. Bullmore, J. Adcock, M. Jiggins and M. Cand, “Wind farm noise predictions and comparison with measurements”, *Proceedings of the 3rd International Meeting on Wind Turbine Noise*, Aalborg, Denmark, 17-19 June 2009
- [6] A. Bullmore, M. Jiggins, M. Cand, M. Smith and S. Von-Hunerbein, “Wind turbine amplitude modulation: Research to improve understanding as to its cause & effect”, *Proceedings of the 4th International Meeting on Wind Turbine Noise*, Rome, Italy, 11-14 April 2011
- [7] D. Bowdler, “Amplitude modulation of wind turbine noise, A review of the evidence”, *Acoustics Bulletin* **33**(4), July/August 2008, pp. 31-35

- [8] C.E. Tickell, J.T. Ellis and M. Bastasch, "Wind turbine generator noise prediction – Comparison of computer models", *Proceedings of Acoustics 2004*, Gold Coast, Australia, 3-5 November 2004, pp. 45-50
- [9] T. Evans and J. Cooper, "Comparison of predicted and measured wind farm noise levels and implications for assessments of new wind farms", *Proceedings of Acoustics 2011*, Gold Coast, Australia, 2-4 November 2011
- [10] J. Cooper, D. Leclercq and M. Stead, "Wind induced aerodynamic noise on microphones from atmospheric measurements", *Proceedings of the 20th International Congress on Acoustics*, Sydney, Australia, 23-27 August 2010
- [11] M. Smith and S. Chiles, "Analysis techniques for wind farm sound level measurements", *Acoustics Australia* **40**(1), 51-56 (2012)
- [12] H. Møller and C.S. Pedersen, "Low-frequency noise from large wind turbines", *Journal of the Acoustical Society of America*, **129**(6), 3727-3744 (2011)
- [13] B. Søndergaard and K.D. Madsen, *Low frequency noise from large wind turbines: Results from sound power measurements*, DELTA Acoustics & Electronics, AV136/08, 2008
- [14] T.H. Pedersen, *Low frequency noise from large wind turbines: A procedure for evaluation of the audibility for low frequency sound and a literature study*, DELTA Acoustics & Electronics, AV1098/08, 2008
- [15] S. Cooper, *Peer review of acoustic assessment*, Flyers Creek wind farm, The Acoustic Group Pty Ltd. Report 41.4963. R1A:ZSC, 15 December 2011
- [16] N. Broner, "A simple outdoor criterion for assessment of low frequency noise emission", *Acoustics Australia* **39**(1), 7-14 (2011)
- [17] D.M. Hessler and G.F. Hessler, "Recommended noise level design goals and limits at residential receptors for wind turbine developments in the United States", *Noise Control Engineering Journal* **59**(1), 94-104 (2011)
- [18] The Senate Community Affairs References Committee, *The social and economic impact of rural wind farms*, Australian Senate June 2011 <http://apo.org.au/node/25321>

LETTER TO THE EDITOR

Marion Burgess

School of Engineering and Information Technology, The University of New South Wales, Canberra, ACT 2600

Australian Standards

At the recent AAS conference in Perth we held a discussion session on Australian Standards to elicit the view from the participants on the direction for the AAS in future dealings with Standards Australia. To explain just a little of the background – the operating model for Standards Australia has changed greatly over the last decade putting more responsibility onto the stakeholder bodies to fully canvas all those who may have any interest in the standard and put forward a submission to Standards Australia for a project. It is then only if that submission is accepted as a project that any work can be done by the Standards Australia committee to update/correct an existing Australian Standard, to replace an outdated Australian Standard with a current ISO or similar as a direct text adoption with or without any additional comment to relate that document to Australian conditions.

A submission prepared by a member under the auspices of the AAS has a reasonable chance of being accepted. There is however considerable effort to get the documentation together so there is a need to prioritise and select those Australian Standards that are desperately in need of amendment, updating or replacement. The discussion at the conference brought forward some proposals of those desperately needing some work – for example AS 2107 and AS 1055 were needing updating or replacement. If any member would like to suggest an Australian Standard that they consider is in desperate need of updating or replacing or removing and could be on the priority listing for an AAS action then please send me an email: m.burgess@adfa.edu.au

Marion Burgess

MESSAGE FROM THE EDITOR

This is just a short note to say thank you to all the lovely people who have been involved with the journal this year, in particular the authors and reviewers (we would not exist without you!), contributors to the various news articles and our advertisers. I believe the journal is gaining momentum in its recognition. In the last twelve months, there were 287,700 requests for the journal – that's a lot of requests! The next issue (April 2013) will be a special issue on Underwater Acoustics. If you would like

to contribute an article to this special issue, please email myself (n.kessissoglou@unsw.edu.au) or Alec Duncan (A.J.Duncan@curtin.edu.au) your submission by the end of January at the very latest. I take this opportunity to wish everyone an enjoyable and relaxing break and a happy new year. Let's hope that 2013 continues to bring much attention to our Acoustics Australia journal.

Nicole Kessissoglou

REDUCTION OF FLOW INDUCED AIRFOIL TONAL NOISE USING LEADING EDGE SINUSOIDAL MODIFICATIONS

Kristy Hansen, Richard Kelso and Con Doolan

School of Mechanical Engineering, University of Adelaide, Adelaide, Australia

kristy.hansen@adelaide.edu.au

Significant tonal noise reduction has been achieved using sinusoidal protuberances, also known as tubercles, on the leading edge of a NACA 0021 airfoil for a Reynolds number, $Re \sim 120,000$. It has also been observed that the overall broadband noise is reduced for a considerable range of frequencies surrounding the peak in tonal noise. It is postulated that tonal noise elimination is facilitated by the presence of streamwise vortices generated by the tubercles and that the spanwise variation in separation location is also an important factor. Both characteristics modify the boundary layer stability, altering the frequency of velocity fluctuations in the shear layer near the trailing edge. This affects the coherence of the vortex generation downstream of the trailing edge, hence leading to a decrease in trailing edge noise generation. An additional effect is the confinement of the suction surface separation bubble to the troughs between tubercles, which may reduce the boundary layer receptivity to external acoustic excitation. Investigations have also revealed that the smallest wavelength and largest amplitude tubercle configuration have the lowest associated tonal and broadband noise

INTRODUCTION

The presence of leading edge tubercles gives rise to several flow effects which could reduce or eliminate tonal noise. For example, the generation of streamwise vortices reduces the coherence of the wake [1] and several researchers have shown evidence of this streamwise vortex formation [2-4]. Furthermore, it has been observed that due to varying locations of separation along the span-wise direction, the separation line becomes somewhat interrupted [3]. This would also lessen the coherence of vortex shedding in the wake. According to Nash et al. [5], airfoil tonal noise is associated with the vortex shedding process and the von Kármán vortex street is shed with the same frequency as the acoustic tone. Suppression of the von Kármán vortex street formation and associated reduction of acoustic disturbance intensity was discussed by Kuethe [6] in relation to vortex generators which generate a similar disturbance to the flow as tubercles.

Other methods of tonal noise reduction and/or elimination include leading edge serrations and boundary layer trips. The acoustic effect of leading edge serrations on a NACA 0012 airfoil was investigated by Hersch et al. [7]. These researchers observed that tones were produced by periodic fluctuating forces, acting on the airfoil near the trailing edge as a result of forces induced by wake vortex shedding. It was found that the serrations caused formation of streamwise vortices on the airfoil suction surface whilst simultaneously tripping the boundary layer on the pressure surface to turbulence. These effects eliminated virtually all tones by changing the wake vortex structure from periodic to random. Arndt and Nagel [8] made similar observations regarding the considerable reduction of tonal noise with leading edge serrations. The effect was attributed to vortex generation caused by the presence of the serrations, which reduced wake-induced tonal noise. A further

method of tonal noise elimination summarised by Nash et al. [5] is through placement of a boundary layer trip on the pressure surface of an airfoil sufficiently far from the trailing edge (i.e. less than 80% chord from the leading edge).

The distinct advantage of tubercles is that the tonal noise reduction is coupled with aerodynamic benefits such as increased maximum lift coefficient and maximum stall angle [9]. In addition, tubercles promote more gradual stall characteristics as well as increased lift post-stall [10]. Noise reduction has been identified as a potential benefit associated with tubercles [11] however there have been no previous studies of the effect of tubercles on airfoil self-noise. This is an important issue, because if aspects of tubercles were to be incorporated into new hydrofoil, airfoil and rotor designs, then it is important to firstly understand how noise is modified, and secondly, to exploit any noise-reduction capability that they may have. Airfoil tonal noise has been identified as a potential problem for wind turbines, gliders, small aircraft, rotors and fans [12, 13]. According to McAlpine et al. [12], tonal noise also occurs in underwater applications such as hydrofoils and propellers and is quite common on fast yachts and dinghys.

Tonal noise generation is believed to be initiated by Tollmein-Schlichting instabilities in a laminar boundary layer [5, 14, 15], which become amplified at the airfoil trailing edge [14] or at a point nearby [12]. Many researchers concur that a necessary condition for the generation of tonal noise is the existence of a self-excited acoustic feedback loop [14-17], however, there are various theories as to its nature and position. More specifically, some researchers suggest that the noise source is at the trailing edge and that the feedback loop exists between this point and a critical point upstream in the boundary layer [16, 17]. On the other hand, some researchers maintain that the acoustic source is in the wake and that the feedback

loop extends from here to the critical point in the boundary layer [14, 15].

The aim of this paper is to present the results from an experimental investigation into the effects of sinusoidal leading edge modifications on airfoil self-noise for a NACA 0021 airfoil at low-to-moderate Reynolds numbers. The ability of tubercles to eliminate tonal noise is demonstrated for both a closed section wind tunnel and an anechoic wind tunnel. A further aim of this paper is to investigate the relationship between the tonal noise frequency and the separation characteristics in order to shed light on the mechanism of airfoil tonal noise generation.

EXPERIMENTAL METHODS

Airfoil Design

Tubercle configurations were incorporated into a NACA 0021 airfoil profile and a baseline airfoil was manufactured for comparison. Airfoils were machined from aluminium and all airfoils have a chord of $c = 70\text{mm}$ and span of $s = 495\text{mm}$, giving a plan-form area of $S = 0.035\text{m}^2$. The limited width of the anechoic wind tunnel, restricted the span to $s = 275\text{mm}$, giving a corresponding plan-form area, $S = 0.019\text{m}^2$. Sinusoidal tubercle configurations are summarised in Table 1 and the dimensions are illustrated in Fig. 1.

Table 1. Tubercle configurations and adopted terminology

Configuration	Label	A/λ Ratio
0021 unmodified	0021 unmod	-
$A = 2\text{mm}$ (0.03c) $\lambda = 7.5\text{mm}$ (0.11c)	$A2\lambda7.5$	0.27
$A = 4\text{mm}$ (0.06c) $\lambda = 7.5\text{mm}$ (0.11c)	$A4\lambda7.5$	0.53
$A = 4\text{mm}$ (0.06c) $\lambda = 15\text{mm}$ (0.21c)	$A4\lambda15$	0.27
$A = 4\text{mm}$ (0.06c) $\lambda = 30\text{mm}$ (0.43c)	$A4\lambda30$	0.13
$A = 4\text{mm}$ (0.06c) $\lambda = 60\text{mm}$ (0.86c)	$A4\lambda60$	0.07
$A = 8\text{mm}$ (0.11c) $\lambda = 30\text{mm}$ (0.43c)	$A8\lambda30$	0.27

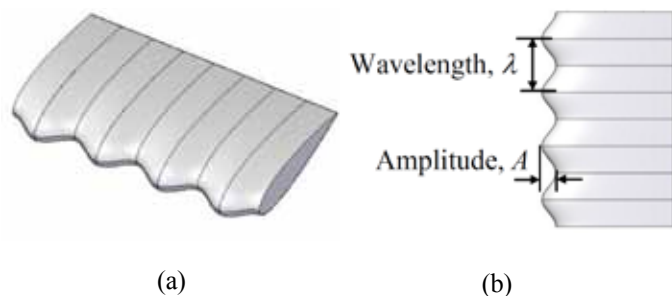


Figure 1. Section view of airfoil with tubercles (a) 3D view, (b) Plan view with characteristic dimensions

Acoustic and Pressure Tapping Measurements

Acoustic and pressure tapping measurements were carried out using a low-speed wind tunnel at the University of Adelaide, which has a 0.5m square cross-section and a turbulence intensity of $TI \sim 0.8\%$. The working section shown in Fig. 2 was bolted to the exit of the wind tunnel and the top of the airfoil was located very close (3mm) to the ceiling of the duct to minimise three-dimensional effects. The free-stream velocity was measured using a Pitot tube and the Reynolds number was $Re = 120,000$, based on the free-stream velocity of $U_\infty = 25\text{m/s}$ and airfoil chord length of $c = 70\text{mm}$. The working section did not have any form of acoustic treatment.

For the acoustic measurements, the microphones were arranged according to Fig. 2 and were fixed in the same positions for all experiments. In the case of the pressure measurements, static pressure ports were incorporated into both the unmodified and modified airfoils at the positions shown in Fig. 3 to observe the surface pressures. The small thickness of the airfoils increased the complexity of incorporating pressure taps into the existing models. Hence, it was decided that it would be more feasible to manufacture airfoils using a casting technique whereby the pressure taps could be moulded into the design during fabrication.

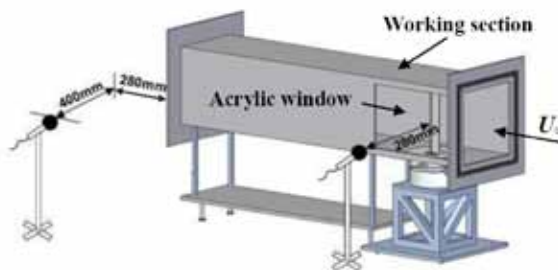


Figure 2. Working section and microphone positions

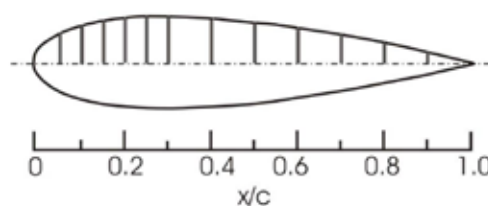


Figure 3. Pressure tap locations for unmodified airfoils

Pressures at the airfoil surface were received by a Scanivalve mechanical pressure multiplexer, model number: 48D3-1404A which was connected to a controller. The output from the Scanivalve was received by a Baratron pressure transducer. The system was controlled using a Labview program which was written to interface with a data logger. A time delay of 5s was included to allow the pressure to stabilise at a given location before the commencement of data acquisition. Measurement duration was 30s, which was followed by another time delay of 5s to eliminate the uncertainties caused by advancement of the Scanivalve to the next position.

Further acoustic results were obtained using the anechoic wind tunnel (AWT) at the University of Adelaide, which has a room size of approximately 2m^3 and walls acoustically treated with foam wedges. The contraction outlet has dimensions of 75mm (height) and 275mm (width). End-plates were manufactured for the model to reduce three-dimensional effects and a circular cut-out section with a 'running fit' tolerance allowed the angle of attack to be adjusted as shown in Fig. 4.

The Reynolds number was $Re = 120,000$, based on the freestream velocity of $U_\infty = 25\text{m/s}$ and airfoil chord length. At this freestream velocity, the corresponding turbulence intensity is $TI \sim 0.4\%$. For these measurements, a single microphone was positioned at a height of 650mm above the airfoil trailing edge and 50mm posterior to the trailing edge.

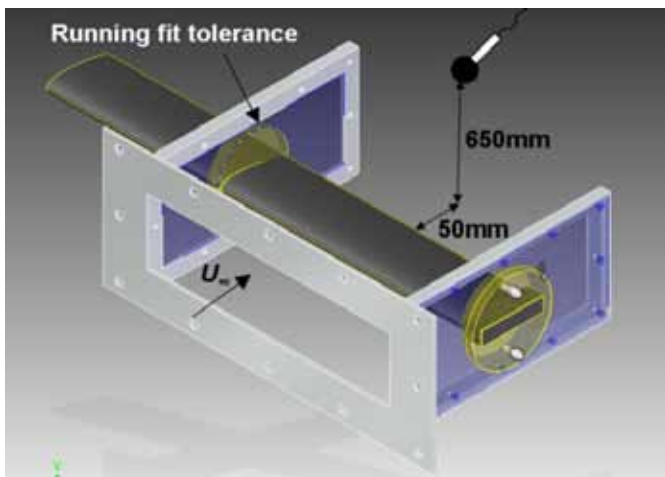


Figure 4. Mount for anechoic wind tunnel

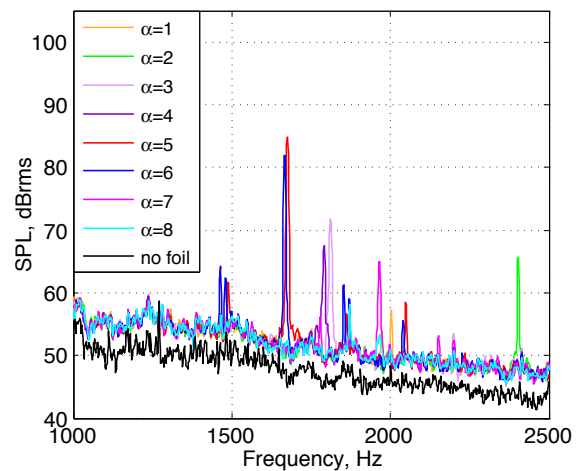
RESULTS AND DISCUSSION

Acoustic Measurements in Hard-Walled Wind Tunnel (HWT)

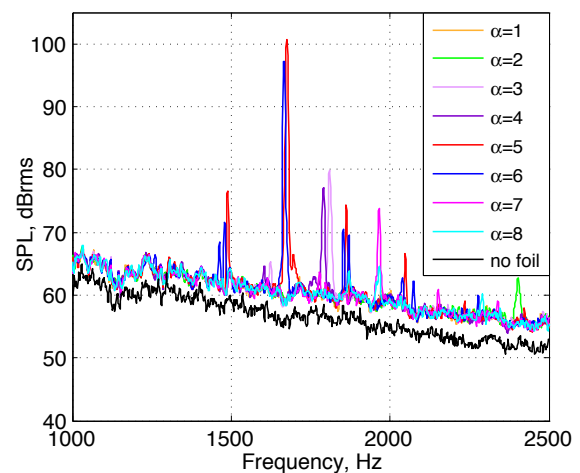
Tonal noise measurements were initially conducted in the hard-walled wind tunnel (HWT) since it was observed that there was an audible difference in tonal noise between models with and without tubercles. Hence, it could be argued that the difference in noise levels was large enough to be measured. The influence of the duct on tonal noise propagation was monitored through comparing the results from two microphones positioned at different streamwise locations. Measurement of the duct modes was not considered pertinent to the investigation because the leading edge tubercles did not change the reflecting surface of the airfoil significantly. Therefore, significant differences in tonal noise for airfoils with and without tubercles were attributed to altered flow characteristics associated with the presence of tubercles. Nevertheless, it should be noted that the absolute values presented in Fig.5 are affected by the highly reverberant nature of the duct and that the relative difference in SPL between the tonal peaks and the broadband noise is more meaningful.

At each angle of attack from $\alpha = 1^\circ$ to $\alpha = 8^\circ$, the unmodified NACA 0021 airfoil generates tonal noise as shown in Fig. 5(a) and (b). According to McAlpine et al. [12], tonal noise would not occur if transition to turbulence occurred sufficiently far from the airfoil trailing edge, which is a possible explanation for the absence of tones for $\alpha > 8^\circ$.

Results are shown for both microphones and it can be seen that the sound pressure level (SPL) at the duct exit is higher due to the transmission loss associated with the acrylic window. There are some slight variations in the two sets of results which can be attributed to the variation in sound directivity with frequency.



(a)



(b)

Figure 5. Sound pressure level (SPL) against frequency, f , for NACA 0021 at angle of attack, $\alpha = 1^\circ - 8^\circ$, $Re = 120,000$ (a) microphone at window, (b) microphone at exit

The results shown in Fig. 6(a) indicate that for airfoils with tubercles, there is a substantial reduction in SPL and that in general, the Strouhal number of the tonal noise is higher for airfoils with tubercles as evident in Fig. 6(b). The Strouhal number, St is defined according to Eq. (1)

$$St = \frac{fc}{U_\infty} \quad (1)$$

where f is the frequency of tone, c is the airfoil chord and U_∞ is the freestream velocity.

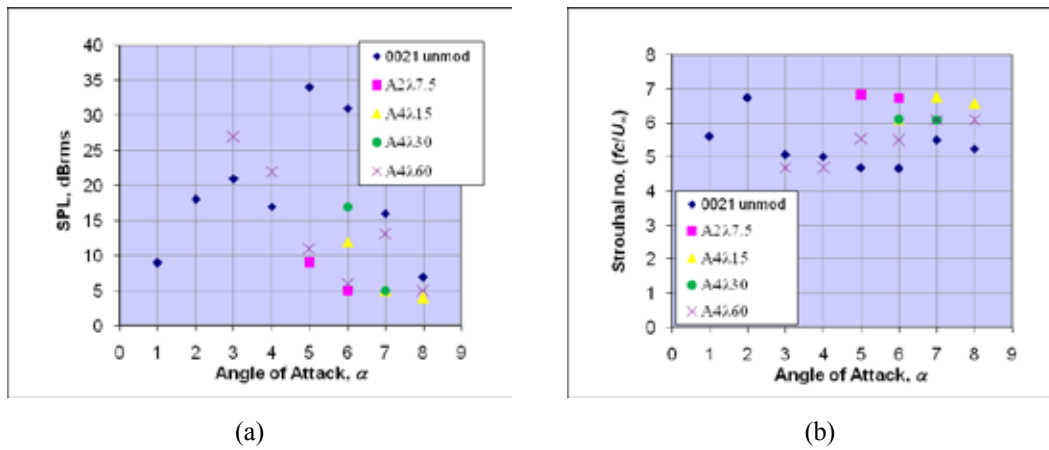


Figure 6. Results at microphone nearest window for NACA 0021 airfoils with tubercles at $1^\circ \leq \alpha \leq 8^\circ$. (a) Sound pressure level (SPL) against angle of attack, α and (b) Strouhal number against angle of attack, α

The largest amplitude tubercles, $A8\lambda30$, and the smallest wavelength case, $A4\lambda7.5$, both of which have relatively large A/λ ratios are not included in the plots since they did not generate any detectable tonal noise. For the tubercle configurations shown in Fig. 6, the smallest wavelength case ($A2\lambda7.5$) has the highest Strouhal number and lowest SPL amplitude at the two angles of attack at which it produces tonal noise. The largest wavelength tubercle case ($A4\lambda60$) generates the tones at the lowest Strouhal number and for a greater number of attack angles and a higher SPL compared to the other airfoils. Note that the results in Fig. 6 were obtained by subtracting the broadband SPL for the corresponding angle

of attack and frequency. In addition, only the largest amplitude tone was considered and thus secondary tones were not plotted.

Acoustic Measurements in Anechoic Wind Tunnel (AWT)

Referring to Fig. 7(b-g), it can be seen that all tubercle configurations experience significantly reduced SPL at the tonal frequency and in most cases the tonal noise is eliminated altogether. Consistent with the results in the HWT, the most successful tubercle configurations for tonal noise elimination are those with a larger value of A/λ ratio as shown in Fig. 7(b), (c), (d) and (g).

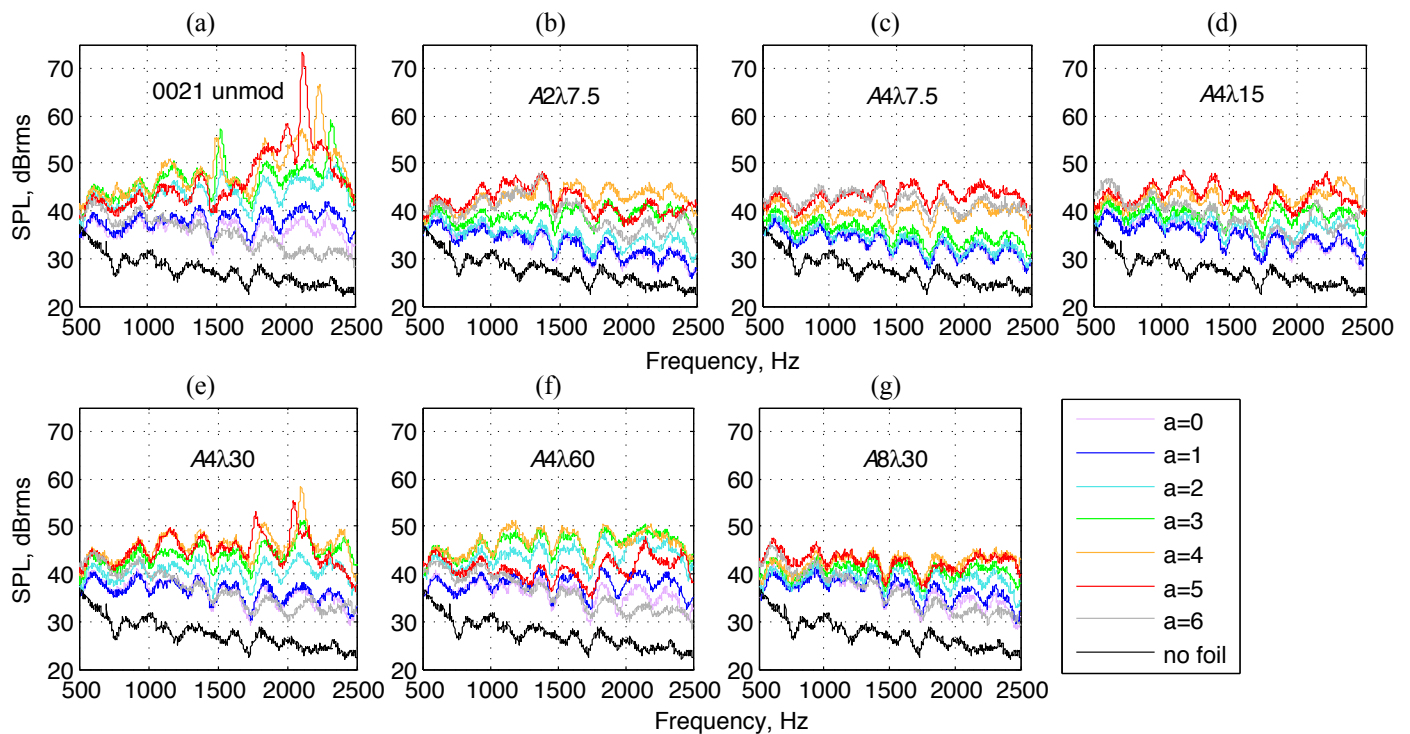


Figure 7. SPL against frequency measured in anechoic wind tunnel (AWT) for (a) unmodified 0021 (b) $A2\lambda7.5$ (c) $A4\lambda7.5$ (d) $A4\lambda15$ (e) $A4\lambda30$ (f) $A4\lambda60$ (g) $A8\lambda30$, $Re = 120,000$

Also, the largest amplitude tone for the unmodified airfoil occurs at $\alpha = 5^\circ$, which can be seen in Fig. 7(a) and is in agreement with the results discussed earlier for the HWT. However, the tonal frequency at this angle of attack is slightly higher in the AWT (2125Hz compared with 1675Hz in the HWT). This is an interesting discrepancy which highlights the sensitivity of the tonal noise generating mechanism to changes in experimental parameters, even after standard corrections have been applied to account for the downwash and flow curvature of the airflow around the model associated with the finite size of the open jet [18]. Another difference between the sets of results is that tonal noise appears over a much wider range of angles when testing in the HWT. A result that was not observable using the HWT is a small reduction in broadband noise, which occurs between 1500 and 2500Hz for all airfoils with tubercles. A higher broadband component appears to be directly related to the presence of the tones for the unmodified airfoil.

Pressure tapping results

The pressure coefficient, C_p , is plotted as a function of the normalised chordwise position for the NACA 0021 unmodified airfoil and the A8230 tubercle configuration in Fig 8. Experimental measurements are compared to values obtained using the XFOIL code [19].

The existence of a separation bubble is reflected in Fig. 8 for both the experimental and XFOIL data at $\alpha = 5^\circ$ and is identified as the section of the suction curve where the pressure gradient starts to decrease, almost reaching a value of zero. After the separation bubble, the pressure gradient increases rapidly and then reaches the value which would be predicted in the absence of the separation bubble. The difference between the results for the unmodified airfoil and the airfoil with tubercles is that the separation bubble is localised to the troughs in the latter case rather than extending over the entire span as shown in Fig. 8(b). This is a possible explanation for the absence of tonal noise for airfoils with tubercles.

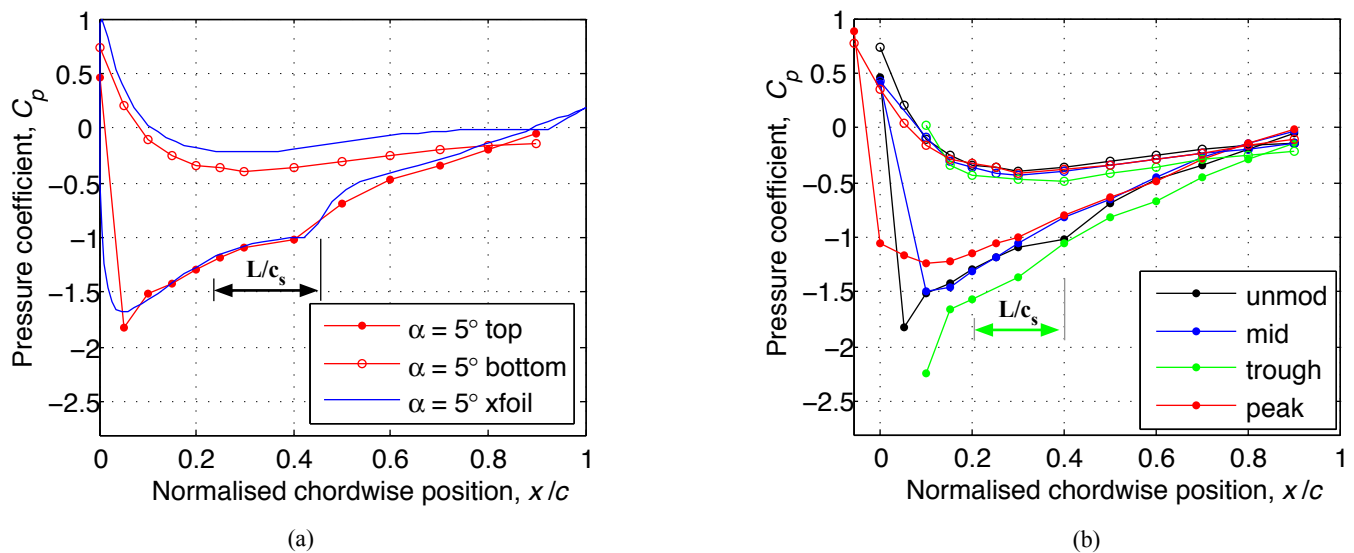


Figure 8. Normalised pressure distribution plots for (a) unmodified airfoil and (b) airfoil with A8230 tubercle configuration at $\alpha = 5^\circ$, where symbols are chosen as follows: “●” suction surface “○” pressure surface, $Re = 120,000$.

CONCLUSIONS

Incorporating tubercles into the leading edge of an airfoil facilitates the reduction and potential elimination of tonal noise for a NACA 0021 airfoil. In addition, the broadband noise is significantly reduced for a range of frequencies adjacent to the tonal peak. It is believed that the mechanism responsible involves the generation of streamwise vortices as well as the spanwise variation in separation location. Both effects alter the boundary layer stability characteristics, influencing the coherence of the vortices downstream from the trailing edge, hence reducing trailing edge noise generation. Also, confinement of separation bubbles to the troughs between tubercles reduces boundary layer receptivity to external acoustic excitation. Consequently, the potential for development of a feedback loop is minimised, which is another explanation for the significant reduction or absence of tonal noise for airfoils with tubercles.

REFERENCES

- [1] P.W. Bearman and J.C. Owen, “Reduction of bluff body drag and suppression of vortex shedding by the introduction of wavy separation lines”, *Journal of Fluids and Structures* **12**, 123-130 (1998)
- [2] F.E. Fish and G.V. Lauder, “Passive and active flow control by swimming fishes and mammals”, *Annual Review of Fluid Mechanics* **38**, 193-224 (2006)
- [3] H.T.C. Pedro and M.H. Kobayashi, “Numerical study of stall delay on Humpback whale flippers”, *Proceedings of the 46th AIAA Aerospace Sciences Meeting and Exhibit*, Reno, Nevada, 7-10 January 2008
- [4] D. Custodio, *The effect of Humpback whale-like leading edge protuberances on hydrofoil performance*, Master’s Thesis, Worcester Polytechnic Institute, 2007
- [5] E.C. Nash, M.V. Lawson and A. McAlpine, “Boundary-layer instability noise on aerofoils”, *Journal of Fluid Mechanics* **382**, 27-61 (1999)

- [6] A.M. Kuethe, "Effect of streamwise vortices on wake properties associated with sound generation", *Journal of Aircraft* **9**, 715-719 (1972)
- [7] A.S. Hersh, P.T. Soderman and R.E. Hayden, "Investigation of acoustic effects of leading edge serrations on airfoils", *Journal of Aircraft* **11**, 197-202 (1974)
- [8] R.E.A. Arndt and R.T. Nagel, "Effect of leading edge serrations on noise radiation from a model rotor", AIAA-Paper No. 72-655 (1972)
- [9] D.S. Miklosovic, M.M. Murray, L.E. Howle and F.E. Fish, "Leading-edge tubercles delay stall on Humpback whale flippers", *Physics of Fluids* **16**, L39-42 (2004)
- [10] H. Johari, C. Henoch, D. Custodio and A. Levshin, "Effects of leading edge protuberances on airfoil performance", *AIAA Journal* **45**, 2634-2642 (2007)
- [11] S.W. Dewar, P. Watts and F.E. Fish, "Turbine and compressor employing tubercle leading edge rotor design", *International patent* WO 2006/042401 A1 (2006)
- [12] A. McAlpine, E.C. Nash and M.V. Lowson, "On the generation of discrete frequency tones by the flow around an airfoil", *Journal of Sound and Vibration* **222**, 753-779 (1999)
- [13] M.J. Kingan and J.R. Pearse, "Laminar boundary layer instability noise produced by an aerofoil", *Journal of Sound and Vibration* **322**, 808-828 (2009)
- [14] C.K.W. Tam and H. Ju, "Aerofoil tones at moderate Reynolds number", *Journal of Fluid Mechanics* **690**, 536-570 (2011)
- [15] G. Desquesnes, M. Terracol and P. Sagaut, "Numerical investigation of the tone noise mechanism over laminar airfoils", *Journal of Fluid Mechanics* **591**, 155-182 (2007)
- [16] S.E. Wright, "The acoustic spectrum of axial flow machines", *Journal of Sound and Vibration* **45**, 165-223 (1976)
- [17] H. Arbey and J. Bataille, "Noise generated by airfoil profiles placed in a uniform laminar flow", *Journal of Fluid Mechanics* **134**, 33-47 (1983)
- [18] T.F. Brooks, M.A. Marcolini, and D.S. Pope, "Airfoil Trailing-Edge Flow Measurements", *AIAA Journal* **24**, 1245-1251 (1986)
- [19] M. Drela and H. Youngren, *XFOIL 6.94 User Guide*, Aeronautical and Astronautical Engineering, MIT, Cambridge, MA, 2001

Inter-Noise 2014

MELBOURNE AUSTRALIA 16-19 NOVEMBER 2014

The Australian Acoustical Society will be hosting Inter-Noise 2014 in Melbourne, from 16-19 November 2014. The congress venue is the Melbourne Convention and Exhibition Centre which is superbly located on the banks of the Yarra River, just a short stroll from the central business district. Papers will cover all aspects of noise control, with additional workshops and an extensive equipment exhibition to support the technical program. The congress theme is *Improving the world through noise control*.

Key Dates

The proposed dates for Inter-Noise 2014 are:

Abstract submission deadline: 10 May 2014

Paper submission deadline: 25 July 2014

Early Bird Registration by: 25 July 2014

Registration Fees

The registration fees have tentatively been set as*:

Delegate	\$840	\$720 (early bird)
----------	-------	--------------------

Student	\$320	\$255 (early bird)
---------	-------	--------------------

Accompanying person	\$140	
---------------------	-------	--

*An additional GST applies to Australian based delegates

The registration fee will cover entrance to the opening and closing ceremonies, distinguished lectures, all technical sessions and the exhibition, as well as a book of abstracts and a CD containing the full papers.

The Congress organisers have included a light lunch as well as morning and afternoon tea or coffee as part of the registration fee. These refreshments will be provided in the vicinity of the technical exhibition which will be held in the Main Foyer.

The Congress Banquet is not included in the registration fee.

Technical Program

After the welcome and opening ceremony on Sunday 16 November, the following three days will involve 10 parallel sessions covering all fields of noise control. Major areas will include Community and



Environmental Noise, Architectural Acoustics, Transport Noise and Vibration, Human Response and Effects of Low Frequencies and Underwater Noise. A series of distinguished lectures and workshops are planned to cover topics such as:

- Noise impact on high density living
- Impact on dense living
- Wind turbine noise
- Active noise control
- Aircraft noise
- Power station noise

Organising and Technical Committee

- Congress President: Dr Norm Broner
- Technical Program Chair: Adjunct Professor Charles Don
- Technical Program Co-Chair: Adjunct Professor John Davy
- Technical Program Advisor: Mrs Marion Burgess
- Proceedings Editor: Mr Terry McMinn
- Sponsorship and Exhibition Manager: Dr Norm Broner
- Congress Treasurer: Ms Dianne Williams
- Social Program Chair: Mr Geoff Barnes
- Congress Secretariat: Ms Liz Dowsett

Further details are available on the congress website

www.internoise2014.org

MODELLING OF PILE DRIVING NOISE BY MEANS OF WAVENUMBER INTEGRATION

Tristan Lippert and Stephan Lippert

Institute of Modelling and Computation, Hamburg University of Technology, Germany

tristan.lippert@tuhh.de

A method for the acoustic simulation of pile driving is presented using the wavenumber integration (WI) approach, in combination with a recently suggested array of point sources, to represent the pile. The fundamentals of the WI are briefly discussed, as are the main acoustic characteristics of pile driving. A reference finite element model is set up to demonstrate these main features and is further compared to a literature example, to ensure its validity. Subsequently, the obtained results are compared to the solutions from WI simulations on the same example. The results are found to be in excellent qualitative agreement, therefore the WI technique seems to be very promising with respect to the acoustic long range prediction in pile driving.

INTRODUCTION

The development and deployment of renewable energy sources is one of the major tasks of our days, since the long term shortage of fossil combustion materials becomes more and more obvious, while the global energy demand continues to rise. To meet this challenge the German government has declared the aim to produce 80% of its total energy consumption from sustainable sources in 2050, with offshore wind energy playing a decisive role [1].

However, one of the major drawbacks of this technology is the possible negative effect on marine wild life during construction. With pile driving being the state of the art foundation for most wind farms, pulses with source sound pressure levels (SPLs) of up to 250dB¹ are produced with each hammer strike. This is likely to cause temporary or even permanent threshold shifts (TTS/PTS) for marine mammals, such as the harbor porpoise, who use their sense of hearing as their primary means of orientation and communication [2]. To protect these endangered species, German authorities have decreed threshold values of 160dB for the sound exposure level (SEL) and 190dB for the peak SPL at a distance of 750m from the pile [3]. To comply with these regulations, sound mitigation measures, such as, bubble curtains or cofferdams, need to be applied. For their design a detailed, numerical model of the pile driving process is needed, both for the assessment of the acoustic impact of planned future wind farms, as well as for the apriority optimization of sound insulation measures to minimize offshore testing time and costs.

Furthermore, apart from offshore wind farms, pile driving takes on a key role in most near shore construction activities, as for example the building of bridges, with comparable possible harm to the environment, see for example Stadler and Woodbury [4].

The relatively large dimensions of several kilometers, in combination with the frequency range of interest stretching up to several kilohertz, make a straight forward, discrete modelling, for example by means of the finite element method (FEM) impractical. Therefore a combined approach of a discrete FE-model that models the complex processes near the

pile with a propagation model that efficiently computes results far from the pile under certain simplifications is desirable.

The present paper focuses on the latter subject, with the wavenumber integration (WI) technique as the propagation method. In this work the basic idea of this method illustrated and the implemented algorithms are briefly discussed. A reference FE-model, that is subsequently explained, is set up and qualitatively compared to results from WI simulations and literature values. Finally, a conclusion and an outlook on planned model extensions are given.

WAVENUMBER INTEGRATION

The simulation of sound propagation in the ocean over long distances via discrete methods is limited by the size of the resulting system of equations. Therefore, a number of alternative schemes have been developed, each involving a number of simplifications, such as normal modes, parabolic equation modelling, wavenumber integration, or ray tracing. For an overview and introduction to each of these schemes, see Jensen et al. [5].

In the present work an investigation by wavenumber integration is used, following Schmidt and Tango [6]. Assuming a two-dimensional, rotational symmetric, stratified (i.e. range-independent) model environment, where sources can only exist on a vertical axis through the origin, the Helmholtz equation reduces to

$$\left[\frac{\partial^2}{\partial r^2} + \frac{\partial^2}{\partial z^2} + k^2(z) \right] \phi(r, z) = S_\omega \delta(r) \delta(z - z_s) \quad (1)$$

where k is the medium wavenumber, ϕ is the potential to be solved for, S_ω is the source strength, $\delta(x)$ is the Dirac function, and z_s is the source depth. The solution of equation (1) can be decomposed into conical wavefronts around the z -axis by means of the forward Hankel transform, from the transform pair

$$f(r, z) = \int_0^\infty F(k_r, z) J_0(k_r r) k_r dk_r \quad (2a)$$

$$F(k_r, z) = \int_0^\infty f(r, z) J_0(k_r r) r dr \quad (2b)$$

¹All dB values are referenced to 1 μ Pascal.

where k_r is the horizontal wavenumber, which can be interpreted as the factor, that determines the inclination of each conical wavefront. The Bessel function J_0 can be expressed by the two Hankel functions $H_0^{1,2}$ by the relation $J_0 = \frac{1}{2} [H_0^1 + H_0^2]$, i.e. identically inclined cones that travel in opposite directions. Thus, the so called depth-separated wave equation is obtained by

$$\left[\frac{\partial^2}{\partial z^2} + (k^2 - k_r^2) \right] \phi(k_r, z) = \frac{S_\omega}{2\pi} \delta(z - z_s) \quad (3)$$

Assuming a purely fluid stratification for a layered waveguide, the solution of equation (3) in each layer m , consists of a particular solution $\hat{\phi}_m$, if a source is present in the layer, and the homogeneous solution of an upward and a downward travelling wave ϕ_m^+ and ϕ_m^- , yielding

$$\phi_m(k_r, z) = \hat{\phi}_m(k_r, z) + A_m^+(k_r) \phi_m^+(k_r, z) + A_m^-(k_r) \phi_m^-(k_r, z) \quad (4)$$

The $2m$ unknown coefficients $A_m^{+,-}$ have to be determined over the $2(m-1)$ continuity conditions for the vertical displacement and the pressure at the $(m-1)$ interfaces between the layers and two boundary conditions, for example a pressure release boundary at the air water interface and an infinite halfspace for the bottom. Analytical solutions for all unknown amplitudes can be found for layers with constant or quadratically varying sound speed profiles, see for example Schmidt [7].

The so-called depth-dependent Green's function $g(k_r, z)$ between a source and a receiver can subsequently be obtained by converting the potential $\phi_m(k_r, z)$ to the physical quantity of interest (e.g. the vertical displacement is defined as $w = \frac{\partial \phi}{\partial z}$). To compute the resulting wave field, $g(k_r, z)$ has to be transformed back from the wavenumber domain to the frequency domain, by means of the backward Hankel transformation, which is given in equation (2).

To automatically obtain frequency results by means of the wavenumber integration approach, e.g. to implement it numerically, some alterations to the described procedure are needed. At first, the infinite integration limit in equation (2) has to be replaced by a finite maximum value $k_{r,max}$ and a horizontal wavenumber discretization Δk_r has to be chosen. Hence, it is crucial to choose $k_{r,max}$ large enough to account for all values of $g(k_r, z)$ that have a meaningful contribution to the integral and to ensure that the wavenumber resolution Δk_r is high enough to avoid aliasing and wrap-around effects in the transformation. For further treatment of numerical transformation requirements, see for example Oppenheim and Schaffer [8].

In the present model, the depth-separated Helmholtz equation (3) is solved by means of the direct global matrix approach suggested by Schmidt and Tango [6]. The algorithm implements an efficient, unconditionally stable solution of the boundary value problem for the pressure p and the displacement w , using an approach resembling finite element discretization of the waveguide in depth. The amplitudes $A_m^{+,-}$ in each layer m are computed for each discrete horizontal wavenumber $k_{r,n}$, with $n = 1 \dots \frac{k_{r,max}}{\Delta k_r}$, what in turn yields the desired, discrete depth-dependent Green's function $g(k_{r,n}, z)$ at all specified receiver depths.

The backward Hankel transformation given in equation (2) is numerically carried out with the help of the so-called fast field approximation (often called fast field program or FFP) suggested by Di Napoli and Deavenport [9]. The approximation is based on the neglect of outgoing waves, i.e. setting the Hankel function $H_0^2 \equiv 0$ in the representation of the Bessel function. Additionally, the remaining Hankel function H_0^1 is replaced by its large argument representation, see for example Abramowitz and Stegun [10]. This yields

$$J_0 = \frac{1}{2} [H_0^1 + H_0^2] \approx \sqrt{\frac{2}{\pi k_r r}} e^{i[k_r r - (m + \frac{1}{2}) \frac{\pi}{2}]} \quad \text{for } k_r r \gg 1 \quad (5)$$

Disregarding the incoming wavefronts is only effecting the wave field close to the source, as is the large argument approximation of $k_r r$ which is already valid for almost all propagation angles at a relatively short distance from the source. The resulting wave field is therefore physically unmeaningful at short ranges r and extremely steep propagation angles, i.e. very small values of k_r . However, steep propagation paths will be damped out rather quickly, due to the multiple reflections at the interfaces and not yield a significant contribution for large values of r and, by definition, the propagation model is used to determine the field at relative large source receiver separations. Hence the use of the fast field approximation is justified in this context.

The main benefit is that the full Hankel transformation, as given in equation (2), reduces to a Fourier transform, as in the FFP representation in equation (5) such that only one exponential function of the argument $k_r r$, multiplied by a constant is left. By doing so, existing, numerically very efficient algorithms can be used for the evaluation of equation (2).

Finally, to better compare the frequency domain results obtained by wavenumber integration with the time domain results from the FE-model, an inverse Fourier transformation is carried out. The convolution of the source signal with the impulse response of the receiver thus reduces to a simple multiplication of the source spectrum S_ω with the Green's function g_ω , and is given by

$$p(r, z, t) = \int_{-\infty}^{\infty} S_\omega g_\omega(r, z) e^{-i\omega t} d\omega \quad (6)$$

For an extensive treatment of time domain transformations and the according requirements see Oppenheim and Schaffer [8].

A tangible illustration of the presented theory of wavenumber integration can be found in figure 1, where it is applied to a simple Pekeris waveguide. As can be seen in figure 1(a), a source is placed in the middle of a fluid layer with a thickness of 100m, which is enclosed by an upper pressure release boundary, i.e. $p(r, z=0) \equiv 0$, and a lower, infinite halfspace of a fluid with higher density and sound speed. In figure 1(b), the solution to equation (4) given by equation (3) is plotted for the receiver depth $z_R = 30$ m for all values of the horizontal wavenumber $k_{r,n}$, at an exemplary frequency of $f = 100$ Hz. Applying the forward Hankel transformation given in equation (2) to this wavenumber spectrum yields the pressure $p(f, r_R, z_R)$. Upon repetition for all frequencies of interest, the frequency response shown in figure 1(c) is

obtained. Convoluting this response with a certain source output signal, here a single sine wavelet, by means of the inverse Fourier transformation given in equation (6), the time series of the receiver $p(t, r_R, z_R)$ is generated. Now the arrival of the direct wave, the first inverse reflection from the pressure release boundary and further reflections can be distinguished, for a full contour plot of the problem see, for example, Lippert et al. [11].

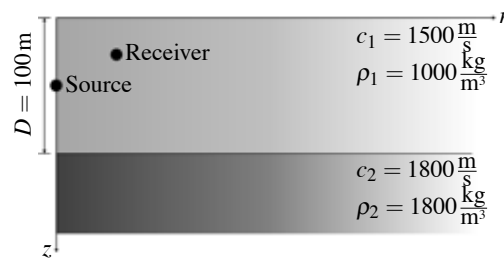
REFERENCE FE-SIMULATION

In this section a basic finite element-model (FE model) is set up to model the acoustics of pile driving. The obtained results are qualitatively compared to an earlier publication of Reinhall and Dahl [12] and used to verify the results obtained with the wavenumber integration.

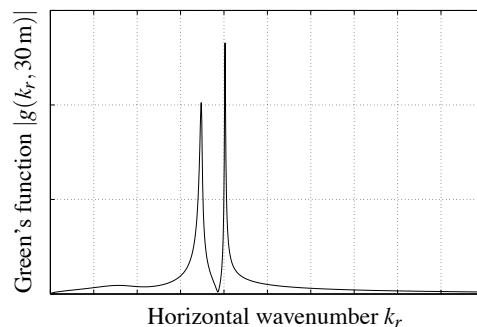
Simplifying, the model is set up as two-dimensional and axis symmetric, assuming a perfectly centered hammer strike. Roughly assuming North Sea offshore conditions, the pile has a total length of 65 m, whereof 20 m are standing in the seafloor, 40 m are surrounded by water, and 5 m protrude from the sea surface. It has a diameter of 3.5 m and a wall thickness of 80 mm. Both the sea bottom and the water column are modeled as fluids, assuming a density of $\rho_w = 1000 \text{ kg/m}^3$ and a sound speed of $c_w = 1450 \text{ m/s}$ for the water phase. The bottom is assumed to be a sandy fluid with a density of $\rho_b = 2034 \text{ kg/m}^3$ and a sound speed of $c_b = 1836 \text{ m/s}$, taken from Hamilton [13]. Additionally, the pile itself is fixed with spring-damper elements, to account for the fact that the vast majority of the strike energy is mechanically absorbed by the intrusion of the pile into the seabed. This somewhat coarse approximation to the real interaction between pile and soil, and the error resulting from it, is accepted, as the results are only to be compared qualitatively. The sea surface is assumed to be a perfect reflector, due to the large difference in impedance between air and water, as is the surface of the protruding part of the pile. The outer boundaries of the model are enclosed by non-reflecting boundary conditions to avoid artificial reflections, thus modelling the surroundings as an infinite layer above an infinite half space. The hammer strike is modelled via a pressure boundary condition. The time-pressure distribution is derived from a simple analytical approach, modelling the pile as a damper with a pile characteristic impedance, acted upon by an accelerated hammer mass, as analytically derived by Deeks and Randolph [14].

The results of three different time steps are depicted in figure 2, where the distinct inclined wavefronts, typical to pile driving can be identified. As shown by Reinhall and Dahl [12] this main contribution of the high sound pressure levels, encountered in acoustic pile driving measurements, can be explained by the occurrence of Mach waves. Typically, Mach waves are associated with jets flying at supersonic speed. Assuming the jet to be an idealized point source, the emitted wavefronts, start to overlap and superimpose each other as the speed of the source is higher than the radiation velocity of the pressure waves (p -waves). The result is a so-called Mach cone, which basically is a high energetic, conical wavefront.

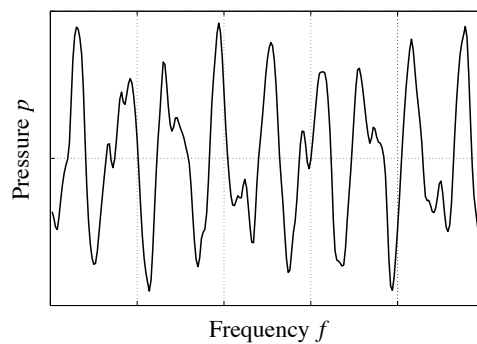
The acoustic radiation from pile driving follows a similar pattern. The hammer strike induces a longitudinal or pressure



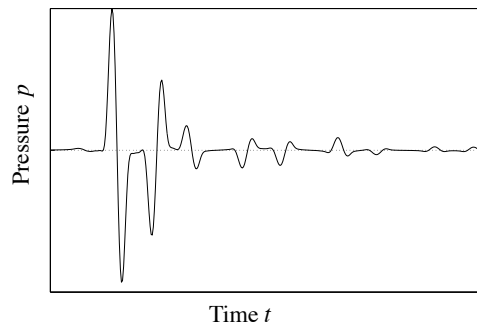
(a) Schematic model sketch (Source: $z_S = 50 \text{ m}$, Receiver: $r_R = 50 \text{ m}$, $z_R = 30 \text{ m}$)



(b) Magnitude of the Green's function at a selected receiver position ($f=100 \text{ Hz}$)



(c) Frequency response at a selected receiver position



(d) Time series at a selected receiver position

Figure 1. Graphic representation of a time series computation with wavenumber integration

wave that travels along down the pile, which in turn triggers a so-called quasi-longitudinal displacement wave. This wave type occurs due to the fact that in solid media, each longitudinal deformation is also coupled to transverse deformation via Poisson's ratio ν , quasi-longitudinal means that the wave is propagating in the longitudinal direction in principle, but with

a transverse component also. In relative slender structures, such as the hollow cylinder regarded here, this transverse deformation component can partly be found to be a surface wave. Additionally, a plate or a rod, for example, have a lower stiffness than an infinite medium consisting of the same material, therefore the propagation speed of an impulse lies below the nominal value, see for example Herbst [15]. As the displacement itself is relatively small, it can be assumed to be a point source. If the pile is simplified as a rod, the propagation velocity of the quasi-longitudinal wave can be determined as $c_{ql} = \sqrt{E/\rho}$, which, depending on the steel used, yields values of approximately $c_{ql} \approx 5000$ m/s. Hence, the analogy to the above mentioned jet example becomes clear, relative to the propagation velocities of the p -waves in the surrounding fluids, the point source is always travelling at supersonic speed, thus producing Mach cones in the same way as described above.

In figure 2, normalized acoustic pressure contours for three exemplary time steps after the hammer impact are depicted. In figure 2(a) the impulse has travelled solely in the water column, developing a clearly identifiable inclined wavefront, e.g. a 2D-slice cut from a Mach cone. The inclination of the wavefront follows directly from the ratio of the propagation velocity of the impulse in the pile c_{ql} and the sound speed in the surrounding fluid c_{fluid} . In this case, the inclination follows as $\phi_w = \arcsin(c_w/c_s) \approx 16$ deg. In figure 2(b) the pulse has passed the interface between the two media and is running in the bottom, the according inclination below the mudline is $\phi_b = \arcsin(c_b/c_s) \approx 20$ deg. The broadening of the resulting wavefront can partly be explained by the higher sound speed c_b in the bottom. In the last figure 2(c) the pulse has reached the lower end of the pile, has been reflected and is now travelling towards the top again. Here one can see that the pressure impulse is subject to a phase shift of 180 deg when it is reflected, due to the drop in impedance between the two media. The less pronounced wavefronts in the bottom are probably partly caused by sound energy leaking from the inner fluid and the inversion of the pulse at the very end of the pile. Additionally imperfections at the nominally non-reflecting boundaries of the model seem to be an issue, as for example discussed by Deeks and Randolph [16].

WAVENUMBER INTEGRATION FOR PILE DRIVING ACOUSTICS

In this section the results produced in the previous section are reproduced with a propagation method, to allow for predictions at large distances from the pile. Based on the exemplified characteristics, Reinhall and Dahl [12] propose a method to model the sound radiation from pile driving by means of a phased point source array. The single contributions from each frequency is determined by means of parabolic equation (PE) modelling. In this contribution, their approach of a point source array is realized with the wavenumber integration technique, described earlier.

The basic idea of the suggested approach is to reproduce the identified Mach waves, by a number of point sources along the pile axis with a fixed spacing. The emitted signal from each of the $n = 1 \dots N$ point sources starts with a time delay of

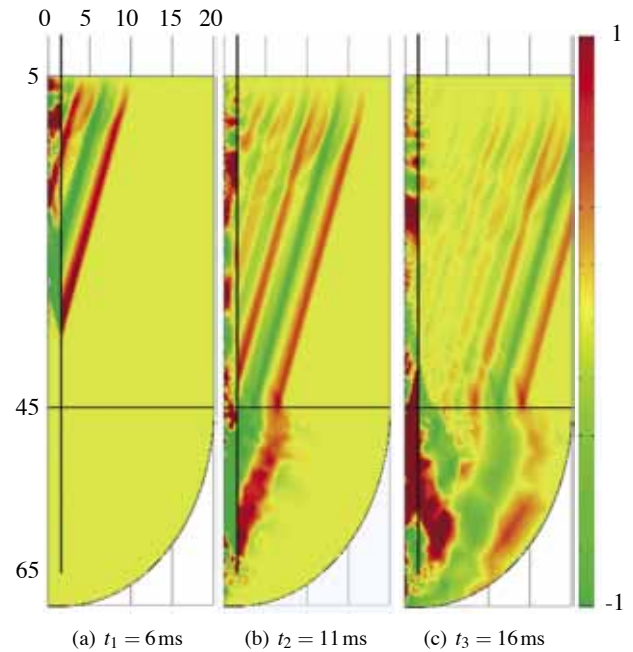


Figure 2. Pressure field contours from the FE model after hammer impact (normalized)

$\Delta t_n = z_{s,n}/c_{ql}$, resulting from the fact that the quasi-longitudinal impulse travels down the pile with a propagation velocity of c_{ql} , which in turn means that at the source position $z_{s,n}$ no signal will be emitted before $t = \Delta t_n$.

The emitted signal from each point source is determined as a single sine wavelet with a frequency of $f_s = 300$ Hz, which is found to be a good approximation for the first wavefront radiated from the pile in the FE simulations. The pile is represented by 13 point sources distributed between the sea surface and the end of the pile, with a spacing of $\Delta z_s = 5$ m. All respective model or material parameters are identical to those described above. The normalized results of the WI simulation are depicted in figure 3.

Before discussion and comparison of the results, some preliminary remarks need to be made. As mentioned above, only the first wavefront is accounted for, hence the noise occurring behind this wavefront cannot be related to the secondary emissions from the FE-results. Also, the region very close to the pile, i.e. the first few metres, are physically unmeaningful, due to the far field approximation discussed earlier. Finally, the relatively wide spacing of the sources leads to somewhat inhomogeneous wavefronts at short distances from the sources, due to the strong curvature. But as the WI is generally used to evaluate the field at some distance from the pile, this problem becomes insignificant, as can be seen from the results. In contrast to its described common application, the WI is subsequently used only in the same range as the FEM to compare the results.

Comparing the simulations, with these reservations, the high consistency of the results becomes obvious. In figure 3(a) the impulse is travelling solely in the water column, while it has reached the end of the pile in figure 3(b). The distinct inclinations of the Mach waves in both media are the same for the FE- and the WI-model, as is the broadening effect of the wavefront in the lower halfspace. In figure 3(c) the impulse has been reflected at the end of the pile and travelling upwards

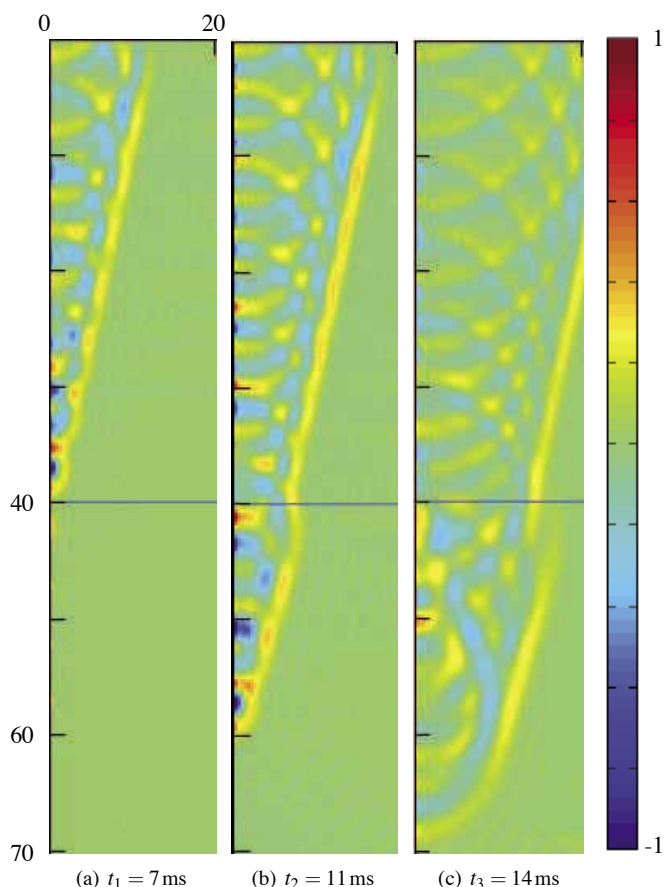


Figure 3. Pressure field contours from the WI-model after hammer impact (normalized)

again, with the expected reversed phase.

It can be seen that developing wavefronts become smooth after approximately 10m. Also, as was the case in the simulations above, the wavefront in the bottom is not as pronounced as it is in the water phase. However, the degree of disfiguration is clearly lower, resulting mainly from the last point source at the pile, which hints to a problem with the non-reflecting boundaries in the FE-model.

Concluding, it can be said that the main characteristics of acoustic pile driving radiation, with the presented WI approach, can be qualitatively reproduced. This could be achieved by means of a relatively simple modelling approach. Therefore, a further enhanced wavenumber integration model is believed to show great promise in the context of acoustic long range predictions of SPLs from pile driving.

CONCLUSIONS AND PROSPECTS

A qualitative modelling of pile driving noise with the help of wavenumber integration is presented and its fundamentals are briefly discussed. To be able to verify the obtained results, an FE model is set up and, first, checked against simulations of Reinhall and Dahl, who identified the main characteristics in pile driving acoustics to be the occurrence of Mach cones. Then, an approach to model the same radiation with the help of parabolic equation modelling, put forward by the same authors, is carried out using wavenumber integration. The qualitative results of the FE and the WI model are compared and found to be in excellent agreement.

As the next step, the comparison of the results on a quantitative basis is planned. After this verification, a validation against extensive planned offshore measurements is envisaged. Therefore, the model is supposed to incorporate both rough boundaries and ambient noise, to account for the actual sea state and weather conditions during the measurements.

ACKNOWLEDGEMENTS

The authors gratefully acknowledge the funding of the BORA project by the Federal Ministry for the Environment, Nature Conservation and Nuclear Safety due to an act of the German Parliament (project ref. no. 0325421 A/B/C). Also, the support of this work by Jonas von Pein is gratefully acknowledged by the authors.

REFERENCES

- [1] Bundesministerium für Umwelt, Naturschutz und Reaktorsicherheit, *Das Energiekonzept der Bundesregierung 2010 und die Energiewende 2011*, 2011
- [2] W.L. Au and M.C. Hastings, *Principles of Marine Bioacoustics*, Springer, Berlin, 2008
- [3] Bundesamt für Seeschifffahrt und Hydrographie, *Leitsätze für die Anwendung der Eingriffsregelung innerhalb der ausschliesslichen Wirtschaftszone*, 2010
- [4] J.H. Stadler and D.P. Woodbury, "Assessing the effects to fishes from pile driving: Application of new hydroacoustic criteria", *Proceedings of Inter-Noise 2009*, Ottawa, Canada, 26-29 August 2009
- [5] F.B. Jensen, W.A. Kuperman, M.B. Porter and H. Schmidt, *Computational Ocean Acoustics*, 2nd edition, Springer, New York, 2011
- [6] H. Schmidt and G. Tango, "Efficient global matrix approach to the computation of synthetic seismograms", *Geophysical Journal of the Royal Astronomical Society* **84**, 331-359 (1986)
- [7] H. Schmidt, *Safari: Seismo-acoustic fast field algorithm for range-independent environments. User's guide*, SACLANTCEN Report no. SR113, Italy, 1988
- [8] A.V. Oppenheim and R.W. Schaffer, *Discrete-time signal processing*, Prentice Hall, 2007
- [9] F.R. Di Napoli and R.L. Deavenport, "Theoretical and numerical Green's function field solution in a plane multilayered medium", *Journal of the Acoustical Society of America* **67**, 92-105 (1980)
- [10] M. Abramowitz and I.A. Stegun, *Pocketbook of mathematical functions*, Verlag Harri Deutsch, Frankfurt, 1984
- [11] T. Lippert, S. Lippert, O. von Estorff, M. Milatz and K. Reimann, "Prediction of pile driving induced underwater noise", *Proceedings of the 19th International Congress on Sound and Vibration*, Vilnius, Lithuania, 8-12 July 2012
- [12] P.G. Reinhall and P.H. Dahl, "Underwater Mach wave radiation from impact pile driving: Theory and observation", *Journal of the Acoustical Society of America* **130**, 1209-1216 (2011)
- [13] E.L. Hamilton, "Geoacoustic modelling of the seafloor", *Journal of the Acoustical Society of America* **68**, 1313-1340 (1980)
- [14] A.J. Deeks and M.F. Randolph, "A simple model for inelastic footing response to transient loading", *International Journal for Numerical and Analytical Methods in Geomechanics* **19**, 307-329 (1995)
- [15] J. Herbst, *Zerstörungsfreie Prüfung von Abwasserkanälen mit Klopferschall*, PhD Thesis, Department of Mechanical Engineering, University of Karlsruhe, 2004
- [16] A.J. Deeks and M.F. Randolph, "Axisymmetric time-domain transmitting boundaries", *Journal of Engineering Mechanics* **120**, 25-42 (1994)

THE VIBRATIONS OF BUBBLES AND BALLOONS

Kirsty A. Kuo and Hugh E.M. Hunt

Faculty of Engineering, University of Cambridge, Trumpington St., Cambridge CB2 1PZ, UK

kan26@cam.ac.uk

Bubbles and balloons are two examples of structures that feature a pressure difference across the skin, a thin, tensioned membrane, and a doubly curved interface surface. While mathematical models have been formulated for bubble vibrations, no such model exists for balloon vibrations. This paper reviews a model of bubble vibrations, and compares its predicted natural frequencies and modeshapes to those of a rubber balloon. It is shown that the bubble model consistently underpredicts the balloon's natural frequencies, and it is concluded that the nonlinear elasticity present in the balloon skin accounts for this result.

INTRODUCTION

There are many examples of thin-walled, inflated shells in our lives – think of airbags, basketballs, tyres, eyeballs, soap bubbles and balloons. These objects may be toroidal, spherical, or some more generalised ovoidal shape, but they all have three features in common: a pressure difference across the skin; a thin, tensioned membrane; and a doubly curved interface surface. This means that for all of these systems, a common set of fundamental equations of motion will form the basis of a derivation of the vibration modes. Hence, once an analytical solution to the vibration of one of these systems (e.g. soap bubbles) has been obtained, theory can be extrapolated to aid in describing another of these systems (e.g. balloons). This is the approach taken in this paper to investigate the vibrations of balloons.

The wider context of this research is the dynamic modelling of high-altitude tethered balloons, which have attracted interest recently due to their potential uses in mobile communications, meteorology, energy harvesting and climate engineering. Recent papers on the dynamics of high-altitude tethered balloons [1-4] treat the balloon as a rigid body. The spherical or streamlined shape of the balloon affects the lift and drag forces, but it is assumed that the forcing from the tether does not result in balloon deformations. However, when the authors observed a 1m-diameter meteorological balloon tethered at 15m, a strong vibration coupling between axial excitation of the tether and ovaling deformations of the balloon was seen. This suggests that higher-order modes can be excited on tethered balloons.

In this paper, the balloon is assumed to have a spherical shape. This is the simplest balloon shape, and is a good approximation to the shape of meteorological balloons and small-scale high-altitude balloons. Streamlined aerostats that exhibit weather-vaning behaviour, and the pumpkin-shaped envelopes that are designed to reduce hoop stresses in large high-altitude balloons are considered beyond the scope of this paper.

A literature search on balloon vibrations revealed that no mathematical model had been specifically derived for balloons, so our attention turned to other inflated shells. Analogous studies of the vibration modes of thin-walled spherical shells were found, including those with application to inflatable

cushions [5], pneumatic tires [6], eyeballs [7], heart ventricles [8], soap bubbles [9-10] and basketballs [11]. These studies use a combination of one or more of analytical techniques, finite element analysis and experimental measurement to determine modeshapes and natural frequencies. Of all the inflated shells that were identified, soap bubbles had received the most attention in the modelling literature, and as they are of a similar spherical geometry to balloons, bubbles were chosen as the closest analogue for the purpose of studying the vibration modes and natural frequencies.

This paper describes a model of soap bubble vibrations, and compares the results of this model to the experimentally measured response of a rubber balloon. The calculated natural frequencies and modeshapes are compared, and conclusions regarding the suitability of this predictive model are made.

BUBBLE VIBRATIONS

The earliest analysis of the bubble vibration problem was performed by Rayleigh [12], in his study of the vibration of a liquid mass about a spherical figure. This analysis was extended by Lamb in 1895, in his book *Hydrodynamics* [13], to account for the surrounding fluid. Lamb's well-known solution describes a spherical bubble of one fluid (e.g. air) immersed within a second fluid (e.g. water), which is often described as a 'droplet'. Lamb begins by assuming an expression for the shape of the common surface, and then uses it to find the corresponding velocity potential and pressure at internal and external points. Using the Theorem for Solid Geometry and the expression for surface tension, he derives this closed-form solution for the natural frequencies ω_j of the bubble

$$\omega_j^2 = \frac{\sigma}{R^3} \frac{(j-1)j(j+1)(j+2)}{(j+1)\rho^+ + j\rho^-} \quad (1)$$

where σ is the surface tension, R is the radius, j is the mode number ($j = 1, 2, \dots$), ρ^+ is the fluid density inside the droplet, and ρ^- is the fluid density outside the droplet. (For an explanation of why $j \neq 0$, refer to the Comparison of Results section).

It was more than one hundred years later that a solution to the vibration of soap bubbles was formulated by Grinfeld [10]. Grinfeld's model includes the inertia of the bubble film,

thus representing a system that comprises three different fluids: the inner fluid, the film fluid, and the outer fluid. To derive this model, Grinfeld begins with the linearised form of Euler's equations governing inviscid flow

$$\frac{\partial v^i}{\partial t} = -\frac{1}{\rho} \nabla^i p \quad (2a)$$

$$\nabla_i v^i = 0 \quad (2b)$$

where v^i is the covariant component of the velocity fields, ρ is the surrounding fluid density (either ρ^+ or ρ^- depending on the domain) and p is the pressure. The momentum and velocity components in each of the three spherical coordinate directions are derived, and the condition that the ambient velocity field in the radial direction must be equal on either side of the bubble film is applied.

The equations for the dynamic behaviour of the bubble film are formulated using a Laplace capillarity model, and include interaction with the ambient air. The detailed formulation of these equations can be found in [14, 15]. For a fluid film with constant thickness, the linearised equation is

$$\tau_0 \frac{\partial^2 c}{\partial t^2} = \sigma (\nabla_\alpha \nabla^\alpha c + \frac{2}{R^2} c) + \left[\frac{\partial p}{\partial t} \right] \quad (3)$$

where τ_0 is the uniform equilibrium two-dimensional mass density of the film, c is the small component of the velocity field, $\nabla_\alpha \nabla^\alpha$ is the surface Laplacian, and the symbol $[p]$ denotes the jump in ambient pressure across the surface of the film.

Equations (2a), (2b) and (3) combine to give a dispersion relationship, which is solved to obtain the natural frequencies of the soap bubble

$$\omega_j^2 = \frac{\sigma}{R^3} \frac{(j-1)j(j+1)(j+2)}{j(j+1)\tau_0 R^{-1} + (j+1)\rho^+ + j\rho^-} \quad (4)$$

As the mass density of the film approaches zero, this equation is shown to reduce to Lamb's 'droplet' solution.

The modeshapes that correspond to these natural frequencies are proportional to the surface spherical harmonics, $Y_{jn}(\theta, \varphi)$, where the mathematical convention for spherical coordinates is adopted such that θ is the azimuthal angle, and φ is the polar angle. In orthonormal form, the surface spherical harmonics are made up of the following two expressions

$$\sqrt{\frac{2j+1}{2\pi} \frac{(j-n)!}{(j+n)!}} P_j^n(\cos \varphi) \cos n\theta \quad (5a)$$

$$\sqrt{\frac{2j+1}{2\pi} \frac{(j-n)!}{(j+n)!}} P_j^n(\cos \varphi) \sin n\theta \quad (5b)$$

where $P_j^n(\cos \varphi)$ are associated Legendre functions of the first kind of degree j and order n . The modeshapes for $j = 0, 1, 2, 3$ are illustrated in Figure 1, where the colouring indicates the amount of deflection in the radial direction. The modeshape corresponding to $j = 0$ is called the 'breathing mode', as it involves uniform radial extension over the entire sphere. The modeshapes corresponding to $j = 1$ represent the three orthogonal rigid-body modes.

To obtain the frequency-response function from the natural frequencies and mode shapes of the bubble, the general equation from Newland [16] can be used. The frequency-response function $H(\mathbf{z}_r, \mathbf{z}_s, \omega)$ of an undamped system, with output measured at location \mathbf{z}_r and subjected to a unit harmonic input force at location \mathbf{z}_s is given in Newland [16] as

$$H(\mathbf{z}_r, \mathbf{z}_s, \omega) = \sum_{j=0}^{\infty} \frac{U_j(\mathbf{z}_r) U_j(\mathbf{z}_s)}{\omega_j^2 - \omega^2} \quad (6)$$

where $U_j(\mathbf{z}_r)$ is the mass-normalised mode function of mode j , evaluated at \mathbf{z}_r . For the case of the vibrating bubble skin, the mass-normalised mode function is represented solely by the contribution of the membrane displacement in the radial direction, that is, the surface spherical harmonics. The mass-normalisation condition is expressed as

$$\lambda^2 \int_0^{2\pi} \int_0^\pi Y_{jn}(\theta, \varphi) \tau_0 R^2 d\varphi d\theta = 1 \quad (7)$$

where λ is the normalisation constant. The normalisation constant is found by numerically evaluating Eq. (7) in the modelling program. For comparison with the experimental results in the next section, the driving-point response of the bubble is to be evaluated at the south pole, that is, at $\mathbf{z}_r = \mathbf{z}_s = (a, 0, \pi)$. This means that only the axisymmetric modeshapes ($n = 0$) are excited, hence the response of the bubble is given by

$$H(\mathbf{z}_r, \mathbf{z}_s, \omega) = \sum_{j=0}^{\infty} \frac{\lambda^2 Y_{j0}(0, \pi) Y_{j0}(0, \pi)}{\omega_j^2 - \omega^2} \quad (8)$$

Having determined the frequency-response function for the vibrations of soap bubbles, we now turn our attention to the vibrations of balloons.

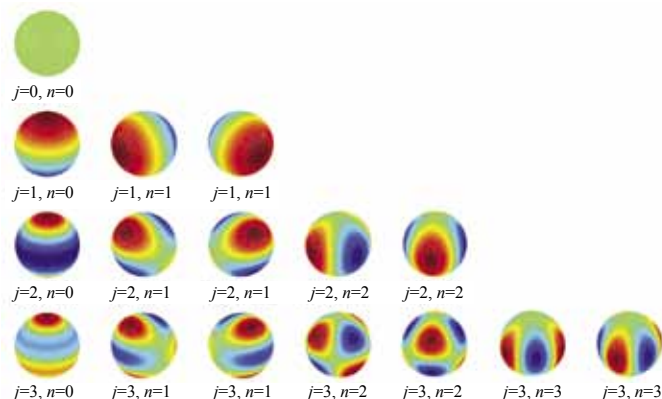


Figure 1. The spherical surface harmonics for $j = 0, 1, 2, 3$

BALLOON VIBRATIONS

There is no mathematical model for balloon vibrations in the literature, hence we embarked on a series of experiments to determine the natural frequencies and modeshapes of a large, spherical, helium-filled novelty balloon.

The natural frequencies were determined by measuring the driving-point frequency-response function of the balloon, using an impact hammer and a laser vibrometer. The impact hammer

was used to deliver an impulse to the base of the balloon, near the neck, and the laser beam was aimed at a piece of reflective tape positioned as close as possible to the impact point. The data from the impact hammer and the laser vibrometer were logged and analysed using a customised Matlab program. The experimental setup is shown in Fig. 2.

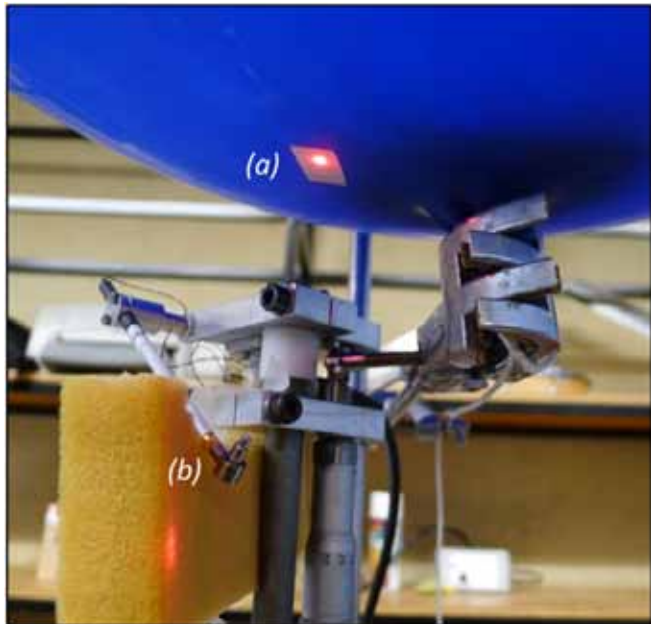


Figure 2. The experimental setup used to measure the balloon vibration modes, showing (a) the laser beam from the vibrometer, aimed at a piece of reflective tape near the base of the balloon; and (b) the impact hammer used to deliver an impulse to the base of the balloon.

The balloon is made of rubber latex, and has a design diameter of 1m, though was only partially inflated for ease of handling. The laser vibrometer is a Polytec OFV302 single-point vibrometer, connected through a Polytec OFV 3001 vibrometer controller. The velocity range is 1000mm/s/V and the velocity filter is set at 2.4kHz. The impact hammer is a miniature instrumented impact hammer, model PCB 086E80. The experimental parameters for this balloon are given in Table 1. The pressure in the balloon was measured by connecting the balloon to a U-tube manometer.

The balloon is very sensitive to disturbances in the surrounding air, and to minimise movement of the balloon it was restrained by a clamp on the neck, below the tie-off point. A total of 50 hammer impacts were used to calculate an averaged velocity frequency-response function. The major peaks of this frequency-response function represent the natural frequencies of the balloon, and the first eight peaks occur at 0.63Hz, 6.8Hz, 55.1Hz, 79.8Hz, 105Hz, 131Hz, 157Hz, and 185Hz. The coherence lies between 0.9 and 1.0 over the measured frequency range of 0Hz to 300Hz, hence the resonant behaviour of the balloon in this range is due to the hammer impact. Figure 3 shows the measured velocity frequency-response function of the balloon, as a function of frequency.

Also overlaid on Fig. 3 is the driving-point response

calculated using the mathematical model of the soap bubble, with the experimental parameters given in Table 1 being used as the input to this model. The surface tension for the soap bubble model is calculated by equating the outwards-acting force due to the internal pressure with the restoring force provided by the surface tension, such that

$$\sigma = \frac{\rho R}{2} \tag{9}$$

(Note that the surface tension in the soap bubble model is a factor of two larger than the surface tension acting in a droplet, as the bubble has two film surfaces as opposed to the one surface that separates the fluids in a droplet). The two-dimensional mass density of the film τ_0 is calculated as the balloon skin mass divided by the surface area of the balloon, $4\pi R^2$. The densities of the helium inside the balloon ρ^+ and the air outside the balloon ρ^- are calculated using the measured pressures and temperature, and the perfect gas law.

Table 1. Experimental parameters

Parameter	Value
Balloon radius	0.32m
Balloon skin mass	3.5×10^{-2} kg
Internal pressure (gauge)	1.27×10^3 Pa
Atmospheric pressure	1.03×10^5 Pa
Atmospheric temperature	291K

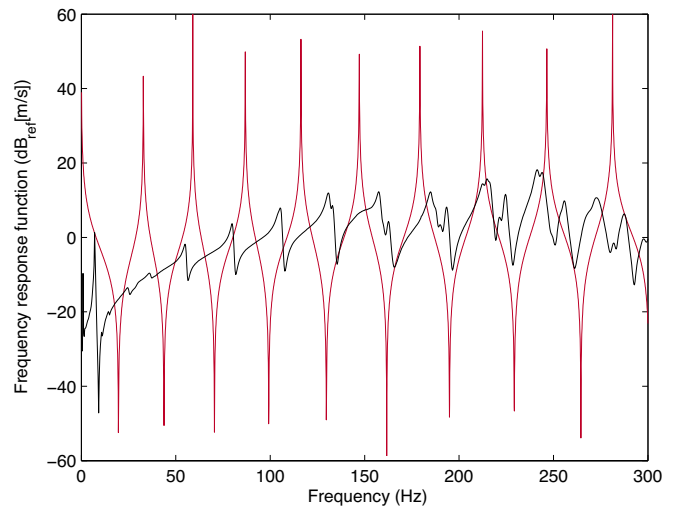


Figure 3. The experimentally measured driving-point response of the balloon is shown in black, and the red line shows the driving-point response predicted using the soap-bubble model, with the balloon parameters as inputs.

COMPARISON OF RESULTS

There are obvious differences between the experimentally measured response of the balloon and the response predicted using the soap-bubble model, and in this section we look at why these differences occur.

For both balloons and soap bubbles, it is reasonable to assume that the gas inside the balloon is incompressible, hence the volume of the sphere is constant and the $j = 0$ breathing mode at 0Hz is not expected to occur. This is consistent with the experimental observations, as no peak at 0Hz is observed.

The first peak in the experimental results occurs at 0.63Hz, and visual observation of the balloon indicates that this peak corresponds to a low-frequency, lightly damped, rigid-body rocking motion of the balloon about the clamp. The balloon was highly sensitive to air-flow disturbances caused by nearby movements, making it particularly difficult to avoid excitation of this mode. As the bottom restraint of the balloon is not included in the soap-bubble model, there is no equivalent natural frequency seen in the predictions of the mathematical model.

The second peak in the experimental results occurs at 6.8Hz, and visual observation of the balloon indicates that this peak corresponds to the theoretical $j = 1$ mode: vertical rigid-body translation of the balloon's centre of mass. Although the soap-bubble model predicts that this occurs at 0Hz, the peak has been shifted slightly. This is because the balloon's neck and the low-tension material at the base of the balloon are acting together as a 'spring' that separates the balloon from the clamp.

To investigate the modeshapes that occur at higher frequencies, the balloon was excited acoustically using an amplifier and speaker system at a pure tone that matched each of the natural frequencies. Visual and tactile observation of the balloon's vibrations indicated that the 55.1Hz mode has two latitudinal nodal lines, arranged identically to the $j = 2, n = 0$ modeshape shown in Figure 1. This suggests that the natural frequency at 55.1Hz is due to the $j = 2$ modeshape. The number of latitudinal nodal lines was observed to increase linearly as the pure tone was matched to the higher natural frequencies: three nodal lines at 79.8Hz ($j = 3, n = 0$), four at 105Hz ($j = 4, n = 0$), and five at 131Hz ($j = 5, n = 0$).

There is a discrepancy between the modelling predictions and the experimental results at these higher frequencies, with the mathematical model consistently underpredicting the natural frequencies of the balloon. The reason for this is believed to be elasticity which is present in the balloon skin, but not accounted for in the bubble model. Grinfeld's bubble model assumes that the bubble film is inelastic, as fluids have a constant value of surface tension, and thus there is no capacity for elastic energy to be stored in the skin during inflation or bubble deformation. The balloon, however, is made of a viscoelastic material that stretches as it inflates and undergoes changes in geometry.

The effect of skin elasticity on the natural frequencies can be evaluated using energy methods. Rayleigh's quotient is a means of approximating natural frequencies, and is based on equating the kinetic and potential energy of vibration, assuming negligible energy loss per cycle, that is, a lightly damped system [17]. The skin elasticity can be incorporated into Rayleigh's quotient by the addition of an extra potential energy term in the numerator. (Note that this extra potential energy term is only relevant for those modes that involve deformation from the spherical 'equilibrium' geometry, and thus only occur for $j \geq 2$). This additional term results in an

increase in the natural frequencies, thus predicting that the natural frequencies of the elastic balloon will be greater than those of a soap bubble with constant surface tension when $j \geq 2$. This is consistent with the results presented here.

It can be seen in Fig. 3 that as the frequency increases, the major peaks in the balloon's driving point response begin to separate into clusters of closely-spaced peaks. This separation is due to the inhomogeneity of the balloon, which has a more pronounced effect on higher frequencies as the modal displacement variation occurs over shorter distances. Inhomogeneity exists in the shape of the balloon, the thickness of the balloon skin, and the surface tension in the balloon skin.

CONCLUSIONS

Bubbles have been well-studied in fluid-mechanics literature, and a mathematical model exists for predicting their natural frequencies and modeshapes. These natural frequencies depend on fluid properties and geometry, and the modeshapes correspond to the spherical surface harmonics. There is no mathematical model for balloon vibrations in the literature, and this paper has shown that the bubble model consistently underpredicts the natural frequencies observed for a balloon. This underprediction is due to the elasticity that is present in the balloon skin, but neglected from the bubble model. Work is currently underway to formulate an analytical solution for the natural frequencies of a spherical, elastic membrane with internal and external fluid interactions.

ACKNOWLEDGEMENTS

The authors would like to thank Professor J. Woodhouse and Professor C.R. Calladine FRS of the University of Cambridge Department of Engineering and Professor J.R. Lister of the University of Cambridge Department of Applied Mathematics and Theoretical Physics who provided valuable comments on this research. This work has been funded by the Engineering and Physical Sciences Research Council UK, reference EP/IO1473X/1.

REFERENCES

- [1] G.S. Aglietti, "Dynamic response of a high-altitude tethered balloon system", *Journal of Aircraft* **46**(6), 2032-2040 (2009)
- [2] K.A. Stanney and C.D. Rahn, "Response of a tethered aerostat to simulated turbulence", *Communications in Nonlinear Science and Numerical Simulation* **11**, 759-776 (2006)
- [3] C. Lambert and M. Nahon, "Stability analysis of a tethered aerostat", *Journal of Aircraft* **40**(4), 705-715 (2003)
- [4] P. Coulombe-Pontbriand and M. Nahon, "Experimental testing and modelling of a tethered spherical aerostat in an outdoor environment", *Journal of Wind Engineering and Industrial Aerodynamics* **97**, 208-218 (2009)
- [5] L.E. Penzes and H. Kraus, "Free vibration of an inflated oblate spheroidal shell", *Journal of Sound and Vibration* **27**(4), 559-572 (1973)
- [6] L.E. Kung, W. Soedel and T.Y. Yang, "Free vibration of a pneumatic tire-wheel unit using a ring on an elastic foundation and a finite element model", *Journal of Sound and Vibration* **107**(2), 181-194 (1986)

- [7] L. Coquart, C. Depeursinge, A. Curnier and R. Ohayon, "A fluid-structure interaction problem in biomechanics: prestressed vibrations of the eye by the finite element method", *Journal of Biomechanics* **25**(10), 1105-1118 (1992)
- [8] A. Singer, "Computed ventricular acoustic frequency", *Bulletin of Mathematical Biophysics* **29**, 465-471 (1967)
- [9] G. Rämme, "Modelling the atom by rotating and vibrating soap bubbles", *Physics Education* **29**, 313-318 (1994)
- [10] P. Grinfeld, "Small oscillations of a soap bubble", *Studies in Applied Mathematics* **128**(1), 30-39 (2012)
- [11] D. Russell, "Basketballs as spherical acoustic cavities", *American Journal of Physics* **78**(6), 549-554 (2010)
- [12] L. Rayleigh, "On the capillary phenomena of jets", *Proceedings of the Royal Society of London (1854-1905)* **29**(10), 71-97 (1879)
- [13] H. Lamb, *Hydrodynamics*, Dover Publications, New York, 1993
- [14] P. Grinfeld, "Exact nonlinear equations for fluid films and proper adaptations of conservation theorems from classical hydrodynamics", *Journal of Geometry and Symmetry in Physics* **16**, 1-21 (2009)
- [15] P. Grinfeld, "Hamiltonian dynamic equations for fluid films", *Studies in Applied Mathematics* **125**, 223-264 (2010)
- [16] D.E. Newland, *Mechanical Vibration Analysis and Computation*, Dover Publications, Inc. Mineola, 1989

ACOUSTICS 2013 VICTOR HARBOR

Science, Technology and Amenity

**VICTOR HARBOR, SOUTH AUSTRALIA
NOVEMBER 17-19, 2013**

THEME

ACOUSTICS 2013, the annual conference of the Australian Acoustical Society, will be held in Victor Harbor, South Australia, at the McCracken Country Club, from 17-19 November 2013.

With its theme of Science, Technology and Amenity, Acoustics 2013 Victor Harbor will include plenary sessions addressing the impact of science and technology on acoustics and amenity, whether it be environmental or internal spaces. Other major streams will address airport / road / railway noise, standards and guidelines including those from EPAs, underwater acoustics, marine bioacoustics and vibration.

Acoustics 2013 Victor Harbor will provide in-depth coverage of many topics of interest to professionals in related fields including educationalists, consultants, planners, developers, government authorities, and EPA/noise officers

VENUE

Acoustics 2013 Victor Harbor will be held at the McCracken Country Club. The 4.5 star McCracken Country Club offers guests luxurious accommodation in the beachside township of Victor Harbor. The country club highlights are its golf course, day spa and the gorgeous panoramic view of Hindmarsh Valley. Visit www.countryclubs.com.au/mccracken/

For up-to-date information regarding the Acoustics 2013 Victor Harbor conference, please visit the conference website:
www.acoustics.asn.au/joomla/acoustics-2013.html

TOPICS

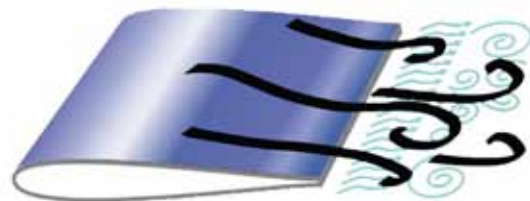
In addition to the main conference themes, Acoustics 2013 Victor Harbor will include sessions on:

- Environmental acoustics
- Industrial acoustics
- Wind turbine noise
- Low frequency noise
- Internal spaces and amenity
- Architectural acoustics
- Underwater acoustics
- Marine bioacoustics
- Legislation and standards
- Transportation noise

WORKSHOPS

A series of workshops are planned. The following workshop will be held:

- Flow induced noise



THE SOUND OF MUSIC: ORDER FROM COMPLEXITY

Neville H. Fletcher

Research School of Physics and Engineering, Australian National University, Canberra, ACT 0200

neville.fletcher@anu.edu.au

Musical and biological sounds have the property of being well organised and usually strictly harmonic in spectrum, though there are a few notable exceptions such as the shimmering crash of a cymbal or the cry of the sulphur-crested cockatoo. It turns out, however, that this apparent simplicity is constructed by the interaction of highly nonlinear feedback generators linked to resonators whose vibrational modes are not in simple harmonic frequency ratios. This paper explores the way in which this apparent simplicity emerges from complex interactions in the generation of instrumental sound and in the songs of humans and other animals.

INTRODUCTION

Musical instruments such as violins, flutes and trumpets are designed to produce sounds that are pleasing to our ears, and analysis shows that these sounds, when played steadily, have exact harmonic spectra. This leads to the expectation that we might hear smooth concords between notes whose frequencies are in simple integer ratios, as is indeed found. This seems to imply that everything about these instruments is simple and linear, but this is very far from being the case. Indeed nonlinearity is essential to produce these apparently simple results. But sometimes nonlinearity takes control, as in cymbals and gongs, giving rise to effects such as pitch glide, subharmonics, and transitions to chaotic vibration. Very much the same is true of the sounds produced in human speech and singing and, more noticeably, in the songs of birds, where we encounter almost pure tones, harmonic spectra, and even chaotic screeches. In this short paper we explore the physics and mathematics underlying this behaviour. The subject has been discussed in more detail by Fletcher and Rossing [1] (chapter 5) and by Fletcher [2, 3, 4] and in less technical form by Backus [5] and by Johnston [6].

IMPULSIVELY EXCITED INSTRUMENTS

Musical instruments came in two types: those that produce steady sustained sounds, such as violins and trumpets, and those that are sharply excited and produce transient sounds, such as plucked strings, bells and gongs. In the first case there is a continuous input of energy and some sort of feedback oscillation is generated, while in the second there is an initial impulse after which the energy stored in the system gradually decays because of internal and radiation losses. In both cases the vibrating system is geometrically extended, whether it be a taut string, a column of air, or a carefully shaped plate or shell, so that it has many possible vibrational modes, and it is the interplay of these modes that controls the sound that is produced.

It might be thought that an elastic string held under tension between two rigid supports is an ideally simple system, but is it really? The “standard theory” treats the string as being ideally thin and the vibration amplitude as being planar and infinitesimal, but none of these assumptions holds in practice.

Instead, even for planar oscillation, the string motion is described by an equation of the form

$$m \frac{\partial^2 z}{\partial t^2} \approx T \frac{\partial^2 z}{\partial x^2} + AEd^4 \frac{\partial^4 z}{\partial x^4} + \frac{BE d^2}{L} \left[\int_0^L \left(\frac{\partial z}{\partial x} \right)^2 dx \right] \frac{\partial^2 z}{\partial x^2} \quad (1)$$

where z is string the displacement at point x , L is the string length, m is the string mass per unit length, and T the string tension. The first term on the right-hand side is that for an ideal string, the second term is the restoring force due to string stiffness, which is proportional to its Young’s modulus E and the fourth power of string diameter d , while the third term is an approximation to the extra tension produced by displacement of the string from a straight line. The stiffness term stretches the mode frequencies so that of the n th mode becomes

$$f_n \approx n f_1 (1 + \alpha n^2) \quad (2)$$

where α is proportional to the ratio of string stiffness to string tension. In the steel strings of the piano this causes a pitch stretch of about half a semitone over the complete keyboard compass because octaves are tuned to match the second harmonic of the octave below.

In a string with inadequate initial tension, plucked with large amplitude, the third term in equation (1) leads to an unpleasant effect in which the tension, and therefore the musical pitch, starts high and then gradually falls. This is avoided by tightening strings to almost their breaking point. The third term also introduces harmonic distortion, so that an initial simple vibration at f_1 generates another vibration at $2f_1$ and so on, or mixes the frequencies of two existing modes. As if this were not enough, the vibrational tension of the third term in equation (1) also excites longitudinal waves in the string, and these couple the transverse modes in the z direction to orthogonal modes in the y direction [7]. And all this is not just mathematics — the effects contribute significantly to the actual sound of a piano! Some piano makers, notably Wayne Stuart in Newcastle Australia, have changed the exact form of the pinning of the strings in their instruments to control some of these effects, but I am not aware of any scientific study of the results, which could well be concealed by other changes in the design anyway. The whole behaviour of piano strings is

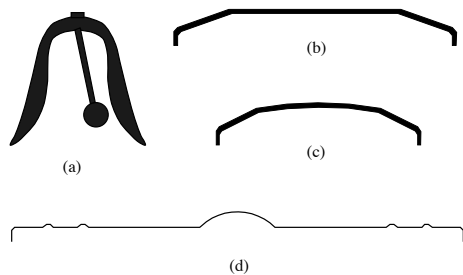


Figure 1. Profiles of (a) a church bell, (b) a flat-centre Chinese Opera gong, (c) a curved-centre Chinese Opera gong, and (d) an orchestral tam-tam

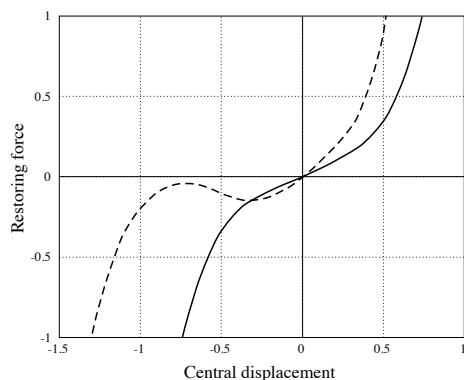


Figure 2. Restoring force as a function of deflection for a flat circular plate pinned at its edges (full curve) and for a slightly curved plate of the same size (broken curve). The units shown are arbitrary

further complicated by the fact that they mostly occur in pairs or triplets for each note, and the strings for a given note interact with each other through the non rigid bridge over which they pass. Weinreich [8] has treated this complication in detail and shown many interesting consequences.

Many musical instruments of the impulsive or percussive variety do not rely primarily on tension, as does the string, but rather on elastic stiffness. The simplest are bells, which have very thick walls, as shown in Figure 1(a), and are almost completely linear in behaviour. The tuning of the modes of such complex shapes is not simple, however. Church and carillon bells are cast to traditional shapes and then adjusted by removing material internally so that the frequencies of their principal modes are in simple integer ratios, giving pleasant musical sounds, one of the characteristics however being a low-pitched musical minor third, with frequency ratio 6/5 relative to the 'prime' or dominant mode, and it is this that gives bells their characteristic sound [1]. Many Eastern bells or gongs, such as the Javanese gamelan, are not tuned in this way however, and this gives rise to musical scales that are quite different from the familiar Western ones [9].

Gongs are another form of percussive instrument, but here the metal shell is thin compared to its diameter, as shown in later panels of Figure 1, so that tension effects become noticeable or even dominant. One very impressive effect is that achieved in Chinese opera gongs, of which there are two types. In the larger gong, shown in Figure 1(b), the main vibrating element in the centre of the gong is quite flat so that any vibration stretches it radially and raises both the tension

and the vibration frequency, as shown by the full curve in Figure 2. As the vibration decays, the pitch falls towards its small-amplitude value over a time of the order of one second. In the smaller gong shown in Figure 1(c), the central portion is slightly domed to a height of about 1 mm over its 10 cm diameter. The tension forces are thus initially compressive for small downward motion of the dome before becoming tensile when the displacement exceeds twice the dome height, though the stiffness maintains a restoring force as illustrated by the dashed curve in Figure 2. For vibrations of moderate amplitude this causes the frequency to rise as the vibration decays, producing a sound that is complementary to that of the larger gong [10].

Sharp changes in shape are important here, since the tension term in equation (1) then acts at an angle and becomes converted in part to a lateral force, generating modes at two and three times the frequency of the original because of further coupling to the original exciting mode slope [11]. The nonlinearity thus leads to a progressive transfer of vibrational energy from low to high modes, an effect that is particularly noticeable in the large Chinese tam-tam gong often used in orchestras, which has two rings of sharp bumps in its outer profile, as shown in Figure 1(d). It is struck with a soft hammer and the low-frequency initial sound becomes transformed over a period of a second or so into a shimmering high-pitched sound that is actually chaotic [12]. Indeed simple experiments with metal gongs or cymbals of simpler shape show that when vibrated at their centre they can display energy transfer to higher harmonics of the exciting frequency, subharmonic generation at frequencies as low as one-fifth of the exciting frequency, or a transition to chaotic oscillation, depending upon minor variations in the exciting frequency. In normal musical playing, of course, cymbals are supported at their centre and driven by a sharp asymmetrical impact, so that essentially all modes are sharply excited. Mode interaction and transitions of the kind discussed above then lead to a wide-band 'shimmering' sound.

SUSTAINED-TONE INSTRUMENTS

Sustained-tone instruments are very different in operation from their impulsive cousins, and each consists of a system of the type shown in Figure 3. The resonant system is normally driven at a sufficiently low level that it is essentially linear in behaviour, with all the nonlinearity being contained in the active driver, the operation of which is controlled by feedback from the resonator. If the driver were linear, then it would simply maintain all the resonant modes of the string (for violin-type instruments) or the air column (for woodwind and brass instruments) at their natural frequencies, which are never in exact integer ratios because of stiffness and end-pinning effects in strings and geometric irregularities and the radiation end-correction in wind instruments. It is clear, therefore, that the nonlinearity of the feedback-driven oscillator must somehow be responsible for producing the exact harmonics observed in the sounds of these instruments. How does this occur?

First let us look at why the driving oscillator is nonlinear. In the case of a string driven by a bow, which consists of

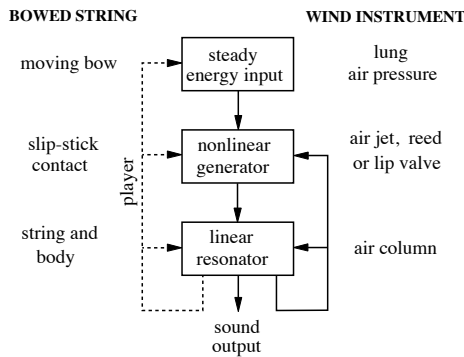


Figure 3. System diagram for a sustained-tone instrument consisting of a feedback-excited nonlinear oscillator coupled to a multi-mode linear resonator. Additional low-frequency control feedback is provided by the performer in the case of a musical instrument

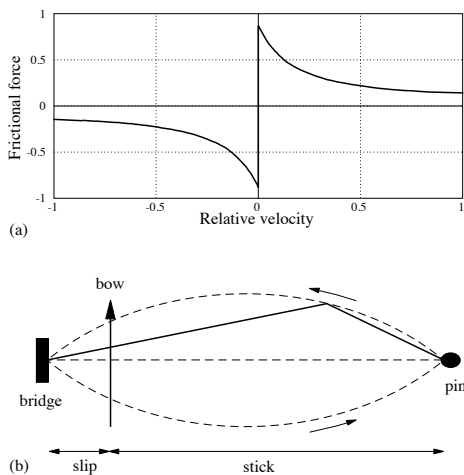


Figure 4. (a) Frictional force of a bow as a function of the velocity of the string relative to that of the bow. Units are arbitrary (b) Motion of the string for bowing in the position and direction shown, the kink moving around the broken curve

hairs coated with rosin, the static friction is very high so that the string essentially sticks to the bow and is drawn sideways. Ultimately, however, the restoring force due to tension exceeds the static frictional force and the string begins to slip. Because sliding friction is much smaller than static friction, as shown in Figure 4(a), the string then slips almost unimpeded until it reaches the farther extreme of its motion, when it is again captured by the bow and the cycle repeats [13, 14]. The envelope of the string motion is shown in Figure 4(b), with the slope discontinuity moving with uniform velocity between two parabolic envelope curves. The string itself does not radiate appreciable sound, but it passes over a bridge support at one end and its varying slope at this point produces an excitation force that is passed on to the body of the instrument. The vibrational response of the instrument body is linear, but is modified by its own resonances, so that the spectrum of the radiated sound depends both upon the string excitation and the instrument body response.

The structure of a woodwind reed instrument such as the clarinet is illustrated in Figure 5(a). For such an instrument, the generator consists of a valve with a fixed aperture covered by a thin cane reed that is partially open in its rest state. Because the

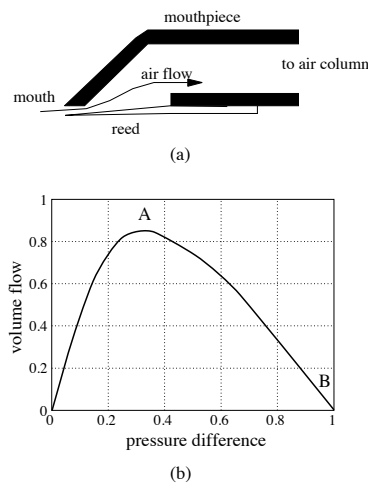


Figure 5. (a) Geometry of the mouthpiece and reed of a clarinet (b) Volume flow through the reed aperture as a function of the pressure difference across the reed. The effective resistance is negative in the region AB

natural vibration frequency of the reed is much higher than that of the note being played, a quasi-static analysis shows what is going on. Initially the volume flow through the reed increases as the pressure difference p across it is increased, conservation of energy dictating that the flow velocity is proportional to the square root of the pressure difference (Bernoulli's law). However the pressure difference also tends to progressively close the reed opening, so that the overall volume flow U has the form

$$U(p) = \begin{cases} \alpha p^{1/2}(1 - \beta p) & \text{if } p < \beta^{-1} \\ 0 & \text{if } p > \beta^{-1} \end{cases} \quad (3)$$

where α and β are constants. This relation is shown in Figure 5(b), and it can be seen that the valve impedance dp/dU is very nonlinear and is negative in the range A to B, which is what allows the valve to act as an acoustic generator. This will work, though with somewhat more complex analysis, at all frequencies up to the free resonance frequency of the reed itself. The constricted double reed of an oboe has an even more complicated flow behaviour because of the flow constriction caused by its narrow channel.

When we consider lip excited brass instruments, the situation is rather different because the lip aperture is blown open by the pressure differential, rather than being blown closed. This complicates the behaviour, and valve oscillations can be maintained only at a frequency just above the natural vibration frequency of the lips, the phase shift again making the resistance negative in this region, at least in a simple model [1, 15]. Because trumpets and trombones are often played very loudly, this is the one case in which the resonator can become nonlinear, leading to distortion of the propagating wave in the cylindrical part of the bore and consequent transfer of acoustic energy from low to high-frequency modes and even to shock waves [16].

Finally, consider instruments such as flutes and organ pipes that are excited by a planar air jet blown across an aperture near one end of the pipe as shown in Figure 6(a). The physics of this jet excitation is rather complicated [1, 17], but essentially the jet is acted on by the acoustic flow through the aperture and this generates a displacement wave that travels along the

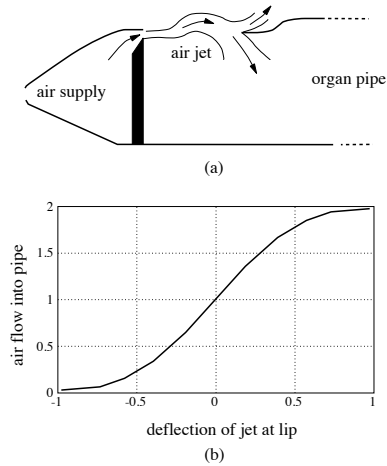


Figure 6. (a) Geometry of the mouth of an organ flue pipe. Waves are excited on the jet by acoustic flow through the mouth of the pipe and grow in amplitude as they propagate towards the pipe lip (b) Flow into the pipe mouth as a function of jet deflection at the lip. Units are arbitrary

jet at about half its airspeed. The jet then blows alternately into and out of the pipe where it meets the other edge of the aperture. The phase shift introduced by the initial excitation and the travel time of the displacement wave along the jet makes the flow resistance negative over a limited frequency range, thus allowing the player to choose which mode of the pipe resonator is being excited. For displacements that are small compared with the jet width, the inflow is linearly related to the excitation, but for larger displacements the flow saturates, as shown in Figure 6(b), generating odd harmonics of the fundamental. If the jet centre-plane is offset with respect to the edge, then the flow waveform becomes asymmetrical and even harmonics are generated as well [18]. These air-jet excited instruments are one of the few cases in which the transition to mode-locked harmonic sound has been studied, as will be discussed in the next section.

FORMAL ANALYSIS

Now that the origins of inharmonicity on the resonator and of nonlinearity in the generator have been explained, it is possible to proceed with a formal analysis of the behaviour of the musical instrument system shown in Figure 3. There are many ways in which this can be done, but one of the simplest is in the frequency domain where one examines the combined response of the resonator modes coupled to the generator using the method of slowly varying parameters [1].

For simplicity, consider first just the case of a single vibrational mode

$$y_n(t) = a_n \sin(\omega_n t + \phi_n) \quad (4)$$

and allow that both the amplitude a_n and the phase ϕ_n may vary with time slowly compared with ω_n . Suppose that, in the system considered, y_n satisfies the equation

$$\ddot{y}_n + \omega_n^2 y_n = g(y_n, \dot{y}_n, t) \quad (5)$$

where the dots signify differentiation with respect to time and the nonlinear function g represents the excitation provided by

the generator under the influence this mode. Substitution of equation (4) into equation (5) gives a complicated result, but this can be simplified if we assume that

$$\dot{y}_n = a_n \omega_n \cos(\omega_n t + \phi_n). \quad (6)$$

This assumption requires that

$$\dot{a}_n \sin(\omega_n t + \phi_n) + a_n \dot{\phi}_n \cos(\omega_n t + \phi_n) = 0, \quad (7)$$

but substituting equations (4), (6) and (7) into equation (5) then leads to the simple results

$$\dot{a}_n = \frac{g}{\omega_n} \cos(\omega_n t + \phi_n) \quad (8)$$

$$\dot{\phi}_n = -\frac{g}{a_n \omega_n} \sin(\omega_n t + \phi_n), \quad (9)$$

where g is expressed in terms of y_n and \dot{y}_n as given by equations (4) and (6).

These two equations (8) and (9) allow us to calculate the steady mode amplitude a_n for which $\dot{a}_n = 0$ and also the steady vibrational frequency $\omega_n + \dot{\phi}_n$, which will generally be different from the resonant frequency ω_n . The whole analysis can also be extended to treat the realistic case of a multi-mode system in which the modes interact because of the nonlinearity of the generator. It can be shown that this interaction leads to the locking of all the mode oscillations into an exactly harmonic (integer frequency ratio) distribution provided the natural mode frequencies are not too distant from this relationship initially [19]. If two prominent modes ω_i and ω_j are very far from integrally related in frequency, as can happen with peculiar fingerings of woodwind instruments, then the resulting oscillation may involve both of them, and the system nonlinearity will produce a “multiphonic” sound containing all frequencies $m\omega_i \pm n\omega_j$ where m and n are integers. These sounds are exploited in certain modern musical compositions for woodwinds [20].

This analysis can also be applied to transient sounds in which the generating function g depends upon time. An obvious example is the case of impulsively excited instruments, but the initial transient is also of great importance in defining the character of sustained-tone instruments, psychoacoustical studies showing that it is largely the initial transients that characterise the identity of a musical instrument, since identity is lost to the hearer if these are removed. This feature is also of great importance in the electronic synthesis of realistic musical sounds.

If the excitation begins abruptly, as is the case at the beginning of a musical note, then this stepwise or even impulsive excitation will excite all the modes of the instrument to vibrate at their natural frequencies, which are never in exact harmonic relationship, and it is only after a significant time, typically ten or more cycles of the fundamental, that the mode frequencies are captured by the nonlinearity in the way discussed above and locked together to produce an exactly harmonic sound. This transition has been examined in detail in the case of organ pipes [21] and an example of the calculated results is shown in Figure 7. The pipe modes, which are not in exactly harmonic relationship, are initially all excited in-phase by the jet impulse. Interaction between the modes

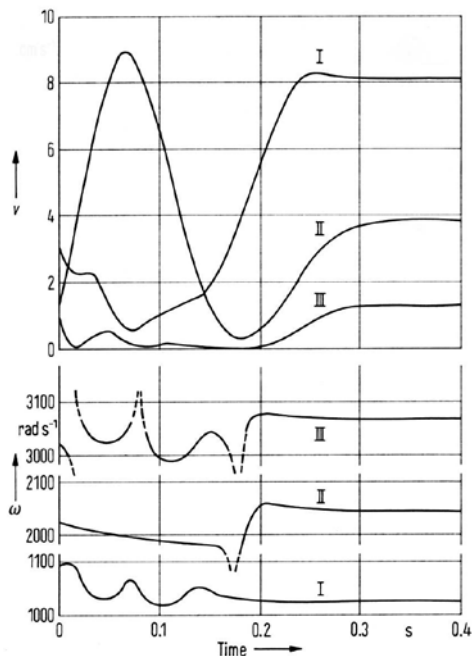


Figure 7. Evolution of the velocity amplitudes and frequencies of the first three modes of an organ pipe as calculated from equations (8) and (9) and a detailed model of wave propagation on the air jet and its interaction with the pipe air-column [21]

through the nonlinear behaviour of the jet then causes both mode amplitudes and frequencies to evolve to a stable harmonic relationship — a typical example of the emergence of order through complex interactions.

ANIMAL SOUNDS

As in musical instruments, the sounds produced by animals can be divided into two classes — those in which the excitation is essentially impulsive and those in which it is continuous — but the division is not so clear since many quasi-continuous insect sounds are really prolonged sequences of impulsive sounds. Once this is recognised, much of the analysis applied to musical systems can also be applied to biological systems [2, 3].

The simplest systems, which are employed largely by water-dwelling crustaceans such as crabs, produce sounds that are just sequences of clicks. This is done by snapping together or flicking apart two body parts that are covered by a stiff elastic shell. Because the shell generally covers some sort tissue, the sound is abruptly damped and has little if any tonal component. In air-dwelling insects such as crickets this system has evolved so that a file containing many teeth, and generally located on a leg, is drawn rapidly across a resonant structure such as a wing. While this bears some resemblance to a bowed string, the damping is again such that the oscillation produced by the impact of each tooth has almost dissipated before the next impact occurs. Since the pic on the structure must slip off the tooth each time, however, there is some chance that these releases will be phase-locked to the vibration, perhaps giving harmonic relations. The loudest insect of all, the cicada, makes its sounds by the rhythmic collapse and release of thin ribbed plates, or tymbals, that cover a large resonant abdominal cavity, giving a rapidly pulsating song near its characteristic frequency,

which ranges from about 600 Hz to above 3 kHz depending upon the species. From the point of view of the present chapter, there is nothing very interesting about these sounds.

The more interesting sounds from the present viewpoint are those produced by air-breathing animals, including birds and humans. These are generally sustained sounds, like the vowels in human speech, punctuated by impulsive or chaotic sounds like the consonants. The vowel-like sounds are produced by a vibrating valve, rather like a tiny pair of human lips, located between the lungs and the mouth. In the case of most mammals, including humans, this valve is near the top of the trachea or wind-pipe near its junction with the mouth, while in birds it is near the base of the trachea. In the case of songbirds there are actually two vocal valves, one in each of the bronchi or tubes leading from the lungs just below their junction with the trachea, allowing them to sing two notes at once if they choose to do so. This structure is known as the syrinx.

In humans, other mammals and many birds the vibration frequency of the vocal valve is below the frequency of the first resonance of the vocal tract, so that there is not the same sort of coupling between the source and the resonant filter provided by the upper vocal tract. Indeed it is reasonable to model these systems as an autonomous vibrating valve producing a pulsating airflow that is rich in harmonics because the valve ordinarily closes once in each cycle, coupled to the upper vocal tract which then provides an adjustable filter that modifies the spectral envelope of the sound to produce distinctive patterns that we know as vowels, each being characterised by maxima in its spectra, known as formants, close to the tract resonance frequencies. This is called the ‘source-filter model’. Only in high soprano singing does the fundamental pitch approach the frequency of one of the higher vocal tract resonances, and there is then a coupling between the two which gives a comparatively pure tone and reduces the distinction between different vowels. Something similar happens in the case of pure-tone songbirds as is discussed below.

While humans can make a pure-tone sound by whistling, involving an air jet and the mouth as a Helmholtz resonator, some birds can produce similar nearly pure-tone songs that are swept over a large frequency range, but they do not do it by whistling. Their vocal tract is connected to an elastic part of the upper esophagus, leading to the stomach, and this can be expanded to produce a quite large vocal cavity of adjustable size. Once again the pitch of the song is adjusted largely by changing the volume of this cavity [22]. Some animals, such as doves and frogs, can even produce pure-tone songs with their beak or mouth closed, a feat which they perform by inflating a vocal sac in the throat with very thin skin surrounding it and exhaling into this through their vibrating vocal valve, which they tune to the resonant frequency of the sac volume loaded by its vibrating walls. In the second or so that the call lasts, the volume of the inflated sac does not change greatly, and the small change is compensated for by the thinning of the walls.

Another interesting case is the very loud cry of the sulphur-crested cockatoo (*Cacatua galerita*). This harsh sound is at odds with the beauty of the bird, but accords well with its destructive behaviour! The interesting thing is that, when the waveform of the recorded cry is examined closely, it is

found to be truly chaotic with a Lyapunov exponent of about 0.3 [23]. The great loudness of the screech is partly explained by its frequency, which covers a broad band from about 2 to 4 kHz where human hearing is most sensitive, but the bird also invests a considerable effort in producing it. The anatomical and physiological basis of this cry (one hesitates to call it a song!) has not yet been established, but it seems likely that the vocal valve, or syrinx, has an extended flap-like structure that can move chaotically like a flag flapping in the wind, even though it is probably secured all around its periphery.

Finally we should mention the interesting combination of vocal and instrumental sounds that is sometimes used in the Australian didjeridu, or yidaki as it is called by the Yolngu people of Arnhem Land who perhaps originated the instrument [24]. The didjeridu consists of a simple tube, about 1.5 m long and 30 to 50 mm in diameter, cut from a small tree trunk that has been hollowed out by termites. The drone sound, typically at about 60 Hz, is made by buzzing the lips as in a brass instrument, and this is accompanied by a full range of upper harmonics. The interesting tonal sounds characteristic of the didjeridu are then made by varying the geometry of the vocal tract, again largely by moving the tongue, so as to produce spectral peaks or formants not unlike those in speech, the emphasised frequencies being those lying close to a minimum in the vocal tract impedance as seen from the lips [25, 26]. Even more interesting in the present context are the sounds that can be made by simultaneously vibrating the folds of the vocal valve, as when singing a note of frequency ω , and also the lips, under the control of the fundamental didjeridu resonance at frequency ω_0 . Since the two vibrating valves are in series, their effect is multiplicative rather than additive, and the resulting flow contains frequencies $m\omega_0 \pm n\omega$ [27]. Thus if the player vocalises a note a musical fifth above the drone fundamental, so that $\omega = (3/2)\omega_0$, then the nonlinearity of the combined valves will produce a subharmonic at frequency $\omega_0/2$, together with all its harmonics. For the singing of more complex sounds, there will be a large variety of frequencies produced.

CONCLUSIONS

In this short paper there has been time only to glance briefly at some of the interesting features of sound production in musical and biological systems. While the systems themselves consist of complex interacting nonlinear elements, the interesting outcome is that these often act together to produce a deceptively simple outcome, with strictly harmonic waveforms and well controlled behaviour. There are a few interesting exceptions, however, and these will doubtless repay detailed study some time in the future.

The work described in this paper has been carried out by many researchers around the world, and the literature documenting it is voluminous. The references I have cited are largely to work with which I have been personally associated, a fault for which I should perhaps apologise.

REFERENCES

[1] N.H. Fletcher and T.D. Rossing, *The Physics of Musical Instruments* second edition, Springer-Verlag, New York (1998)
 [2] N.H. Fletcher, *Acoustic Systems in Biology* Oxford University Press, New York (1992)

[3] N.H. Fletcher, "Acoustic systems in biology: from insects to elephants" *Acoustics Australia* **33**, 83–88 (2005)
 [4] N.H. Fletcher, "The nonlinear physics of musical instruments" *Reports on Progress in Physics* **62**, 723–764 (1999)
 [5] J. Backus, *The Acoustical Foundations of Music* W.W. Norton, New York (1969)
 [6] I. Johnston, *Measured Tones: The Interplay of Physics and Music* (second edition) Institute of Physics Publishing, Bristol (2002)
 [7] P.M. Morse and K.U. Ingard, *Theoretical Acoustics* McGraw-Hill, New York, pp. 828–882 (1968)
 [8] G. Weinreich, "Coupled piano strings" *J. Acoust. Soc. Am.* **62**, 1474–1484 (1977)
 [9] W.A. Sethares, *Tuning, Timbre, Spectrum, Scale* Springer-Verlag, New York (1998)
 [10] N.H. Fletcher, "Nonlinear frequency shifts in quasispherical-cap shells: Pitch glide in Chinese gongs" *J. Acoust. Soc. Am.* **78**, 2069–2073 (1985)
 [11] K.A. Legge and N.H. Fletcher, "Nonlinear mode coupling in symmetrically kinked bars" *Journal of Sound and Vibration* **118**, 23–34 (1987)
 [12] K.A. Legge and N.H. Fletcher, "Nonlinearity, chaos, and the sound of shallow gongs" *J. Acoust. Soc. Am.* **86**, 2439–2443 (1989)
 [13] L. Cremer, (1984) *The Physics of the Violin* MIT Press, Cambridge Mass. (1989)
 [14] G. Müller and W. Lauterborn, "The bowed string as a nonlinear dynamical system" *Acustica* **82**, 657–664 (1996)
 [15] N.H. Fletcher, "Autonomous vibration of simple pressure controlled valves in gas flows" *J. Acoust. Soc. Am.* **93**, 2172–2180 (1993)
 [16] A. Hirschberg, J. Gilbert, R. Msallam and A.P.J. Wijnands, "Shock waves in trombones" *J. Acoust. Soc. Am.* **99**, 1754–1758 (1996)
 [17] N.H. Fletcher, "Sound production by organ flue pipes" *J. Acoust. Soc. Am.* **60**, 926–936 (1976)
 [18] N.H. Fletcher, and L.M. Douglas, "Harmonic generation in organ pipes, recorders and flutes" *Acustica* **68**, 767–771 (1980)
 [19] N.H. Fletcher, "Mode locking in non-linearly excited inharmonic musical oscillators" *J. Acoust. Soc. Am.* **64**, 1566–1569 (1978)
 [20] B. Bartolozzi, *New Sounds for Woodwind* Oxford University Press, London (1982)
 [21] N.H. Fletcher, "Transients in the speech of organ flue pipes — a theoretical study" *Acustica* **34**, 224–233 (1976)
 [22] N.H. Fletcher, T. Riede and R.A. Suthers, "Model for vocalization by a bird with distensible vocal cavity and open beak" *J. Acoust. Soc. Am.* **119**, 1005–1011 (2006)
 [23] N.H. Fletcher, "A class of chaotic bird calls?" *J. Acoust. Soc. Am.* **108**, 821–826 (2000)
 [24] K. Neuenfeldt (Ed.) *The Didjeridu: from Arnhem Land to Internet* John Libbey, Sydney (1997)
 [25] A.Z. Tarnopolsky, N.H. Fletcher, L.C.L. Hollenberg, B. Lange, J. Smith and J. Wolfe, "Vocal tract resonances and the sound of the Australian didjeridu (yidaki): I. Experiment" *J. Acoust. Soc. Am.* **119**, 1194–1204 (2006)
 [26] N.H. Fletcher, L.C.L. Hollenberg, J. Smith, A.Z. Tarnopolsky and J. Wolfe, "Vocal tract resonances and the sound of the Australian didjeridu (yidaki): II. Theory" *J. Acoust. Soc. Am.* **119**, 1205–1213 (2006)
 [27] J. Wolfe and J. Smith, "Acoustical coupling between lip valves and vocal folds" *Acoustics Australia* **36**, 23–27 (2008)

DESIGN OF HELMHOLTZ RESONATORS IN ONE AND TWO DEGREES OF FREEDOM FOR NOISE ATTENUATION IN PIPELINES

S. Mekid and M. Farooqui

King Fahd University of Petroleum and Minerals

Department of Mechanical Engineering, Dhahran, 31261, Saudi Arabia

smekid@kfupm.edu.sa, maazfarooqui@kfupm.edu.sa

A thorough design methodology of one and two degrees of freedom Helmholtz resonators leading to optimised transmission loss is described and validated in this paper. Numerical simulations of acoustic wave propagation in pipelines fitted with designed resonators have shown great agreement with analytical modelling and experimental tests. The Helmholtz resonator concept has been analysed in various configurations to evaluate the effect of the size and arrays on the overall noise attenuation performance. Using this method to directly dimension geometry aspects of the resonators followed by numerical computation of the sound pressure levels has shown that considerable sound attenuation could be achieved.

INTRODUCTION

Excessive noise from compressors is a major concern in industries and refineries. The biggest impact of this noise is the discomfort to the personnel working at the facility as observed in practice. The primary concern is that the noise may drown/hide the sound of the emergency alarms of the facility. The noise levels in compressors vary over a wide range from 70–120 dB(A) [1-3]. As the compressor operates over its lifetime, the noise and vibration levels expectedly increase, since centrifugal compressors are continuous flow machines and are extensively used in Saudi Arabia at crude oil processing facilities such as Saudi Aramco. Maintenance is periodic and stopping the operation every time noise levels exceed the desired threshold can be very expensive. Currently Dresser Rand uses Duct Resonator arrays (DR arrays) as an add-on solution [1, 2]. This solution was applied successfully to a 2528 PSIG (172 BARG) multistage centrifugal compressor on a platform in the North Sea and was shown to successfully give a reduction of up to 12 dB(A). Although the DR arrays give appreciable noise reduction since they are machined directly on the diffuser, the challenge lies in the manufacturing and application cost of this solution. The aim of this work is to formulate a design procedure for Helmholtz resonators that will be considered as an add-on device to existing pipelines to further reduce noise levels in a compressor line (Fig. 1).

Two levels of noise reduction are usually requested in a compressor line i.e. compressor and pipeline. The first one is at the compressor level as introduced previously and the other one is within the pipelines. In this paper, the focus will be on the design of a fit resonator for pipelines bearing in mind that characteristics of the compressor are known. The objective is then to identify a design method to fit the right resonator in terms of shape and size on the current pipeline connected to a known compressor.

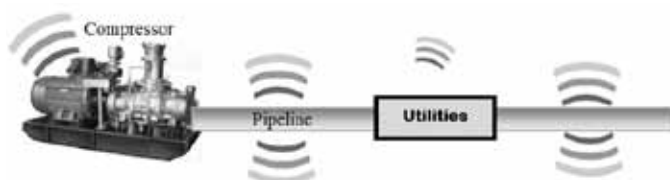


Figure 1. Source of noise reduction in a compressor line

SOURCES OF NOISE IN CENTRIFUGAL COMPRESSORS

Noise originates from various sources within compressors in downstream oil sector. The most critical source of noise in centrifugal compressors is considered to be the blade passing noise which mostly characterizes the gas flowing to the pipelines. This noise arises from the interaction between the impeller blade and the stationary diffuser vanes [1-3]. It is widely known that blade passing frequency (BPF) noise components come from the circumferential flow distortions upstream and downstream of the impeller [4]. The interaction between the impeller blades as it passes by the stationary diffuser vane causes a pressure pulsation which leads to the development of positive and negative vortices.

The interaction of these vortices as they move along the flow path creates the discrete frequency noises of the blade passing frequency. Conventionally the BPF falls between 1000 Hz to 4500 Hz, usually depending on the speed of the compressor and the number of impeller blades [1]. This range falls within human hearing sensitivity which adds to the irritating nature of this noise. Although the BPF may be considered to be the most annoying aspect of compressor noise, at supersonic flow conditions another source of noise arises in the form of buzz saw noise. The BPF noise and the buzz saw noise coupled together can lead to structural failure due to fatigue especially at pipe nipples, stubs, and instrumentation connections. In any centrifugal compressor as the fluid flow exits the impeller, the

flow distribution is distorted. Specifically, such distorted flow is characterised by a low angle (relative to a tangent to the impeller circumference) fluid flow exiting most prominently adjacent to the shroud side of the diffuser. In the past, this distorted flow has been shown to cause severe compressor performance problems [5]. Due to the design of the compressor, the inlet and discharge pipes are relatively more susceptible to noise transmission than the compressor casing itself. Noise propagates through the medium of least resistance and since the piping at the inlet has thinner walls when compared to the compressor casing, this provides a path of lower resistance for noise propagation. Between the inlet and the discharge, investigations have found that higher vibration and noise levels emanate from the discharge. At the inlet, the primary source of noise is the rotor-alone noise, while at the diffuser the BPF noise is dominant [2].

HELMHOLTZ PRINCIPLE

However in recent years, an add-on solution using the Helmholtz concept has been developed in the form of Helmholtz resonators. A Helmholtz resonator operates on the phenomenon of air resonance in a cavity, the pressure inside a cavity increases when air is forced into it. When the air source is removed, the air pressure inside the cavity flows outwards. This outward air pressure tends to overcompensate due to the inertia of the air in the neck this causes the pressure inside the cavity lower than the outside letting the air to come back into the cavity. This continues with a decrement in the pressure magnitude every time. There exist many variations of the Helmholtz resonators in the form of a quarter-wavelength resonator [6], branched type resonator [5] and duct resonators [1, 2]. Some of them are already studied and published with some of their characteristics [7]. The authors have focused on a lumped element model for this study because of the expected practical application in industrial plants.

LUMPED ELEMENT MODEL OF THE HELMHOLTZ RESONATOR

The Helmholtz resonator acts as an acoustic filter element. The dynamic behavior of the Helmholtz resonator can be modelled as a lumped system if the dimensions of the Helmholtz resonator are smaller than the acoustic wavelength. The air in the neck is considered as an oscillating mass and the large volume of air is taken as a spring element [4]. Damping appears in the form of radiation losses at the neck ends and viscous losses due to friction of the oscillating air in the neck. Figure 2 shows this analogy between the Helmholtz resonator and a vibration absorber with defined parameters [8]. In Fig. 2, M_a is the acoustic mass of the resonator and M_m is the mass of the mass-spring-damper system. F is the force applied at the resonator neck entrance and P is the pressure at the neck entrance. V and R_a are respectively the cavity volume and acoustic damping capacity of the Helmholtz resonator. K and R_m are respectively the stiffness and damping capacity of the mass-spring-damper system. ω is the excitation frequency.

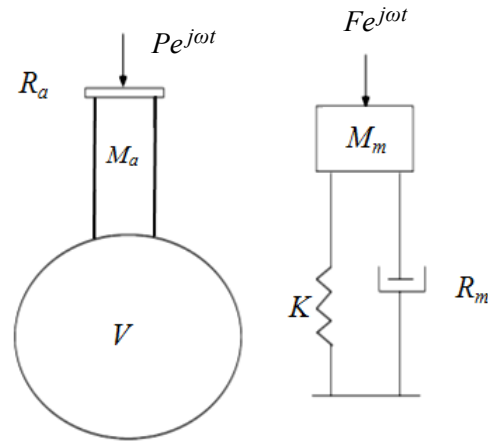


Figure 2. Helmholtz resonator and vibration absorber

DESIGN PROCEDURE FOR ONE AND TWO DOF RESONATORS

It is aimed in this part of the paper to establish a parametric design procedure which will be used to dimension resonators of one and two degrees of freedom (DOF) capable of reducing noise and securing a great transmission loss of noise starting from a known compressor line where the blade passing frequency and the pipeline geometry are already known. The procedure proposed by the authors considers the resonating frequency and transmission loss equations from [9] and [10]. The procedures are explained hereafter. The one DOF resonator has only one resonant frequency hence one peak for transmission loss while two DOF resonators exhibit two resonant frequencies, thereby giving two peaks for transmission loss [11].

Design of a one degree of freedom resonator

The resonating frequency and transmission loss for a one DOF Helmholtz resonator are represented by Eqs. (1) and (2), respectively [8, 10]. There are four design parameters corresponding to L_c , L_n , a_c and a_n that represent the cavity and corrected neck lengths, and the cross sections, respectively, as shown in Fig. 3. Damping appears in the form of radiation losses at the neck ends, and viscous losses due to friction of the oscillating air in the neck.

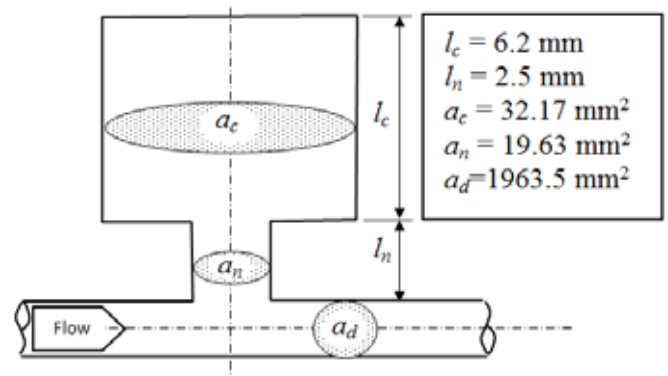


Figure 3. Single degree-of-freedom Helmholtz resonator

Relationships need to be defined to proceed with a suitable design. The design procedure to estimate the optimal size for the resonator needs to satisfy a couple of conditions derived from Eqs. (1) and (2).

$$f = \frac{c}{2\pi} \sqrt{-\frac{3L_n + L_c A}{2L_n^3} + \sqrt{\left(\frac{3L_n + L_c A}{2L_n^3}\right)^2 + \frac{3A}{L_n^3 L_c}}} \quad (1)$$

where A is the area ratio defined in Eq. (4) and c is the speed of sound in the medium. The only restriction in the theory is the cavity diameter that must be less than a wavelength at the resonance frequency. On applying the transfer matrix method [7], the transmission loss is obtained as

$$TL = 10 \log_{10} \left[1 + \left(\frac{a_n}{2a_d} \frac{(1/A) \tan(kL_c) + \tan(kL_n)}{(1/A) \tan(kL_n) + \tan(kL_c) - 1} \right)^2 \right] \quad (2)$$

where k is the wave number.

Expressing the areas a_n and a_c given by Eqs. (A2) and (A3) respectively, and using the condition of solution existence (see appendix A), this leads to a condition on the frequency given by

$$f < 0.2756 \frac{c}{L_c} \quad (3)$$

This condition will be considered as an initial necessary condition for the design of the resonator when the BPF is known.

The second equation given by Eq. (4) is defined as the ratio between the cross sections. It is derived from the optimum transmission loss of Eq. (2) in which the denominator provides a relationship for the resonance frequency, as shown in Eq. (2). The frequency is a function of the cavity dimensions as expressed in Eq. (1) [12]. This second condition will be considered as the sufficient condition to complete the design of a single degree of freedom resonator.

$$A = \frac{a_c}{a_n} = \tan(kL_n) \cdot \tan(kL_c) \quad (4)$$

Since the procedure is based on one-dimensional wave propagation, for a successful noise attenuator, the length to diameter ratio of the neck connected should not be less than 1 as the discrepancy between the analytical results and the experiment is largest for *length/diameter* of this order [7, 13].

The design procedure is organised hereafter:

- i. Specify the frequency to be attenuated.
- ii. Assume values for A (sections ratio) within the range 0.1 to 1.
- iii. Determine the maximum value of L_c from Eq. (3).
- iv. Calculate the values of L_n from Eq. (4) using next step.
- v. Define a value of A to determine a set of lower values for L_c using $L_c = L_c - A$, and hence the corresponding L_n set of values. A is chosen to be small in the same unit as L_c and

L_n , if mm then A will be 1, 2 or 3 mm for example (this will show optimum values of both L_c and L_n for maximum TL).

- vi. The optimum dimensions i.e. L_c and L_n are selected when satisfying Eq. (2) and to provide the maximum transmission loss.
- vii. In order to combine the effects of end correction factors, Eq. (5) can be used [7, 14]

$$l_n = L_n - \delta_1 - \delta_2 \quad (5)$$

The end correction factor δ_2 is given by [10]

$$\delta_2 = 0.48 \sqrt{a_n} (1 - 1.25 \sqrt{A}) \quad (6)$$

The end correction δ_1 between the circular neck and main duct is approximated by

$$\delta_1 = 0.46 \frac{\sqrt{a_n}}{2} \quad (7)$$

- viii. After calculating the optimised dimensions, the resonator can be designed for $l_c = L_c$ and $l_n = L_n - \delta_1 - \delta_2$ for the A which gives maximum transmission loss. Figure 3 shows one of the examples based on this design methodology.

Design of a two degree of freedom resonator

Let the dual frequencies f_1 and f_2 to be attenuated,

- a. Following the procedure for two DOF resonators calculate the values of the radius, neck length and the volume of the first resonator i.e. R_{n1} , l_{n1} , V_1 , respectively. Calculate the ratio (γ_a/γ_l) which satisfies the necessary condition derived from Eq. (B1) (procedure explained in Appendix B).
- b.

$$\frac{f_1^2}{f_2^2} + \frac{f_2^2}{f_1^2} \geq 2 \left(1 + \frac{2\gamma_a}{\gamma_l} \right) \quad (8)$$

where $2\gamma_a = \frac{a_{n2}}{a_{n1}}$, $\gamma_l = \frac{l_{n2}}{l_{n1}}$, and a_{n1} , a_{n2} are the area of cross sections of the first and the second neck and l_{n1} and l_{n2} their respective lengths.

- c. Let $\alpha = \frac{a_{n1}}{l_{n1}}$ and $\beta = \frac{a_{n2}}{l_{n2}}$

$\frac{\gamma_a}{\gamma_l}$ can be determined from Eq. (8) as well as $\frac{\alpha}{\beta}$ since it is equal to the same ratio.

- d. By using the following frequency equation, V_1 and V_2 can be calculated in terms of α and β .

$$f_{1,2} = \frac{c}{2\sqrt{2}\pi} \sqrt{\left(\frac{\alpha}{V_1} + \frac{\beta}{V_1} + \frac{\beta}{V_2} \right) \pm \sqrt{\left(\frac{\alpha}{V_1} + \frac{\beta}{V_1} + \frac{\beta}{V_2} \right)^2 - 4 \frac{\alpha}{V_1} \frac{\beta}{V_2}}} \quad (9)$$

Equation (9) is the dual frequency expression rewritten in this form from Xu et al. [10].

- e. Now the transmission loss can be calculated using Eq.(10) but rewritten and plotted with respect to α and β for getting the optimum $\frac{\alpha}{\beta}$ or maximum transmission loss. The corrected lengths can be converted to original lengths used for design by following step (vi) of the one degree-of-freedom design procedure.

$$TL = 20\log_{10} \left| 1 + \frac{\alpha}{2a_d \left(ik + \frac{\alpha}{ikV_1} \left(1 - \frac{V_2}{V_2 + V_1 - \frac{V_2V_1k^2}{\beta}} \right) \right)} \right| \quad (10)$$

where a_d is the cross section area and k is the wave number.

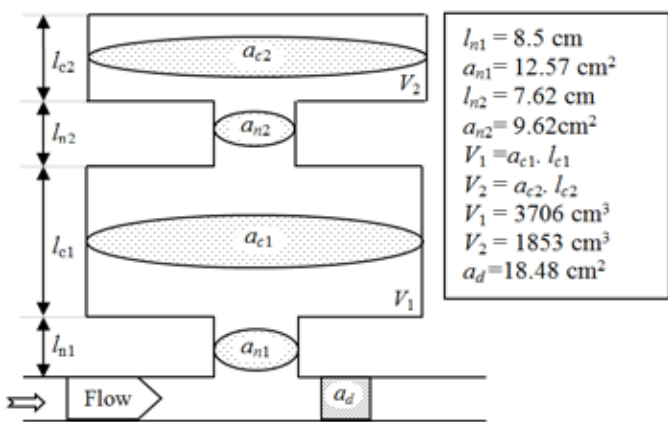
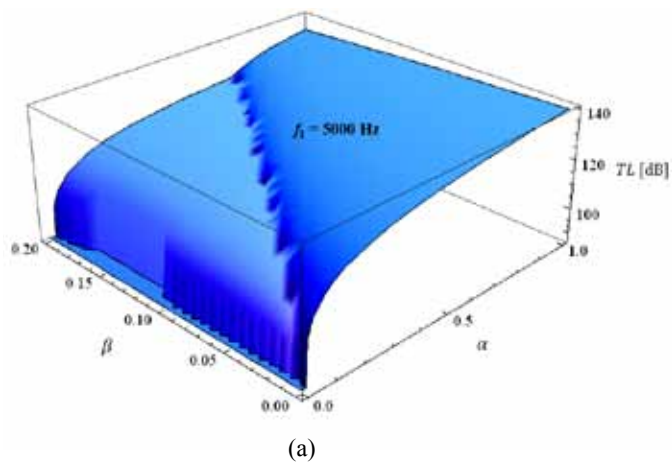


Figure 4. Dual Helmholtz resonator [10]

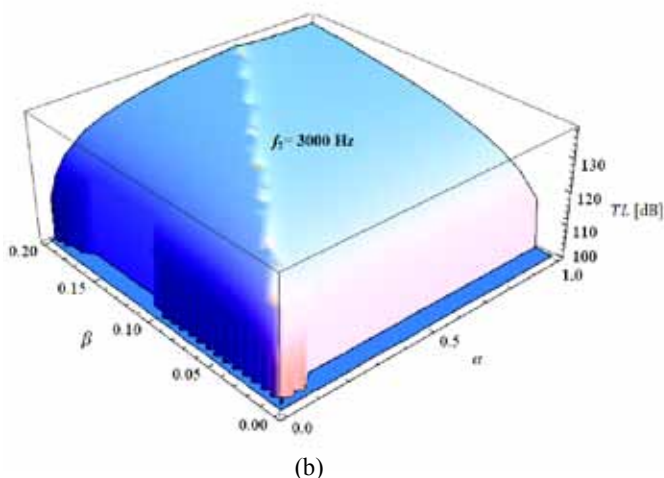
This method has been applied to design a two DOF resonator for a pipeline. Referring to Fig. 4, the values can be correlated. The corresponding volume of the first and second cavities simulated have $V_1=3706 \text{ cm}^3$ and $V_2=1853 \text{ cm}^3$, respectively. Figure 5 shows the transmission loss distribution depending on the dimensional parameters ratios α and β . An in-depth analysis of the level of transmission loss that could be achieved shows that optimisation can be done based on the acceptable manufactured necks in terms of diameters and lengths. Hence as shown in Fig. 5(a) the maximum transmission loss obtained from simulation could be achieved with α towards 1 while β within 0.2. Therefore, the first neck cross section a_{n1} is proportional to its length L_{n1} e.g. the neck length will be two orders higher than the neck's diameter ($d_{n1}^2=4L_{n1}/\pi$), while β shows that the second neck cross section is less than 20% of the length L_{n2} . As α moves towards zero and β towards 0.2, the first neck cross section becomes very small with respect to its

length ($d_{n1}^2=4L_{n1}/\pi$), while the second cross section remains similar as in previous case. This trend is fairly conserved for the second frequency in Fig. 5(b).

It is worth noticing from the numerical simulations using COMSOL Multiphysics that these frequencies are higher enough so that higher modes, in addition to planar wave, can propagate depending on the size of the main duct.



(a)



(b)

Figure 5. Transmission loss distribution versus ratios α and β for two degrees of freedom resonator applied to a pipeline for two different frequencies at 5000 Hz (a) and 3000 Hz (b)

NUMERICAL SIMULATIONS FOR ONE AND TWO DOF RESONATORS

3-Dimensional numerical simulation for one degree of freedom resonator

The following example is applied to an industrial plant. A cylindrical Helmholtz resonator was designed using the design procedure for one degree-of-freedom discussed earlier. Sound pressure levels showing transmission loss have been numerically computed using the COMSOL Multiphysics Acoustics module. The blade passing frequency that was attenuated was measured at the suction pipe of a compressor located in one of the plants of Saudi Aramco. Figure 6 shows

the corresponding sound pressure level versus frequencies. The simulation results are shown for a pipe with one resonator in Fig. 7, and with an array of resonators in Fig. 8. The maximum achieved noise attenuation was around 30 dB. The dimensions that were taken to model the resonators were found for $A=0.1$ corresponding to $r_{neck}=1$ mm, $l_{neck}=3.74$ mm, $r_{cavity}=3.16$ mm, $l_{cavity}=6.21$ mm. A sudden decrease in the sound pressure levels can be visualized in Fig. 9 when comparing a pipe fitted with a resonator whether it is single or in an array with a non-fitted pipe. When an array of identical resonators is added on the same location around the perimeter of the pipe (Fig. 8), it was observed from the numerical simulation that the sound pressure attenuation has improved by about 15% as shown in Fig. 9(b). This shows the advantage of using arrays rather than single resonator although the attenuation offered by the array has a very limited incremental range (Fig. 9). Also, the reduction of sound pressure level at the resonance frequencies is very narrow since damping and viscosity effect were not considered in the simulation. The little increase in noise level above the resonating frequency may indicate that the reference pressure used for the computations is higher than the measured pressure level. As known from Helmholtz resonators, the damping appears in the form of radiation losses at the neck ends, and viscous losses due to friction of the oscillating air in the neck. Neglecting the damping at this stage of numerical simulations by COMSOL will only have little effect on the results since the structure is stiff while the system with resonators is by definition damping-controlled.

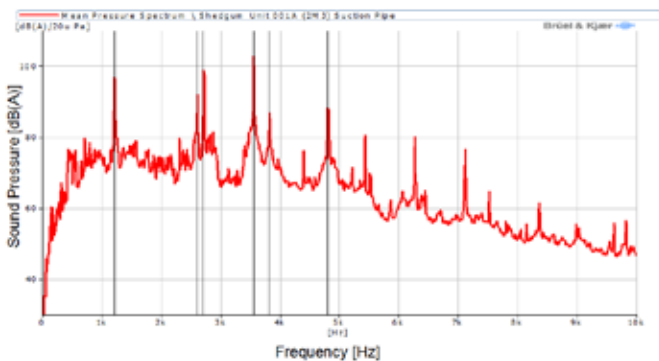


Figure 6. Suction pipe narrow band sound pressure level of a measured compressor (from Dresser Rand)

3-Dimensional numerical simulation for two degrees of freedom resonator

The dual resonators used by Xu et al. [10] were used as a benchmark test to validate the analytical design method described previously. The same dual resonator was used in the COMSOL simulation to validate the level of transmission loss obtained analytically.

Validation of results

The dual resonator described in Fig. 4 was used in the numerical simulation. The main duct was considered with a square cross-section of 4.3cm x 4.3cm. The square main

duct is then connected to a circular impedance tube with smooth transitions that retain a constant cross-sectional area development. The following figures show the results of simulation as generated by COMSOL Multiphysics in the Acoustics module, and showing relative noise attenuation in Figs. 7 and 8 and in Figs. 12 and 13. The input frequency was varied and the acoustic response of the system was recorded. As the figures show, there is a noticeable reduction in noise levels. There is nearly a 20 dB decrease in noise levels at the 73 Hz resonant frequency and a 25 dB decrease in noise levels at the 166 Hz resonant frequency. The noise response of the dual Helmholtz resonator versus frequency is shown in Fig. 11. Using the stated equations for two DOF resonators, the results match the analytically calculated values with an error of 1%.

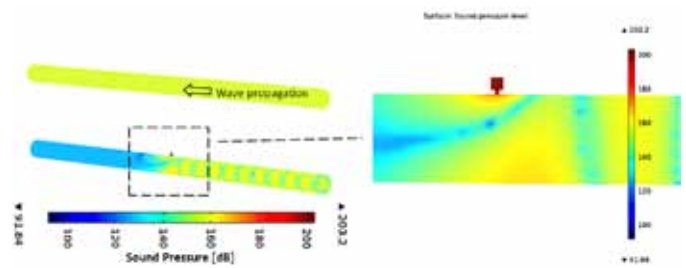


Figure 7. Sound pressure levels distribution at 3556 Hz on the surface of the pipe without and with one DOF single designed resonator with a closer view of the tuned resonator.

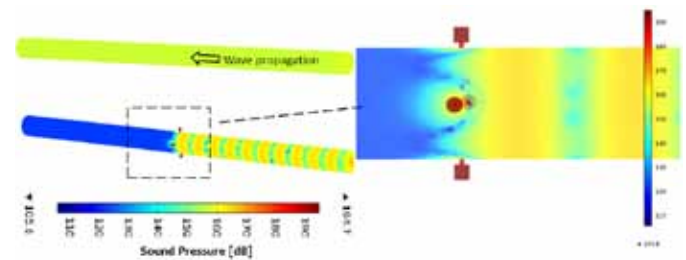
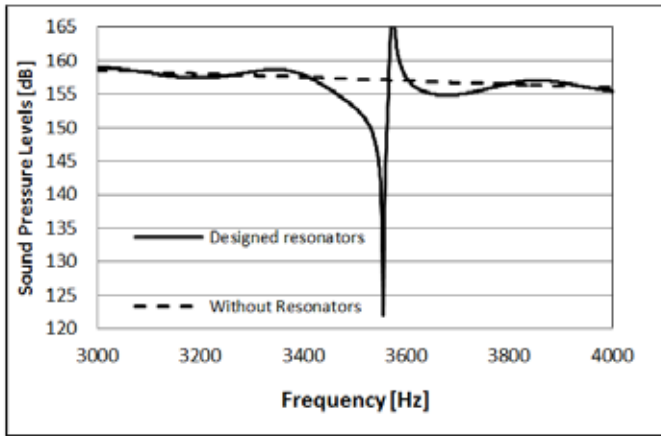


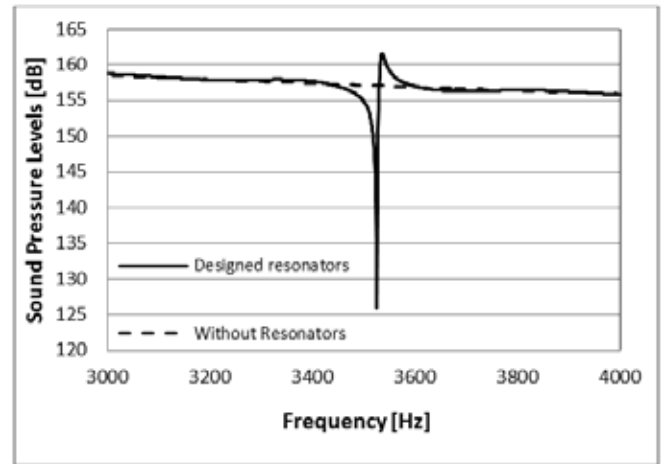
Figure 8. Sound pressure levels distribution at 3556 Hz on the surface of the pipe without and with one DOF of four designed resonators with a closer view of the tuned resonator.

Experimental tests

The experiment included a main square section duct (43x43mm) and one two degree of freedom resonator formed of two cylinders which dimensions are shown in Fig 4 [10]. The main duct has a square cross section and was connected to a circular impedance tube. The apparatus used in the experiments to measure the transmission loss is based on two-microphone technique applied on the impedance tube set-up [15]. Along with the random sound input, B&K Multichannel Analysis System Type 3550 has been used. Throughout the frequency range of interest, the reflection coefficient measured on the downstream side of the resonator was ensured, by an appropriate termination, to remain below 0.1 which translates to accurately measured transmission loss.

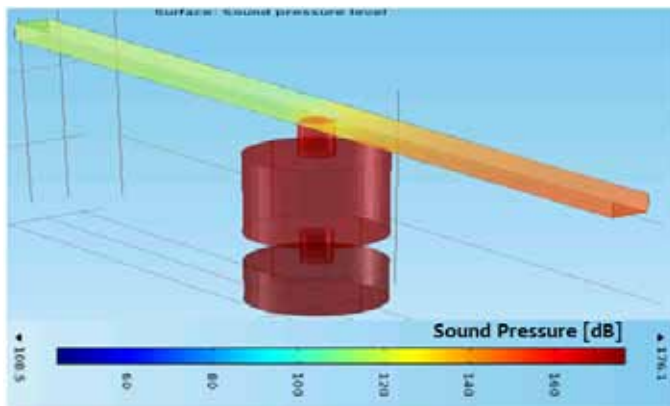


(a)

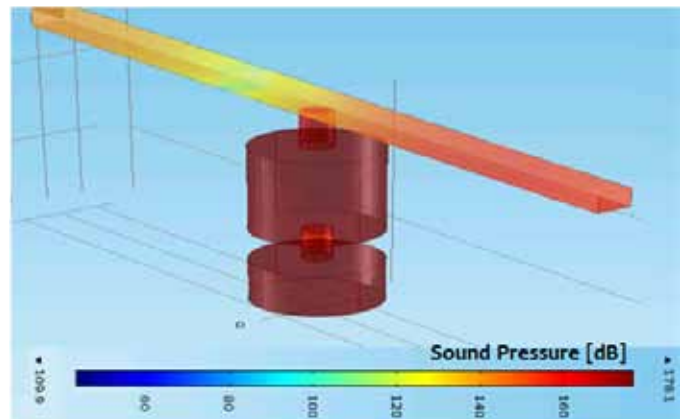


(b)

Figure 9. Sound pressure levels comparison without and with resonators, (a) pipe with a single designed one DOF resonator, (b) pipe with four designed single DOF resonators. Sound pressure measured at the end of the main duct which length is 1.2m and hosting the resonators. The source is a random noise signal



(a)



(b)

Figure 10. Sound pressure levels at the resonating frequency (a) 73 Hz, (b) 166 Hz

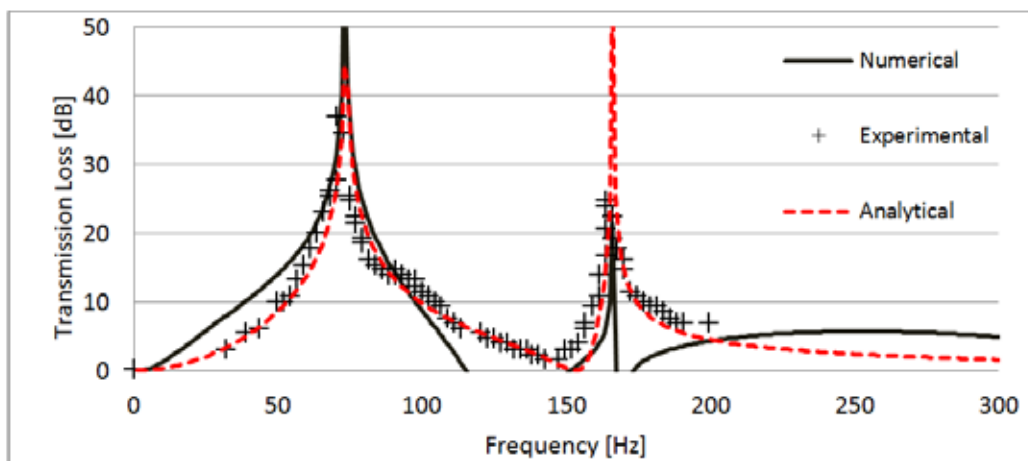


Figure 11. A comparison of transmission loss with published experimental results [10] for a single 2 DOF resonator

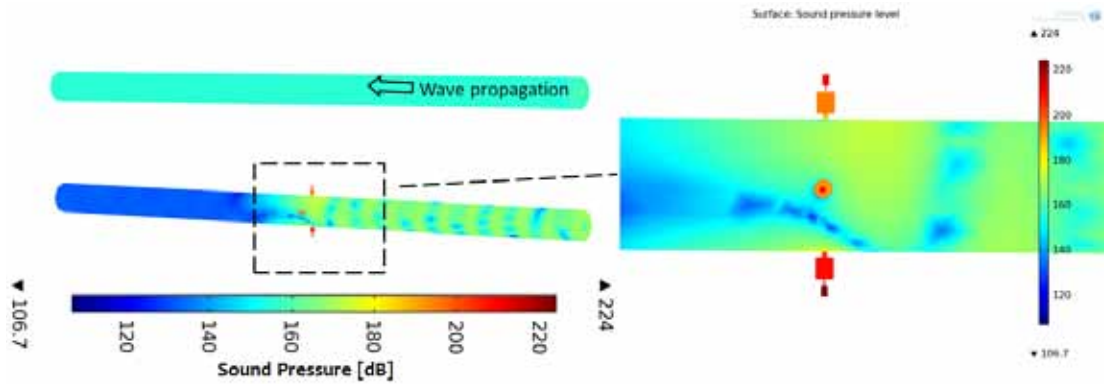


Figure 12. Sound pressure levels distribution at 3556 Hz on the surface of the pipe without and with two DOF designed resonators. A closer view of sound pressure levels distribution at 3556 Hz on the surface of the pipe with and without two DOF designed resonators

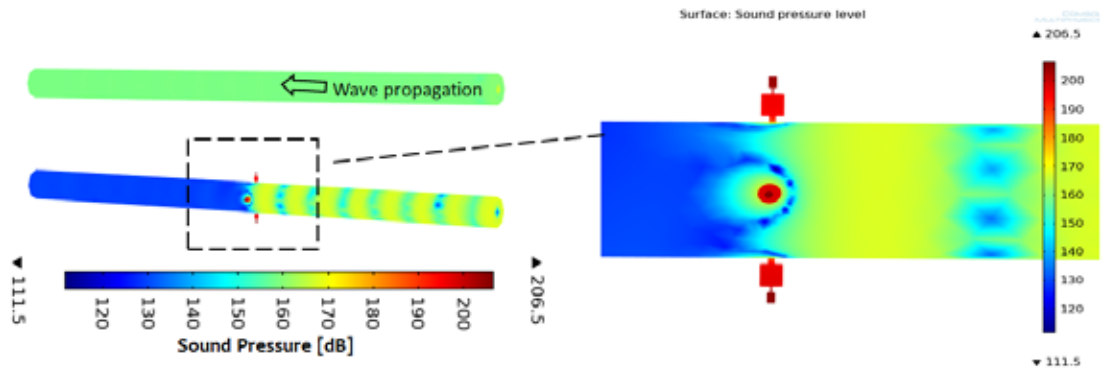


Figure 13. Sound pressure levels distribution at 2712 Hz on the surface of the pipe without and with two DOF designed resonators. A closer view of sound pressure levels distribution

Simulation of array resonators

A 2 DOF cylindrical Helmholtz resonator was designed using the design procedure. This time two highest peaks from Fig. 6 were taken to be attenuated by designing resonators. The simulation shown in Figs. 12 and 13 gives an idea of the degree of attenuation received where the pipes with the array of resonators is able to attenuate the noise by around 30-40 dB for both frequencies. The values of α and β used are 1.2 and 0.07142 so as to satisfy Eq. (9), i.e. the ratio, $\alpha/\beta \leq 0.07522$ for frequencies 3556 and 2712 Hz.

CONCLUSIONS

A new design procedure has been proposed and validated in this paper for noise attenuation using Helmholtz resonators in pipelines. Applied to one and two of Helmholtz resonators, the designed models of resonators have been verified numerically using COMSOL. All analytical and numerical results were validated using experimental results from published data. Attenuation of around 40 dB has been achieved which proves not only the efficiency of the proposed design procedure but also the straightforward method to dimension the resonators.

ACKNOWLEDGMENTS

The authors would like to acknowledge the support

provided by the research collaboration between King Fahd University of Petroleum & Minerals (KFUPM) and Dresser-Rand Company (USA).

Appendix A - One degree of freedom resonator

The equation for angular resonating frequency of one degree of freedom resonator is given by [7]

$$\omega = c \sqrt{-\frac{3L_n + L_c A}{2L_n^3} + \sqrt{\left(\frac{3L_n + L_c A}{2L_n^3}\right)^2 + \frac{3A}{L_n^3 L_c}}} \quad (A1)$$

where

$$A = \frac{a_n}{a_c}$$

a_n is the cross section area of the neck, a_c is the cross section area of the cavity, L_n is the corrected neck length, L_c is the length of the volume, and c is the speed of sound.

Solving Eq. (A1) for the two areas of cross sections results in

$$a_n = \frac{a_c (-3c^2 \omega^2 L_n L_c - \omega^4 L_n^3 L_c)}{c^2 (-3c^2 + \omega^2 L_c^2)} \quad (A2)$$

$$a_c = \frac{a_n c^2 (-3c^2 \omega^2 L_c^2)}{(-3c^2 \omega^2 L_n L_c - \omega^4 L_n^3 L_c)} \quad (A3)$$

From these two equations it is obvious for the two cross section areas to be positive, the denominator should be negative for Eq. (A2) while the numerator should be negative for Eq. (A3), that is

$$-3c^2 + \omega^2 L_c^2 < 0 \quad (A4)$$

where

$$\omega < \sqrt{\frac{3c^2}{L_c^2}}$$

The resonating frequency then becomes

Therefore, Eq. (B1) can be expressed as

$$f_{1,2} = \frac{c}{2\sqrt{2\pi}} \sqrt{\left(\frac{a_{n1}}{l_{n1}V_1} + \frac{a_{n2}}{l_{n2}V_1} + \frac{a_{n2}}{l_{n2}V_2}\right) \pm \sqrt{\left(\frac{a_{n1}}{l_{n1}V_1} + \frac{a_{n2}}{l_{n2}V_1} + \frac{a_{n2}}{l_{n2}V_2}\right)^2 - 4\frac{a_{n1}}{l_{n1}V_1} \frac{a_{n2}}{l_{n2}V_2}}} \quad (B2)$$

Equation (B2) can be solved for the volumes of the first and second cavities, which are given by

$$V_1 = \frac{(8a_{n1}^2 a_{n2}^2 c^4)}{l_{n1} \left(2a_{n1} a_{n2} c^2 f_1^2 + 2a_{n1} a_{n2} c^2 f_2^2 - \sqrt{\left(4a_{n1}^2 a_{n2}^2 c^4 f_1^4 - 8a_{n1}^2 a_{n2}^2 c^4 f_1^2 f_2^2 + 4a_{n1}^2 a_{n2}^2 c^4 f_2^4 - \frac{16a_{n1} a_{n2}^3 c^4 f_1^2 f_2^2 l_{n1}}{l_{n2}} \right)} \right)} \quad (B3)$$

$$+ \frac{(8a_{n1} a_{n2}^2 c^4)}{l_{n2} \left(2a_{n1} a_{n2} c^2 f_1^2 + 2a_{n1} a_{n2} c^2 f_2^2 - \sqrt{\left(4a_{n1}^2 a_{n2}^2 c^4 f_1^4 - 8a_{n1}^2 a_{n2}^2 c^4 f_1^2 f_2^2 + 4a_{n1}^2 a_{n2}^2 c^4 f_2^4 - \frac{16a_{n1} a_{n2}^3 c^4 f_1^2 f_2^2 l_{n1}}{l_{n2}} \right)} \right)}$$

$$V_2 = \left(\frac{0.5 \left((a_{n1} a_{n2} c^2)(2f_1^2 + 2f_2^2) - \sqrt{\left(a_{n1}^2 a_{n2}^2 c^4 (2f_1^2 + 2f_2^2)^2 - \frac{16a_{n1} a_{n2}^2 c^4 f_1^2 f_2^2 (a_{n2} l_{n1} + a_{n1} l_{n2})}{l_{n2}} \right)} \right)}{f_1^2 f_2^2 (a_{n2} l_{n1} + a_{n1} l_{n2})} \right) \quad (B4)$$

The two volumes V_1 and V_2 are real if the expressions in square root are positive or zero. Hence, a new condition emerges and is given by

$$\left(\frac{f_1^2}{f_2^2} + \frac{f_2^2}{f_1^2} \right) \geq 2 \left(1 + \frac{2a_{n2} l_{n1}}{a_{n1} l_{n2}} \right) \quad (B5)$$

which can also be written as

$$\left(\frac{f_1^2}{f_2^2} + \frac{f_2^2}{f_1^2} \right) \geq 2 \left(1 + \frac{2\gamma_a}{\gamma_l} \right)$$

$$\gamma_a = \frac{a_{n2}}{a_{n1}}, \quad \gamma_l = \frac{l_{n2}}{l_{n1}}$$

$$f < \left(\frac{1}{2\pi} \sqrt{\frac{3c^2}{L_c^2}} = 0.2756 \frac{c}{L_c} \right)$$

Appendix B - Two degree of freedom resonator

The equation for angular resonating frequency of two degree of freedom resonator is derived from Eq. (1) and is given by

$$f_{1,2} = \frac{c}{2\sqrt{2\pi}} \sqrt{\left(\frac{\alpha}{V_1} + \frac{\beta}{V_1} + \frac{\beta}{V_2}\right) \pm \sqrt{\left(\frac{\alpha}{V_1} + \frac{\beta}{V_1} + \frac{\beta}{V_2}\right)^2 - 4\frac{\alpha}{V_1} \frac{\beta}{V_2}}} \quad (B1)$$

where

$$\alpha = \frac{a_{n1}}{l_{n1}} \quad \text{and} \quad \beta = \frac{a_{n2}}{l_{n2}}$$

REFERENCES

- [1] Z. Liu and M.J. Kuzdzal, "Noise control of an 11,000 horsepower single stage pipeline centrifugal compressor", *Proceedings of the ASME Turbo Expo 2007: Power for Land, Sea, and Air (GT2007)*, Montreal, Canada, 14-17 May, 2007, pp. 1489-1496
- [2] Z. Liu and M.J. Kuzdzal, "Turbo compressor noise reduction by D-R™ duct resonator arrays", *Insights* **8**, 10-14 (2002)
- [3] T. Raitor and W. Neise, "Sound generation in centrifugal compressors", *Journal of Sound and Vibration* **314**, 738-756 (2008)
- [4] J. Kim and I. Imam, *Compressor noise attenuation using branch type resonator*, US Patent 4927342, 1990
- [5] W. Neise and G.H. Koopmann, "Reduction of centrifugal fan noise by use of resonators", *Journal of Sound and Vibration* **73**, 297-308 (1980)

- [6] P.K. Tang and W.A. Sirignano, "Theory of generalized Helmholtz resonator", *Journal of Sound and Vibration* **26**, 247-262 (1973)
- [7] A. Selamat, P.M. Radavich, N.S. Dickey and J.M. Novak. "Circular concentric Helmholtz resonators", *Journal of the Acoustical Society of America* **101**, 41-51 (1997)
- [8] S. Khelladi, S. Kouidri, F. Bakir and R. Rey "Predicting tonal noise from a high rotational speed centrifugal fan", *Journal of Sound and Vibration* **313**, 113-133 (2008)
- [9] D. Li, *Vibroacoustic behavior and noise control studies of advanced composite structures*, PhD Thesis, University of Pittsburgh, USA, 2003
- [10] M.B. Xu, A. Selamat and H. Kim, "Dual Helmholtz resonator", *Applied Acoustics* **71**, 822-829 (2010)
- [11] D.M. Wan and D.T. Soedel, "Two degree of freedom Helmholtz resonator analysis", SAE Technical Paper 2004-01-0387, 2004
- [12] P.K. Tang and W.A. Sirignano, "Theory of a generalized Helmholtz resonator", *Journal of Sound and Vibration* **26**, 247-262 (1973)
- [13] N.S. Dickey and A. Selamat, "Helmholtz resonators: one-dimensional limit for small cavity length-to-diameter ratios", *Journal of Sound and Vibration* **195**, 512-517 (1996)
- [14] U. Ingard, "On the theory and design of acoustic resonators", *Journal of the Acoustical Society of America* **25**, 1037-1061 (1953)
- [15] M.L. Munjal, *Acoustics of ducts and mufflers with application to exhaust and ventilation system design*, John Wiley and Sons, New York, 1987

Distance Learning for Acoustics

The Professional Education in Acoustics program was established some years ago on the request from the industry due to a lack of regularly available appropriate courses in the formal University programs. It is aimed at providing appropriate modules to meet the needs of those embarking on a career in Acoustics and has the support of the Association of Australian Acoustical Consultants (AAAC). It is also be of value for those working in government agencies and allied organisations needing a fundamental understanding of acoustics. The program is based on a similar program that has been offered via universities and the UK Institute of Acoustics (IOA).

The program is fully flexible and all undertaken in distance learning mode. This means the modules can be commenced at any time and there is no requirement to complete at a specific date. This is an advantage to those who are unsure of future work demands – but of course a disadvantage as the lack of a deadline means that completion depends on the commitment of the registrant.

Each module of the program will be offered separately in distance learning mode so that it can be undertaken throughout Australia or elsewhere in the world and can be commenced at any time. Each module comprises course notes, assignments and two modules include practical exercises and a test. Registrants work through this material at their own pace and in their own location submitting the work electronically. The practical work and the test are undertaken at the registrant's location under supervision of their employer. It is expected that those registrants working for acoustical consultancies will receive support and supervision by their supervisors. For registrants who are working on the program without support from their employer will be given assistance by phone or email from the course coordinator. This assistance can be supplemented with assistance from a company that is a member of the AAAC.

For more information on the program see <http://www.aaac.org.au/au/aaac/education.aspx>



DESIGNING & FABRICATING SMART ACOUSTIC SOLUTIONS ALL DEPENDS ON WHAT'S BETWEEN YOUR EARS.

For intelligent solutions from design to installation,
pick our brains. Contact Robert at Peace Engineering now.



Peace

NOISE & VIBRATION CONTROL

www.peaceengineering.com



Ph [02] 4647 4733

VIBRATION FIELD OF A DOUBLE-LEAF PLATE WITH RANDOM PARAMETER FUNCTIONS

Hyuck Chung

School of Computing and Mathematical Sciences, Auckland University of Technology, PB 92006, Auckland, New Zealand

hchung@aut.ac.nz

This paper shows how to compute vibrations of a double-leaf plate with random inhomogeneities in its components. The components are two plates and reinforcement beams. The modelling method is based on the variational principle for elastic plates and beams. In addition to the deformation of individual components, the model includes contributions from junctions between components, e.g., rigidity of the connection between a beam and a plate. The model does not restrict the junctions to be perfectly straight. The beams are allowed to have a small random twist. The junction rigidity is included as potential energy in addition to the strain and the kinetic energies of the components. The random inhomogeneities are simulated as continuous smooth random functions. A random function is realized using a predetermined probability density function and a power spectral density function. The vibration is then computed from a set of random functions. The numerical simulations show that the random stiffness affects the behaviour of the structure in a wide frequency range. Whereas the junctions affect the a lower frequency vibrations. The root-mean-square velocity of surface vibration level shows changes at resonance frequencies depending on the random functions.

INTRODUCTION

This paper presents a theoretical and computational model of vibrations of a double-leaf plate when it is subjected to some external forces. Double-leaf plates have a high strength-to-weight ratio, and are used in many lightweight constructions. Acoustic properties of double-leaf plates are more difficult to predict than those of single plates, because of a high number of components that make up typical double-leaf plates. A simple design of a double-leaf plate would have two plates sandwiching reinforcement parallel beams. There are various methods of joining the two components such as nails and glue. The large number of distinct components and the complexity of the junctions make the mathematical representation of the double-leaf plate difficult. The often used finite element method (FEM) would represent the junction between a plate and a beam as a 'T' shaped continuous object. This is not true in most cases because the connection at the junction is not perfect, while additionally the material properties of the plate and the beam may be completely different. In other cases, the FEM would require microscopic descriptions of the junction, for example describing how the nails react to various forces and affect the surrounding material. This paper uses an alternative way of modelling the junctions. A junction is modelled by the amount of energy required for any particular way of deformation of the junction. The amount of energy at the junction will be large or small if the bonding is strong or weak.

The conventional deterministic models of double-leaf plates that use the partial differential equations of Kirchhoff plates and Euler beams can predict low frequency vibrations (see [1, 2, 7, 8, 9]). The parameters of the equations are constants such as mass density and Young's modulus. However the vibration of a double-leaf plate becomes unpredictable above the 5th resonant

frequency, which in the case of a 3.2m-by-5.1m structure is about 80 Hz. This particular dimension is chosen because of author's past experience with an experimental programme on timber-framed floor/ceiling systems (see [2]). One can find variations in the vibrations of apparently identical composite structures. The discrepancy may come from the manufacturing inconsistencies or random inhomogeneities in the components themselves. The unpredictability of the vibrations of composite structures have been known for many years, and modelled using various methods such as perturbation, scattering, and asymptotic methods. All of these methods assume the irregularities in the structure to be small compared to the wavelengths, and hence terms higher than first-order are negligible. This is not true for most engineered products.

Another popular modelling method for double-leaf plates is Statistical Energy Analysis (SEA). In order to use SEA, a structure needs to be divided into sub-systems that interact with their neighbouring systems. Two neighbouring sub-systems are related by a loss factor that is determined either from experiments or theoretical models. Measurements and theoretical predictions of various types of double-leaf plates are considered in [3, 4]. SEA has been used successfully to predict the surface vibration level above 300 Hz. However SEA is not suitable for computing the vibrations in the frequency range of concern here.

In this paper the deformation of each component is computed using the variational principle. The energy density functions for individual components and junctions are derived using the Kirchhoff plate, Euler beam models and Hooke's law. Once the integral form of the total energy in the double-leaf plate is obtained from the functions of the deformation of individual components of the double-leaf plate, the true solution will give the minimum of the integral form. The solution will be computed using the Fourier series expansion of the solution

over the basis functions in the x and y -directions, which is possible because of the rectangular shape of the structure. The irregularities, the stiffness (Young's modulus) of the two plates, junctions and the small twist in the beams, are included using their Fourier components. The Fourier representation of the solution keeps the computation cost low. The computation cost is determined by the number of Fourier terms. In this paper 20×20 terms are used for a plate and 20 terms for a beam. On the other hand, the computation cost of using FEM is dependent on the resolution of the finite element mesh that must be generated for a whole 3-dimensional double-leaf plate. The junctions will need high resolution mesh to capture the small deformation.

In addition to the simplified junction model, a few selected parameters are simulated as random functions (or random process) with pre-assigned power spectral density (PSD) functions and probability density functions (PDFs). The parameters are the stiffness of the plates, the rigidity of the junction, and shape of the beams. Each random function is assumed to be stationary, and thus its PDF is identical everywhere at any spatial location. This paper follows the method given in [6], in which only 1-dimensional examples are given. In this paper, 2-dimensional random functions are used to simulate the irregular stiffness of the top and bottom plates. The extension from 1 to 2 dimensional random function is straightforward. The computation is carried out for each of the random functions and the results (vibrations of the top plate) are studied using the root-mean-square velocity and the spatial distribution of the variance of the vibration amplitude. The computation time of, say 5000 simulations, for each random function was approximately 2 to 3 hours using MatLab on a desktop computer.

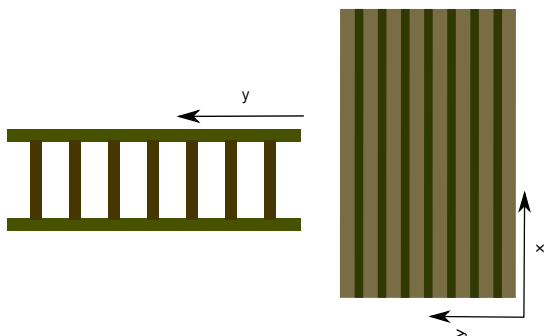


Figure 1. Depiction of a double-leaf plate. Cross section (left) and the view from the top (right). The origin of the coordinate system is at the lower corner

MODELLING AND MATHEMATICAL FORMULATION

Variational formulation

The deflection of the individual components is the solution, which will be computed in this paper. A local coordinate

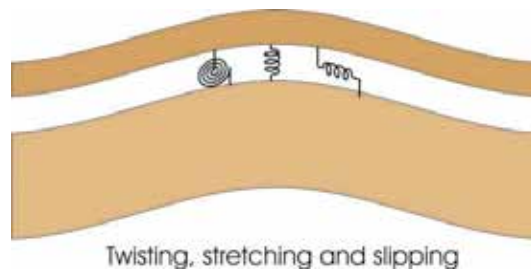


Figure 2. Depiction of the model for the coupling conditions between the plate (top) and the beam (bottom). The springs give the resistance to the rotational (left), vertical (centre), and horizontal (right) movements

system is used for each component, that is, the origin is placed at the corner of each plate, and each beam has the origin at one end (see Fig. 1). Here the simple harmonic vibration is considered, and hence the solutions will have the form $\mathbf{Re}[w(x,y)\exp i\omega t]$ where ω is the radial frequency. The deflection of each component is denoted by $w_1(x,y)$, $w_2(x,j)$, and $w_3(x,y)$ for the top plate, j th beam, and the bottom plate, respectively. Other parameters and functions will be denoted with the corresponding subscripts 1, 2, or 3 for the top plate, beams, and bottom plate, respectively. For example, the thickness of the top plate is denoted by h_1 , and the mass density of the bottom plate will be ρ_3 , and so on. The length (x -direction) and the width (y -direction) are A and B , respectively. Hence the plates cover the area $(x,y) \in [0,A] \times [0,B]$, and the beams are modelled as one dimensional objects for $x \in [0,A]$. The beams have the same size, density, and elastic modulus.

We choose the variational formulation using the Lagrangian of the deflection to compute the vibration field of the structure. The vibration field of the structure is found by constructing the Lagrangian of the total energy in the structure (see [10]). The solution will be found by minimizing the Lagrangian. The Lagrangian for the whole structure is given by the following general form for the given deformation of the structure.

$$\mathcal{L} = \int_0^T \int_V \{ \mathcal{P}(t) + \mathcal{K}(t) - \mathcal{F}(t) \} dv dt, \quad (1)$$

where \mathcal{P} is the potential energy, \mathcal{K} is the kinetic energy, and \mathcal{F} is the work done to the object. The integral is taken over the volume of the elastic body and the period of time T . Here the integral will be taken over the plates and beams. The integral over time need not be considered because the vibration is simple harmonic.

The classical Kirchhoff (thin elastic) plate model expresses the strain energy and kinetic energy of a thin elastic plate, which has non-moving boundary, by

$$\mathcal{P}_1 = \frac{1}{2} \int_0^A \int_0^B D_1(x,y) |\nabla^2 w_1|^2 dx dy \quad (2)$$

$$\mathcal{K}_1 = \frac{\rho_1 h_1 \omega^2}{2} \int_0^A \int_0^B |w_1(x,y)|^2 dx dy \quad (3)$$

where $D_1(x,y) = E_1(x,y)h_1^3 / (12(1-\alpha^2))$ is the flexural rigidity and ρ_1, h_1, E_1 and α are the density, the plate thickness,

Young's modulus and Poisson ratio, respectively. Note that the effect of rotation is neglected in \mathcal{K}_1 . The minima of Eq. (1) is the solution of the thin plate equation,

$$\nabla^2 (D_1(x,y)\nabla^2 w_1(x,y)) - \omega^2 m_1 w_1(x,y) = p(x,y) \quad (4)$$

where $m_1 = \rho_1 h_1$ is the mass density per unit area, and p is the effective pressure acting on the plate. The above differential equation is useful when an analytical solution can be considered. We however deal with irregular structural properties, and therefore the solution method is numerical. The energies for the bottom plate are given by the same formulae with \mathcal{P}_3 and \mathcal{K}_3 for w_3 .

The strain and kinetic energies for the Euler beams are given by

$$\mathcal{P}_2 = \frac{1}{2} \sum_{j=1}^S \int_0^A E_2 I |w_2''(x,j)|^2 dx \quad (5)$$

$$\mathcal{K}_2 = \frac{\rho_2 h_2 \omega^2}{2} \sum_{j=1}^S \int_0^A |w_2(x,j)|^2 dx \quad (6)$$

where E_2 and I are the Young's modulus and the moment of inertia of the beam, and ρ_2 and h_2 are the mass density per unit length and the thickness of the beam, respectively. The primes '' on w indicate the second derivative with respect to x .

The combination of Kirchhoff plates and Euler beams has been used successfully in [2] to predict vibrations of timber-framed floor/ceiling systems. An example of comparison between the theoretical prediction and the experimental measurement is shown Fig. 3. Figure 3 shows the root-mean-square velocity of the bottom plate. The theoretical prediction disagrees with the experimental measurement above 80 Hz. The model of the double-leaf plate in [2] includes cavity air, damping in timber components, and various attachments used in construction of real building structures. In this paper the model is simplified to keep the computation minimum. Furthermore the purposes of this paper are to study the effects of the randomness in the structure and show how the random functions can be included in the method of solution.

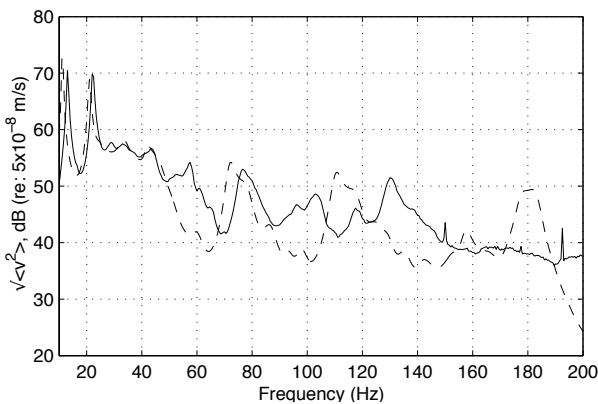


Figure 3. Comparison between the theoretical prediction (dashed) and the experimental measurements (solid)

Coupling at the junctions

In addition to the strain and kinetic energy, we include the energy contributions from the junctions due to the discrepancy in the displacement of the two components (see Fig. 2). The potential energies at the junctions are given by

$$\mathcal{P}_{1,2}^{\text{sep}} = \frac{1}{2} \sum_{j=1}^S \int_0^A \sigma_{\text{sep}}(x,j) |w_1(x,y_j) - w_2(x,j)|^2 dx \quad (7)$$

$$\mathcal{P}_{1,2}^{\text{slip}} = \frac{1}{2} \sum_{j=1}^S \int_0^A \sigma_{\text{slip}}(x,j) |h_1 w_1'(x,y_j) + h_2 w_2'(x,j)|^2 dx \quad (8)$$

$$\mathcal{P}_{1,2}^{\text{rot}} = \frac{1}{2} \sum_{j=1}^S \int_0^A \sigma_{\text{rot}}(x,j) |w_1'(x,y_j) - w_2'(x,j)|^2 dx \quad (9)$$

where ' indicates the derivative with respect to x and σ_{sep} , σ_{slip} , and σ_{rot} are the Hooke's constants for springs resisting the relative separation, slippage and rotation, respectively. These functions are defined along the beams and have the single variable x . The subscripts of \mathcal{P} indicate the interaction between either top plate and beams ((1,2)), or bottom plate and the beams ((3,2)). A simpler model of the junction may let the separation constant σ_{sep} become very large, that is, the separation is nearly zero and the plate and the beams are always in contact. The total potential energy, \mathcal{P} in Eq. (1), is the sum of all potential energies from the individual components and the junctions. In [2] the slippage at the junctions have been proven to be necessary for predicting the vibration level over the frequency range shown in Fig. 3.

Method of solution

The method of solution chosen in this paper is the Fourier expansion method, which is ideal because of the rectangular shape of the structure. Furthermore the boundary of the plate is assumed to be simply supported. Thus the basis functions are sine-functions, further simplifying the solution. Different basis functions must be chosen when the boundary conditions are different. There are a few example sets of basis functions shown in [10] for free or clamped boundaries. Whatever the basis functions may be, a linear system of equations for the coefficients of the expansion over the chosen basis functions can be formulated. Hence the method of solution shown here will be applicable.

The deflection of the top plate, bottom plate and beams are expressed by

$$w_1(x,y) = \sum_{m,n=1}^N C_{mn}^{(1)} \phi_m(x) \psi_n(y) \quad (10)$$

$$w_3(x,y) = \sum_{m,n=1}^N C_{mn}^{(3)} \phi_m(x) \psi_n(y) \quad (11)$$

$$w_2(x,j) = \sum_{m=1}^N C_{mj}^{(2)} \phi_m(x) \quad (12)$$

for $j = 1, 2, \dots, S$, respectively. The basis functions are given by $\phi_m(x) = \sqrt{2/A} \sin k_m x$, and $\psi_n(y) = \sqrt{2/B} \sin \kappa_n y$, and the

wavenumbers are given by $k_m = \pi m/A$ and $\kappa_n = \pi n/B$. Note that the basis functions are orthonormal. The positions of the joists are given by $y = y_j, j = 1, 2, \dots, S$. Note that the number of terms in the series has already been truncated to N to construct the finite system for the numerical computation. The operations in Eq. (1) are then expressed using the column vectors of the coefficients, $\mathbf{c}_1 = (C_{11}^{(1)}, C_{21}^{(1)}, \dots, C_{NN}^{(1)})$,

$\mathbf{c}_2 = (C_{11}^{(2)}, C_{21}^{(2)}, \dots, C_{NS}^{(2)})$, and $\mathbf{c}_3 = (C_{11}^{(3)}, C_{21}^{(3)}, \dots, C_{NN}^{(3)})$. The variational formulation then becomes

$$\frac{1}{2} \begin{bmatrix} \mathbf{c}_1 \\ \mathbf{c}_2 \\ \mathbf{c}_3 \end{bmatrix}^t \mathbf{L} \begin{bmatrix} \mathbf{c}_1 \\ \mathbf{c}_2 \\ \mathbf{c}_3 \end{bmatrix} = \mathbf{f}^t \begin{bmatrix} \mathbf{c}_1 \\ \mathbf{c}_2 \\ \mathbf{c}_3 \end{bmatrix} \quad (13)$$

where \mathbf{L} is the matrix from the integrals and \mathbf{f} is the vector of the external forcing, whose elements are given by

$$\int_0^A \int_0^B f(x, y) \phi_m(x) \psi_n(y) dx \quad (14)$$

with zero padding for the parts corresponding to \mathbf{c}_2 and \mathbf{c}_3 . Here the forcing on the top plate is given by the Delta-function $f(x, y) = f_0 \delta(x - x_0, y - y_0)$ for some fixed point (x_0, y_0) and a constant force amplitude f_0 , which makes the integrals unnecessary. The following will give details how the elements of \mathbf{L} are obtained.

Substituting the Fourier series expansion for the deflections w_1 and w_2 into Eq. (8) gives

$$\begin{aligned} \mathcal{P}_{1,2}^{\text{slip}} = & \sum_{j=1}^S \int_0^A \sigma_{\text{slip}}(x, j) \left| h_1 \sum_{m,n=1}^N k_m C_{mn}^{(1)} \phi_m(x) \psi_n(y_j) \right. \\ & \left. + h_2 \sum_{m=1}^N k_m C_{mj}^{(2)} \phi_m(x) \right|^2 dx \end{aligned} \quad (15)$$

where $\phi_m(x) = \sqrt{2/A} \cos k_m x$. Then the above integral will be obtained by

$$\begin{aligned} & \int_0^A \sigma_{\text{slip}}(x, j) \phi_m(x) \phi_{m'}(x) dx \\ & = \frac{1}{A} \int_0^A \sigma_{\text{slip}}(x, j) \left(\cos \frac{\pi(m-m')}{A} x - \cos \frac{\pi(m+m')}{A} x \right) dx \end{aligned} \quad (16)$$

Notice that this integral is simply the Fourier cosine coefficients of the function $\sigma_{\text{slip}}(x, j)$, which can be computed using the fast Fourier transform (FFT). The matrix that corresponds to the separation σ_{sep} can be obtained by the similar derivation. More details for calculating the elements of the matrix are given in Appendix .

Substituting the series expansion for $w_1(x, y)$ into Eq. (2) for \mathcal{P}_1 leads to vector and matrix expression for the strain energy of the top plate. Let the function D_1 be separated into $D_1(x, y) = \bar{D}_1 + d_1(x, y)$ where \bar{D}_1 is the average stiffness and $d_1(x, y)$ is the deviation from the average. The elements of the matrix \mathbf{L} due to the varying stiffness $d_1(x, y)$ are computed

using the integral

$$\begin{aligned} & \sum_{m,n,m',n'=1}^N \int_0^A \int_0^B d_1(x, y) C_{mn}^{(1)} C_{m'n'}^{(1)} (k_m^2 + \kappa_n^2) (k_{m'}^2 + \kappa_{n'}^2) \\ & \times \phi_m(x) \phi_{m'}(x) \psi_n(y) \psi_{n'}(y) dx dy \end{aligned} \quad (17)$$

The constant stiffness \bar{D}_1 will give us a diagonal matrix with its element $\bar{D}_1(k_m^2 + \kappa_n^2)^2$ because of the orthogonality of the functions $\{\phi_m\}$ and $\{\psi_n\}$. The above integral is the formula for the Fourier cosine coefficients for the function $d_1(x, y)$, which can be found using the FFT. Furthermore, the products of *cosine* components are obtained by taking the real part of the FFT in x and y directions. The contribution from the bottom plate can be derived using the same formula for w_3 .

In order to include not-so-straight shape of beams, we here make a few assumptions and keep the model simple. The strain energy of the beams is computed in the same way as before by integrating over the x from 0 to A . The shape of j th beam is denoted by the function of $x, \theta_j(x)$. Thus the contact between the top plate and the beam is given by $y = y_j + \theta_j(x)$. We first take the Taylor expansion of the basis functions along the junction and omit the higher order terms because $\theta_j(x)$ is assumed small.

$$\psi_n(y_j + \theta_j(x)) \approx \psi_n(y_j) + \kappa_n \theta_j(x) \chi_n(y_j) \quad (18)$$

where $\chi_n(y) = \sqrt{2/B} \cos \kappa_n y$. Then the displacement of the plate along the junction, denoted by B_j are given by

$$w_1|_{(x,y) \in B_j} = \sum_{m,n=1}^N \{ \psi_n(y_j) + \kappa_n \theta_j(x) \chi_n(y_j) \} C_{mn}^{(1)} \phi_m(x) \quad (19)$$

The expansion for the twisting beams remains the same, i.e., $w_2(x, j) = \sum_{m=1}^N C_{mj}^{(2)} \phi_m(x)$. The energy contributions $\{ \mathcal{P}_{i,j}^{\text{slip}}, \mathcal{P}_{i,j}^{\text{sep}} \}_{(i,j)=(1,2),(3,2)}$ are now calculated from the above two expressions.

The potential energy due to the slippage at the twisting beams is modified and given by

$$\mathcal{P}_{1,2}^{\text{slip}} = \frac{\sigma_{\text{slip}}}{2} \sum_{j=1}^S \int_0^A \frac{|h_1 w_1'(x, y_j + \theta_j(x)) + h_2 w_2'(x, j)|^2}{1 + (\theta_j'(x))^2} dx \quad (20)$$

and the potential energy due to the separation is

$$\mathcal{P}_{1,2}^{\text{sep}} = \frac{\sigma_{\text{sep}}}{2} \int_0^A |w_1(x, y_j + \theta_j(x)) - w_2(x, j)|^2 dx \quad (21)$$

The constant σ_{sep} will be set to be large so to keep the plates and the beams in contact always. Here we assume that $|\theta_j(x)|^2 \ll 1$ and $|\theta_j'(x)|^2 \ll 1$. We then have the following simplified formula.

$$\mathcal{P}_{1,2}^{\text{slip}} = \frac{\sigma_{\text{slip}}}{2} \sum_{j=1}^S \int_0^A (h_1 + h_2)^2 |w_2'(x, j)|^2 dx \quad (22)$$

Substituting the series expansion of $w_2(x, j)$ gives

$$\mathcal{P}_{1,2}^{\text{slip}} = \frac{(h_1 + h_2)^2}{2} \sum_{j=1}^S \sum_{m,m'=1}^N k_{mm'} C_{mj}^{(2)} C_{m'j}^{(2)} \times \int_0^A \sigma_{\text{slip}}(x, j) \varphi_m(x) \varphi_{m'}(x) dx \quad (23)$$

SIMULATION OF RANDOM FUNCTIONS

The parameter functions, $d_i(x, y)$, $\sigma_{\text{slip}}(x, j)$ and $\theta_j(x)$, must be continuous and smooth because they model real components and junctions. Thus a series of discrete random numbers along the junctions or a plate surface will not be adequate. The methods of generating continuous smooth random functions have been studied by the signal processing community for many years (see [5, 11, 12]). Here the random functions are simulated using the method given in [6], in which a stationary random process is simulated using a prescribed PDF and PSD. As an example, the Gaussian distribution is used for the prescribed PDF here. There are two reasons for the choice of Gaussian distribution. First, the computation of normally distributed random functions is simple. Second, the author has not been able to find any measurements of the PDF of stiffness of timber products and their junctions. However there is a set of data of timber beam shape (2.5 m long beams) obtained by SCION Research in New Zealand (through personal communication). The histogram of the twist amplitude is shown in Fig. 4. The standard deviation of the measurements is approximately 0.8 mm. 301 beams were measured at 500 positions. Figure 4 shows the histogram of the measurements at all positions.

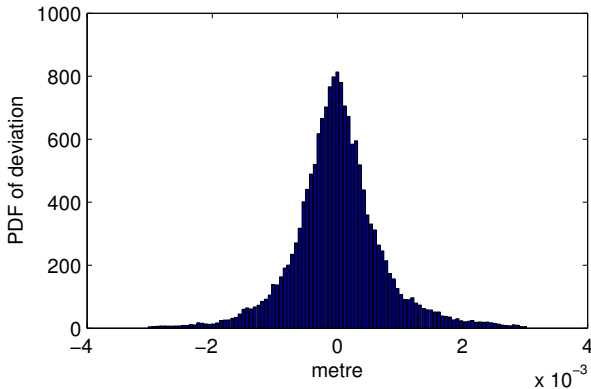


Figure 4. PDF of the twist of dried timber beams

Let $S(x)$ be a random function (or random process) for the spatial variable $0 \leq x \leq A$. We assume that $S(x)$ has the probability $p(S \leq s)$ and the probability density function $p_S(s)$ at any $x \in [0, A]$. The PDF $p_S(s)$ is assumed to be identical for any x . In other words $S(x)$ is a stationary process. It is further assumed that $S(x)$ can be expressed by

$$S(x) = \sqrt{\frac{2}{M}} \sum_{i=1}^M Q_i \cos(2\pi F_i x/A + \Phi_i) \quad (24)$$

where Q_i , F_i , and Φ_i are the random variables with some probability densities. Here M needs to be sufficiently large,

and is set to 100. The above series makes the mean of $S(x)$ zero for all $x \in [0, A]$. Let us follow the procedure given in [6] to formulate the PDFs for Q_i , F_i , and Φ_i .

First, the amplitudes $\{Q_i\}$ are assumed to be independent and identically distributed (i.i.d) random variable with PDF denoted by $p_Q(q)$ for $q > 0$. The phases $\{\Phi_i\}$ are also assumed to be i.i.d and their PDF is given by the uniform distribution in $[-\pi, \pi]$. The frequencies $\{F_i\}$ are i.i.d with the marginal first order continuous PDF denoted by $p_F(f)$ for $0 \leq f \leq V/2$.

The PDF of F_i and the PSD of $S(x)$ denoted by $P_S(f)$ are related by the formula

$$p_F(|f|) = \frac{2}{\mathbb{E}[Q^2]} P_S(f), \quad -\frac{V}{2} \leq f \leq \frac{V}{2} \quad (25)$$

where V is some large enough value so that $P_S(f)$ is nearly zero outside of the range $[-V/2, V/2]$. Setting the variance of S to be v^2 gives $\mathbb{E}[Q^2] = v^2$. The PSD function $P_S(f)$ here is chosen to be simple bell shaped, for example, $P_S(f) = K \exp(-(f - \delta)^2/2\mu^2)$, where K , δ , and μ will be varied to simulate effects of changing parameters. An example is shown in Fig. 7(left).

The characteristic function of the random function $S(x)$ is given by

$$\psi_S(\gamma) = \mathbb{E}[e^{i\gamma S}] = \left[\int_0^\infty p_Q(q) J_0\left(\frac{\gamma q}{\sqrt{M/2}}\right) dq \right]^M \quad (26)$$

where J_0 is the Bessel function of the first kind of order zero. The PDF for Q is related to the characteristic function of $S(x)$ by

$$p_Q(q) = q \int_0^\infty \left(\psi_S(v\sqrt{M/2}) \right)^{1/M} J_0(qv) v dv \quad (27)$$

which is the inverse Hankel transform. For the Gaussian parameter, the characteristic function is given by $\psi_S(\gamma) = \exp(-v^2 \gamma^2/2)$. Hence the inverse Hankel transform gives the following PDF of the amplitude

$$p_Q(q) = q \int_0^\infty \left(\exp\left(-\frac{Mv^2}{4}\right) \right)^{1/M} J_0(qv) v dv \quad (28)$$

The above integral has the closed form, which is

$$p_Q(q) = \frac{2q}{v^2} \exp\left(-\frac{q^2}{v^2}\right) \quad (29)$$

This is a Rayleigh PDF, which can be simulated from the two Gaussian random variables. For example, when the variance is $v^2 = 2$, then the amplitudes are simulated by $U_1 \sim \mathcal{N}(0, 1)$ and $U_2 \sim \mathcal{N}(0, 1)$, then $Q \sim \sqrt{U_1^2 + U_2^2}$. The histogram of the simulation result is shown in Fig. 5 along with the target PDF of normal distribution with the standard deviation $\sqrt{2}$. The slippage function $\sigma_{\text{slip}}(x, j)$ will be generated using the distribution shown in Fig. 5. The standard deviation of the distribution will be set to be $3 \times 10^6 \text{ Nm}^{-1}$, which is 10% of the average slippage resistance constant $3 \times 10^7 \text{ Nm}^{-1}$. This

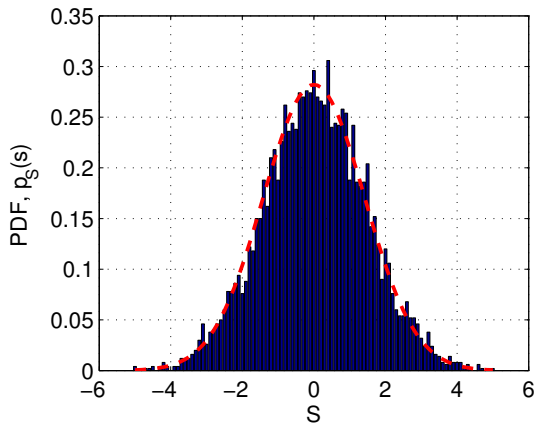


Figure 5. PDF of the simulated 1 dimensional function (not scaled) and target normal distribution (dashed) with standard deviation $\sqrt{2}$

average value comes from the experimental measurements in [2] for the junction between a plywood panel and a timber joist.

The stiffness function $d_1(x,y)$ can be similarly simulated using the expansion

$$d_1(x,y) = \frac{1}{M} \sum_{i,j=1}^M Q_{ij} \cos\left(\frac{2\pi F_i x}{A} + \Phi_i\right) \cos\left(\frac{2\pi G_j y}{B} + \Psi_j\right) \quad (30)$$

where the coefficients $\{Q_{ij}\}$ are random variables with the Rayleigh distribution, and Φ_i and Ψ_j are uniformly distributed random values in $[-\pi, \pi]$. The frequencies F_i and G_j are also generated from Eq. (25) and Eq. (26). In order to prove that the above expression correctly simulates the random realization in 2-dimensional space with the correct PSD and PDF, one needs to extend the derivation given in [6], which is beyond the scope of this paper. Instead, only the simulated realizations are numerically confirmed here. The histogram of the simulations is shown in Fig. 6 with the target PDF of normal distribution with the standard deviation 1. Again the PSD of d_1 (and d_3) is chosen to be a simple bell shaped function. An example is shown in Fig. 7(right). In the numerical simulations, the standard deviation of the stiffness of the plates $d_1(x,y)$ and $d_3(x,y)$ will be set to be 3% of the average stiffness of the plates in the following section. The value 3% has been chosen because the effects of inhomogeneous stiffness start to show at that value.

NUMERICAL COMPUTATION

The computation results of the solution $w_1(x,y)$ are studied here using the simulated functions $\sigma_{\text{slip}}(x,j)$, $d_i(x,y)$ and $\theta_j(x)$. The number of terms for the Fourier expansion was set to be $N = 20$. All computation was done using MatLab on a standard personal desktop computer. No special numerical packages were used. The parameters for the beams and the plates are chosen from the well used values for plywood and timber beams, $E_1 = E_3 = 10^{10}$ Pa, $E_2 = 1.4 \times 10^{10}$ Pa, $m_1 = m_2 = m_3 = 500 \text{ kgm}^{-3}$, $A = 5.1$ m, $B = 3.2$ m, $h_1 = h_3 = 0.015$ m, $h_2 = 0.3$ m, $\alpha = 0.3$, $y_j = jB/8$, $j = 1, 2, \dots, 7$, and the width of

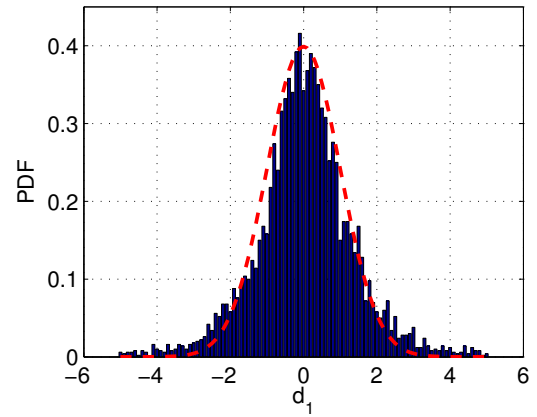


Figure 6. PDF (not scaled) of the simulated $d_1(1.2,1.2)$ and target normal distribution (dashed) with standard deviation 1

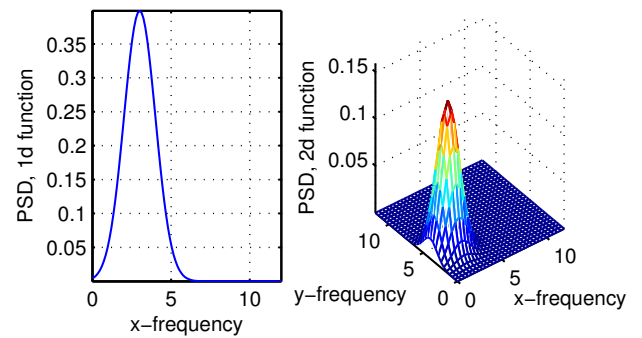


Figure 7. Examples of PSDs for the 1 and 2 dimensional random functions

the beams is 0.045m. The average slippage constant is $3 \times 10^7 \text{ Nm}^{-1}$, which was determined from the experiments in [2]. The location of the forcing is $(2.85, 2.1)$ with $f_0 = 1000\text{N}$.

The PSD of random functions is chosen to mimic what might be happening at the junctions. It is not obvious to the author how the conditions can be measured in real composite structures. On the other hand, the PSD of the shape $\theta_j(x)$ may be chosen based on actual measurements. Here each PSD is simply set to be a bell shaped smooth curve with a peak (Fig. 7). Two different peak positions have been used to compare the effects of spatial variations on the solution.

Figures 8 and 9 show the distributions of the variance of the surface deflection of the top plate when slippage and stiffness are randomized, respectively. There seems to be no particular rule how the variance is distributed over the plate. The distribution varies as the frequency changes. The slippage affects lower frequency vibrations than it does the higher frequency ones as shown in Figs. 11(a) and (b). In Fig. 8, the variance distribution changes from even to localized distribution as the frequency increases. Figure 9 shows that the stiffness affects the higher frequency vibrations evenly over the plate. On the other hand the random stiffness shows localized effects at lower frequencies. Figure 10 shows the distributions of the variance of the surface deflection of the top plate when there is small random twist in the beams. The variance is more

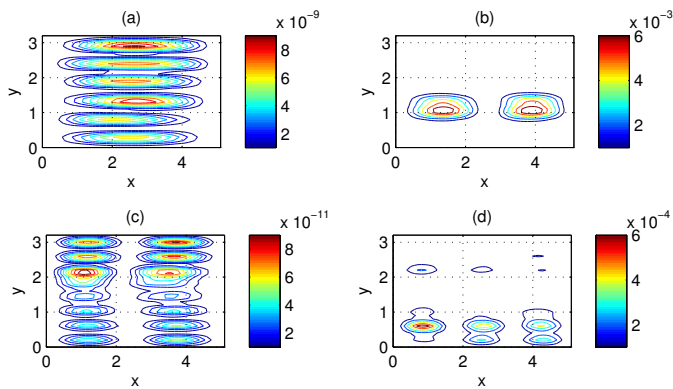


Figure 8. Contour plot of the variance distribution of the deflection over the top plate when slippage is random at 100 Hz (a), 150 Hz (b), 200 Hz (c) and 250 Hz (d)

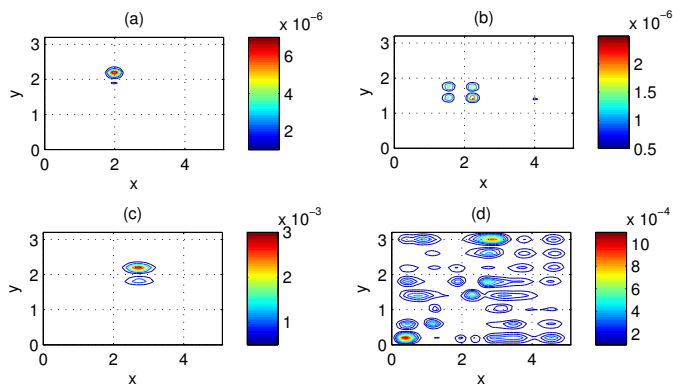


Figure 9. Contour plot of the variance distribution of the deflection over the top plate when stiffness of the two plates is random at 100 Hz (a), 150 Hz (b), 200 Hz (c) and 250 Hz (d)

evenly spread over the plate compared to Figs. 8 and 9.

Figures 11 and 12 show the root-mean-square velocity at the frequencies from 150 Hz to 250 Hz. The vertical axis is in a log scale without any reference velocity. The velocity is not converted to decibels because this study is not about sound pressure. The slippage is randomized for Figs. 11(a) and (b), and the stiffness is randomized for Figs. 11(c) and (d). Figures 11(a) and (b) correspond to the PSDs with peaks at spatial frequencies at 3 m^{-1} and 5 m^{-1} , respectively. Figures 11(c) and (d) correspond to the PSDs with peaks at spatial frequencies of (x,y) components at $(2 \text{ m}^{-1}, 4 \text{ m}^{-1})$ and $(4 \text{ m}^{-1}, 8 \text{ m}^{-1})$, respectively. The randomness of the slippage affects the surface velocity near the resonant frequencies at lower frequencies. However there is little effect showing between 220 Hz and 240 Hz, even though there are several resonance frequencies in that range. The random stiffness affects the vibration at the higher frequencies and the vibration level is flattened. Furthermore the variance of the vibration level is small. In both slippage and stiffness cases, the smaller variations of the random functions lead to smoother vibration levels. Figure 12 shows the root-mean-square velocity when there is small random twist in the beams. The standard deviations of the twist are 1.25 mm (Fig. 12(a)) and 2.5 mm (Fig. 12(b)), which are

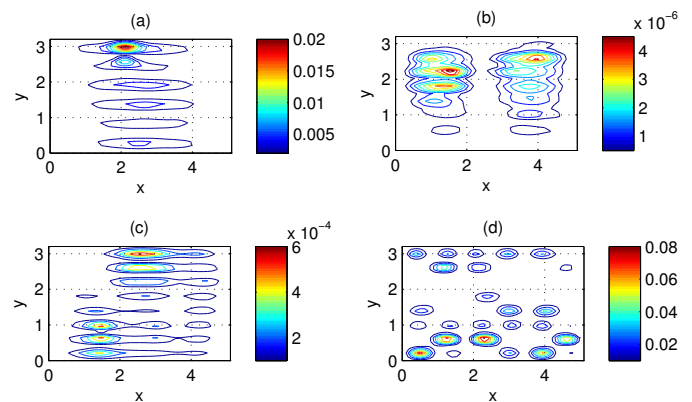


Figure 10. Contour plot of the variance distribution of the deflection over the top plate with the random twist in the beams at 100 Hz (a), 150 Hz (b), 200 Hz (c) and 250 Hz (d)

larger than the measured standard deviation shown in Fig. 4. The larger values were chosen to show clearly the effects of the twist. The larger twist affects the higher frequency vibrations in a similar way the random stiffness does in Fig. 11.

The numerical simulations show that the random irregularities affect the vibration over the whole plate surface. Thus the modelling of a composite structure, even this moderately complex double-leaf plate, requires the random irregularities to be taken into account. In particular, both Figs. 11 and 12 show that the vibrations at the higher frequencies are greatly affected by the random functions.

SUMMARY AND CONCLUSION

The simulations of the vibration of a double-leaf plate with random parameters have been carried out. The parameters are slippage, stiffness and small twist of beams, which are given by continuous smooth functions of x or (x,y) . The computation cost of the simulations is kept low using the Fourier series solutions and the variational formulation. The simulations show that each random function affects the vibration differently in different ranges of frequencies. Also the spatial distributions of the variance show that the randomness along the junctions (slippage and twists) leads to more even spread over the plate than that of the random stiffness results. More definitive studies are needed to understand the effects of random parameters on the vibration. The method shown in this paper can include more random parameter functions as additional energy terms in the variational formulation. The method of solution changes little because only the elements of the matrix \mathbf{L} in Eq. (13) that correspond to a new random function will need to be modified.

REFERENCES

- [1] J. Brunskog, "The influence of finite cavities on the sound insulation of double-plate structures", *Journal of the Acoustical Society of America* **117**, 3727–3739 (2005)
- [2] H. Chung and G. Emms, "Fourier series solutions to the vibration of rectangular lightweight floor/ceiling structures", *Acta Acustica United with Acustica* **94**, 401–409 (2008)

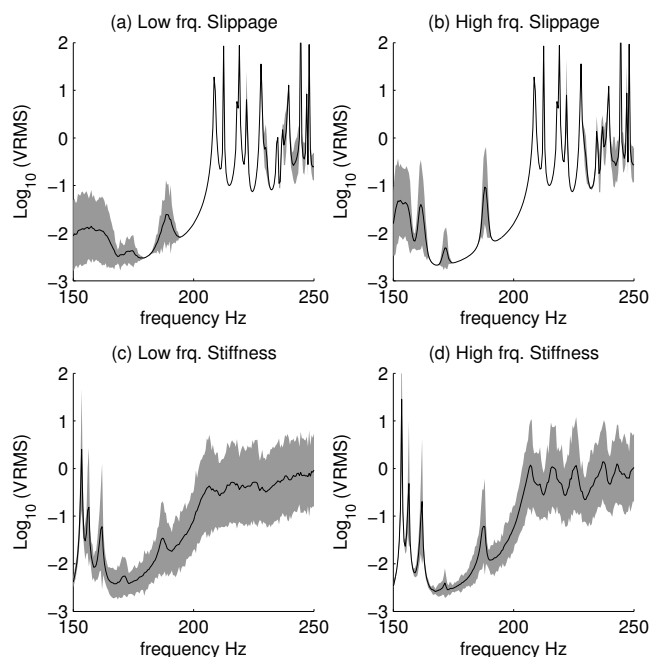


Figure 11. Velocity root mean square of when the slippage (a), (b) and the stiffness (c), (d) are randomized. The variance is shown by the gray area, and the mean of the simulations is shown by solid curve

- [3] R.J.M. Craik, "Sound transmission through double leaf lightweight partitions. Part I: Airborne sound", *Applied Acoustics* **61**, 223–245 (2000)
- [4] R.J.M. Craik, "Sound transmission through double leaf lightweight partitions. Part II: Structure-borne sound", *Applied Acoustics* **61**, 247–269 (2000)
- [5] M. Grigoriu, "Simulation of stationary non-gaussian translation processes", *Journal of Engineering Mechanics* **124**, 121–126 (1998)
- [6] S. Kay, "Representation and generation of non-gaussian wide-sense stationary random process with arbitrary PSDs and a class of PDFs", *IEEE Transactions on Signal Processing* **58**, 3448–3458 (2010)
- [7] B.R. Mace, "Periodically stiffened fluid-loaded plates, I: Response to convected harmonic pressure and free wave propagation", *Journal of Sound and Vibration* **73**, 473–486 (1980)
- [8] B.R. Mace, "Periodically stiffened fluid loaded plates, II: Response to line and point forces", *Journal of Sound and Vibration* **73**, 487–504 (1980)
- [9] B.R. Mace, "Sound radiation from a plate reinforced by two sets of parallel stiffeners", *Journal of Sound and Vibration* **71**, 435–441 (1980)
- [10] I.H. Shames and C.L. Dym, *Energy and finite element methods in structural mechanics*. Taylor & Francis, New York, SI units edition, 1991
- [11] M. Shinozuka, "Simulation of multivariate and multidimensional random process", *Journal of the Acoustical Society of America*, **49**, 357–368 (1971)
- [12] M. Shinozuka and C.M. Jan, "Digital simulation of random processes and its applications", *Journal of Sound and Vibration* **25**, 111–128 (1972)

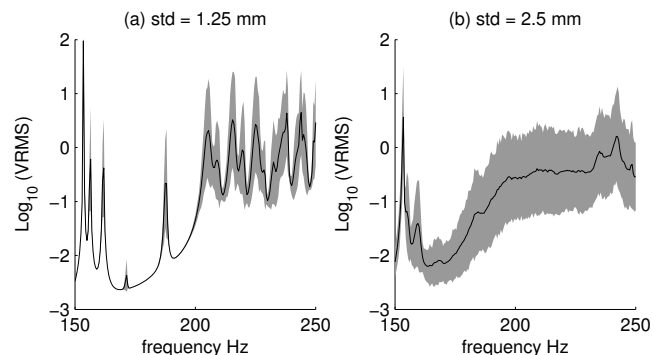


Figure 12. The root-mean-square velocity when there is small random twist in the beams. The variance is shown by the gray area, and the mean of the simulations is shown by solid curve

Appendix - Formulae for the simple coupling between a plate and beams

When the coupling parameter σ_{sep} is constant along the beams, the lagrangian matrix for the coupling energy contribution is given by

$$\frac{\sigma_{sep}}{2} \sum_{j=1}^S \int_0^A |w_1(x, y_j) - w_2(x, j)|^2 dx \quad (A1)$$

The above expression can be expressed by the vector operation

$$\frac{1}{2} \begin{pmatrix} \mathbf{c}_1 \\ \mathbf{c}_2 \end{pmatrix}^t \begin{bmatrix} \sigma_{sep} M^t M & -\sigma_{sep} M^t \\ -\sigma_{sep} M & \sigma_{sep} I \end{bmatrix} \begin{pmatrix} \mathbf{c}_1 \\ \mathbf{c}_2 \end{pmatrix} \quad (A2)$$

where the matrix M represents the operation

$$\sum_{n=0}^N C_{mn}^{(1)} \psi_n(y_j) \quad (A3)$$

Then, the total matrix is given by

$$\begin{bmatrix} L_1 + \sigma_{sep} M^t M & -\sigma_{sep} M^t \\ -\sigma_{sep} M & L_2 + \sigma_{sep} I \end{bmatrix} \quad (A4)$$

where I is the identity matrix. The matrices for the interaction between the beams and the bottom plate can be obtained in a similar way. We have the complete matrix

$$\begin{bmatrix} L_1 + \sigma_{sep} M^t M & -\sigma_{sep} M^t & 0 \\ -\sigma_{sep} M & L_2 + 2\sigma_{sep} I & -\sigma_{sep} M \\ 0 & -\sigma_{sep} M^t & L_3 + \sigma_{sep} M^t M \end{bmatrix} \quad (A5)$$

where L_i , $i = 1, 2, 3$ are the strain and kinetic energy matrices for the top plate, the beams, and the bottom plate, respectively.

ADDING NOISE TO QUIET ELECTRIC AND HYBRID VEHICLES: AN ELECTRIC ISSUE¹

Ulf Sandberg

Swedish National Road and Transport Research Institute (VTI), Linköping, Sweden

ulf.sandberg@vti.se

It has been suggested that hybrid and all-electric automobiles are so quiet at low speed in electric drive that they constitute a safety hazard for pedestrians and bicyclists. This trait has been especially troubling to vision-impaired people who rely on sound cues to avoid approaching vehicles. Assumptions have been made linking the quietness of such vehicles with fatalities and serious injuries. The U.S. Pedestrian Safety Enhancement Act of 2010, requires the use of Audible Vehicle Alerting Systems (AVAS) in hybrid and all electric vehicles. Rules are now being developed and are expected to be issued by January 2014. Similar regulations are being promulgated in Japan and the European Union. The UN/ECE is developing a Global Technical Regulation after extensive preparatory work. SAE International and ISO are developing a method of measuring the lowest accepted noise level for vehicles. This article first notes firm evidence that the noise difference between electric-driven and internal combustion engine (ICE) vehicles exists only at speeds below about 20 km/h; also that AVAS makes vehicles traveling at low speeds detectable from a longer distance, absent masking background noise. Some electric and hybrid cars on the market already have AVAS installed. The author explores the assumptions related to the problem in regard to traffic safety and the harmful effects of noise on humans. One statistical study from the United States seems to suggest that vehicles driven in electric mode cause relatively more accidents involving pedestrians than do ICE vehicles. However, multiple studies in the U.S., Japan and Europe leave this causal relationship unconfirmed. The author then shows that quiet vehicles, very hard to hear when approaching at low speeds, existed in urban traffic already many years before hybrid cars became common, and if quietness would create accidents this should have been apparent already earlier and not be something occurring only when hybrid and electric cars entered the market. A number of non-acoustical ways to alert pedestrians, not the least blind people, of quiet vehicles near them are discussed and suggested in the article. The article also describes the intensive work to explore the problem as well as to develop and specify AVAS systems that has been made from 2008 until now. The author argues that it would be more beneficial to human health and safety to reduce the maximum noise of vehicles rather than increasing the minimum noise of them. Consequently, the article ends with the recommendation to discontinue the work with AVAS, to limit rather than require the use of such systems, and instead focus on limitation of the worst masking noise emissions in urban areas.

A NEW PROBLEM IDENTIFIED

It has been suggested in later years that road vehicles, driven in electric mode, either hybrid electric vehicles (HEV) or all-electric vehicles (EV), are so quiet that they constitute a safety hazard for vulnerable road users (VRU) in traffic, especially to blind pedestrians. Following such fears, EVs and HEVs have sometimes in various documents and press articles been portrayed as “some kind of shark in the water” [1].

The “problem” seems to have been noted first in the United States in 2008 in meetings with the car industry and the US DoT following complaints by the National Federation of the Blind (NFB) against the growing trend for automobile manufacturers to design extremely quiet vehicles. Already in 2007, the SAE International started to work out a draft specification J2889-1 for the measurement of “minimum noise” of vehicles. Due to, among

other things, pressure from the California Legislative Counsel in 2009 [2], in 2010 the Pedestrian Safety Enhancement Act was introduced in the US, and approved by the President in January 2011, requiring “means of alerting blind and other pedestrians of motor vehicle operation”. This, in practice, requires the addition of artificial sound, also known as acoustic alerting systems, to EVs and HEVs [3].

The Japanese automotive industry, enjoying great commercial success with vehicles such as the Toyota Prius, seems to have reacted quickly to this potential threat to hybrid vehicles and already in 2009 had established own work towards Japanese standards for acoustic alerting systems for HEVs and EVs [4].

Internationally, a special informal group “Quiet Road Transport Vehicles (QRTV)” to deal with this “problem” was established within the UN/ECE/WP29/GRB in 2010 [5]. Japan had then already been working on guidelines for approaching vehicle alerting systems (AVAS), which later were essentially accepted also by the QRTV. Following the QRTV recommendations, the

¹ Originally published in Noise/News International, Vol. 20, No. 2, June 2012, and a shorter version reprinted with permission.

GRB (noise) group within the UN ECE [6] accepted them, which is now also part of a present proposal to the European Parliament regarding more stringent vehicle noise limits [7].

Concerning standardisation, the SAE International draft specification J2889-1 for the measurement of “minimum noise” of vehicles is at “Measurement of minimum noise emitted by road vehicles” was initiated also within the ISO; largely based on the SAE draft. The intention is to work out an international standard ISO 16254 for measurement of “minimum noise” of a vehicle.

Never before has the author in his 38 year career in transportation noise seen any subject being so quickly and non-critically accepted by the legislators, vehicle industry, university acoustics departments, acoustic consultancies and other research organisations; and as it appears almost in total agreement. This is in sharp contrast to when it comes to reducing vehicle noise. Vehicle noise standards in Europe and as specified by the UN ECE (accepted by several nations outside Europe) have been unchanged since 1996 and when now, after 16 years, somewhat lower limits are proposed, the industry and some MPs are hesitant [9]. On the other hand, the interest in adding sound to quiet vehicles is enormous.

The vehicles operating at exceptionally low noise levels are mostly called “quiet vehicles”. The systems that are intended to save the world from the assumed pedestrian road massacres have been named Audible Vehicle Alerting Systems (AVAS), although some documents let the A stand for “Approaching” instead of “Audible”.

In this paper, the author presents a review and discussion of the problem, based on his earlier conference papers [10, 11], but with focus on the development during 2011-2012. This article is an abridged version of a much longer article appearing in Noise/News International earlier in 2012 [12].

NOISE EMISSION PROPERTIES

The very low noise emission from electric motors means that power unit noise is almost totally absent for EVs and HEVs in electric mode, and that only tyre noise remains. The effect will be that at low vehicle speeds, approximately up to 20 km/h for cars and up to 50-70 km/h for heavy vehicles, the acoustic environment will improve substantially.

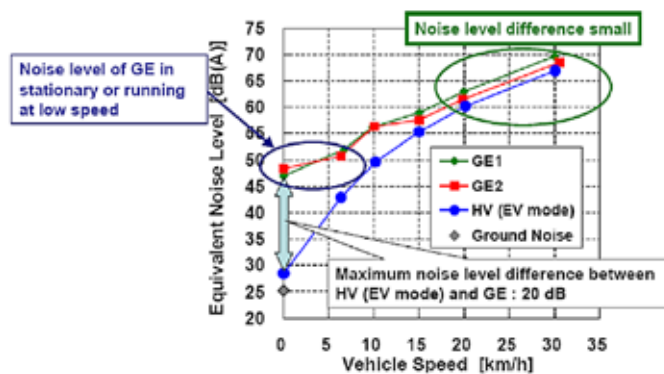


Figure 1. Equivalent A-weighted noise levels from an HEV car, compared to two ICE cars in Japan at low speeds [13]

This subject was the main issue in an earlier paper by the author [10]. It has been shown by many researchers, with consistent results, that it is only at speeds below approximately 20 km/h for cars when there is a significant difference in noise emission from ICE vehicles and vehicles driven in electric mode. The example shown in Figure 1 is typical of most test results.

TRAFFIC SAFETY ASPECTS

Traffic accidents due to lack of sound cues?

There is no doubt that acoustical cues are important in the interactions between road users of all kinds; and in particular among the visually impaired pedestrians. However, this does not mean that the lack of sound cues automatically lead to serious traffic accidents. There are many other things of importance and the lack of sound cues is associated only with very low speeds.

As yet, the lack of sound cues has never been identified in accident statistics as a major cause of accidents; at least as far as this author has found in literature searches and when asking colleagues specialised in traffic accident statistics. The only exception is a study presented by NHTSA, which concluded that [14]:

- “This study found that HEVs have a higher incidence rate of pedestrian and bicyclist crashes than do ICE vehicles in certain vehicle maneuvers”
- “In situations where cars drive slowly (slowing down, stopping, backing up, parking maneuvers) hybrid cars were involved twice as much compared to conventional cars”.

When looking critically at these conclusions, one finds that the evidence of the conclusions is rather weak and that alternative causes for the findings are possible [10, 15]. An update of the NHTSA report when more data had been added became available in 2011, but the conclusions are essentially the same [16].

Other studies of statistics, in the Netherlands and Japan, have been unable to confirm this [15]. Another US study of deaths and accidents of blind people involving Toyota Prius (this car was especially studied as it dominated the US HEV park) gave a different picture [18]:

- No deaths of legally blind pedestrians 2002-2006 involved a Prius or any other hybrid vehicle (out of an average of five legally blind pedestrians per year killed in US motor vehicle accidents)
- For all US pedestrian deaths, a Prius was no more likely to be involved in a pedestrian death than the average passenger vehicle.

A study in the U.K. to explore the safety aspect of quiet vehicles was undertaken for vehicle accident statistics in the period 2005-2008 and showed that [18]:

- Relative to the number of registered vehicles, for the combined vehicle group of passenger cars, car-derived vans and vans < 3500 kg GVW, EV/HEV vehicles were 10 % less likely to be involved in a collision with a pedestrian than ICE vehicles

- Although the relative number of EV/HEV vehicles involved in accidents is smaller, proportionately more of these vehicles hit a pedestrian than ICE vehicles
- The reason for the latter observation may be that these accident rates reflect different usage patterns of EV/HEV vs ICE vehicles
- There were only two EV/HEV accidents (out of 497) involving a collision with a pedestrian who was disabled in some way (CF810) so it was not possible to make a judgment on the perceived risk to vision-impaired pedestrians.

It is indeed strange that such extensive activities as started on this subject are not based on robust traffic accident data. As so many pedestrian accidents happen, and we have now had quiet vehicles for a long time; if lack of sound were a problem, it should be relatively easy to identify this in current accident statistics.

The common procedure is that a problem is addressed and solved when the problem has been reliably identified. In this case, the safety problem seems to be more psychological than “real” and yet work is extremely intensive to solve the assumed problem. It seems that one has started in the “opposite end” to what is customary. If legislators and industry had acted with equal speed and efficiency when it comes to high noise emissions from vehicles, it would have been wonderful.

Special fears of the blind

Organisations such as the National Federation of the Blind (NFB) in USA [19] and the World Blind Union (WBU) have put pressure on the NHTSA and the QRTV in order to produce a solution to the problem that they identify as the lack of sound cues for this group of people who depend largely on sound cues. Some national organisations for the blind have also reacted. The WBU was rather critical to the guidelines for AVAS produced in 2011; the organisation thought that the guidelines are not sufficiently strong or far-going [20].

There is of course no doubt that the blind perceive their situation as worrying when the sound cues are becoming less audible. Yet, this does not necessarily lead to accidents. The situations where, the situations where and when the EVs and HEVs may pose a problem due to weak sound are relatively few and not with very serious effects as seen in relation to the entire traffic work.

We have had numerous electric driven vehicles for a very long time and we have had relatively quiet ICE vehicles, some of which are almost equally quiet as EVs, for at least 15 years. Thus, the reaction of the blind organisations should have come much earlier, and be a result of many more encounters than from electric drive, if lack of sound were a “real” accident problem.

However, at the time, it must be recognised that the problem is at least a psychological problem, since the blind see their possibilities to navigate safely as pedestrians in traffic relying on sound cues becoming reduced with the increasing number of EVs, HEVs and quiet ICE cars.

The author has searched very extensively on the web (in English and Swedish) for reports about accidents where blind pedestrians have been injured due to quietness of the car. No such case has been found to date (July 2012), whereas cases when pedestrians are killed due to distraction by using electronic

devices in traffic (not involving quiet cars) are frequent.

Distraction due to use or misuse of sound

Especially for the blind people it must seem strange, if not stupid, that a large proportion of the seeing people deliberately choose to totally neglect sound cues from vehicles and from other pedestrians. More and more pedestrians and joggers, in many situations a majority of them, wear some kind of system producing music or speech in earphones, or they use cell phones, which effectively obscure sounds of approaching vehicles. Figure 2 shows an example. It may sometimes be impossible even to hear warning sounds as was, e.g., an observation in the study in [21].

A study conducted by three U.S. universities in 2005 indicated that 48 percent of pedestrians using a cell phone stepped into a crosswalk in what the researchers defined as “unsafe” condition, compared to 25 % not using cell phones [22].

These people have acceptable vision, but often they seem to fail concentration to the traffic as they talk or listen to whatever they use the electronic equipment for. The latest trend is to walk around and read and write text messages. It is not necessary to watch a pedestrian crosswalk many minutes until one will see a situation as the one in Figure 3. This may well be the unsafest behavior of all.

In the Australian state of New South Wales, this is already identified as a serious problem. In the last 12 months 26 Sydney pedestrians died after being hit by vehicles, twice as many as the year before. Experts say that both drivers and people crossing roads are distracted by texting or listening to technology like iPods and mobile phones [23]. “Last week an 18-year-old woman listening to music on an iPod was hit this week as she crossed a road in Marrickville, Sydney. Maybe if she wasn't listening to an iPod she would have heard the horn of a car, the screech of tyres or other people warning her”, it was reported [23].

The New York State “distracted walking legislation”, first proposed in 2007, would keep pedestrians who are in crosswalks from using handheld cell phones, Blueberries, MP3 players such as iPods, PDAs and similar attention-grabbing devices. The proposal restricts the law to cities with a population of at least 1 million, meaning only Manhattan [24]. However, as far as this author could find, it has not yet materialised into a law.



Figure 2. Woman crossing a street while listening to something in her earphones (Sydney, Australia) (photo by the author)

Since the number of people choosing to neglect sound cues, as described above, may outnumber the blind by several magnitudes, this author wonders if not this would be a far greater accident cause than the missing acoustical cues for the blind. And, sadly, this is a self-chosen situation among seeing pedestrians.

QUIET VEHICLES IN OUR SOCIETY

In a previous paper by this author on this subject [10], a number of vehicle types are described which have operated in traffic since many years ago and which produce no or very low propulsion noise (that list is supplemented here with newer findings by the author):

- Volvo and Scania supplied city busses for the Scandinavian market which met very stringent noise limits already in the early 1970's. These had encapsulated diesel engines at the very rear (Scania) or in the middle (Volvo) resulting in mainly tyre noise being heard towards the front in cruising or coasting conditions.
- Also modern CNG-driven busses with rear engine used in some Swedish cities, are very quiet when approaching and also when leaving a bus stop; propulsion noise can hardly be heard towards the front.
- From 1996, cars in Europe have had to meet the same noise level limits for type approval as today (74 dB(A)). The spread in results has been and is dramatic; some have measured only 68 dB(A). The more fancy variants of these cars are usually designed with quiet (ICE) engines since this gives an impression of a luxury car and is a selling argument. In many countries such luxury cars and limousines have been common for many decades. It is undisputable that such cars are so quiet that it may be hard to hear other than tyre/road noise from them when they approach a listener at cruising or coasting; even at very low speeds.
- Bicycles may not be so much used in most US or Australian cities but in some European cities (such as in the Netherlands, Denmark and Sweden) they are the dominating vehicle types for personal transportation. What you hear from them

is weak tyre noise and maybe sometimes chain noise and a bell, but they run very close to pedestrians, even among them. Collisions pedestrian-bicyclist at 20-30 km/h may be fatal.

- Trackless trolley bus networks have existed or exist in e.g. Vancouver, San Francisco, Philadelphia, Zurich, Arnhem, Geneva, and three cities in Poland. In some cases such vehicle types have been used for several decades. They are essentially as quiet as a regular EV. See Figure 4. Note that tyre noise from heavy trucks and buses is sometimes no worse than from automobiles; depending on tyre equipment fitted [25].
- On the 16th Street Mall in Denver, CO, the main shopping and entertainment street, partly only open for pedestrians and busses, hybrid busses which are very quiet have been operating for approximately a decade. No accidents due to the quietness had been reported, according to the Denver transit company in 2010, but the busses have bells that may be activated by the driver when needed, and often is so when starting from a stop.

Increasingly popular, particularly in densely populated urban areas, electric two-wheel vehicles is a category that includes Segways, electric bicycles, electric kick scooters, electric motorcycles, and electric scooters. Walmart sells a range of electric scooters that can run at up to 25 km/h.

None of these vehicle types, busses and electric two-wheelers, which run in quiet mode especially close to pedestrians, have been considered in the work so far by QRTV, although they are not formally excluded, as all attention has been focused on cars.

It is concluded that pedestrians and bicyclists have been exposed to numerous quiet vehicles (where no or very little propulsion noise can be heard) for many years, even before the EV and HEV era; some very quiet vehicle types have been around for decades.

Therefore, the potential problem of missing sound cues is not new and occurring only recently with the modern EVs and HEVs. It has existed for a long time and yet significant accident types caused by the quietness of vehicles have not



Figure 3. Woman crossing a street while “texting” (Braga, Portugal) (photo by the author)



Figure 4. Trolley bus in Seattle, USA, in 2008 (photo by the author)

been reported, as far as this author has found. Also, blind people have of course been exposed to this situation for a long time.

CRITICAL DRIVING CONDITIONS

There is a wide consensus, supported by data in [10], that EVs and HEVs in general are significantly quieter than ICE (light) vehicles only at the following driving conditions:

- At speeds below approx. 20 km/h while ICE vehicles would be using the lowest gear. This hardly ever includes decelerating and stopping at a traffic light, since first gear would not normally be engaged, but it does include the first few seconds of starting from standstill. Whenever 2nd or higher gear is used, tyre and overall noise is approx. the same for EVs/HEVs as it is for ICE vehicles.

- When reversing; for example backing out from a parking lot.

It follows that if artificial sound is added with the aim to make EVs and HEVs equally recognisable in traffic as regular ICE vehicles, this sound shall be in operation only when driving 0-20 km/h and when reversing (“back-up”).

It seems that the many proponents of adding extra sound to EVs and HEVs have not yet understood that the assumed safety problem would be potentially greater for trackless trolley busses and other heavy vehicles than for light vehicles, as the “loss” of sound in electric drive versus combustion is much bigger for the heavier vehicles; yet AVAS for these have not yet been proposed (?). If they will ever be proposed, the conditions would include cruising and coasting at speeds lower than 30-50 km/h and accelerations up to probably around 60 km/h, and this would normally mean a dramatically larger effect than for light vehicles, but it depends on how much of the “lost” sound that will be compensated for.

Note that at speeds lower than 20 km/h, stopping distance (reaction and braking times) is shorter than 6 m.

It follows that an accident involving a car-to-pedestrian collision would potentially happen more frequently for EV/HEVs without extra sound than for ICE vehicles only when the EV/HEV is starting or turning from standstill up to about 20 km/h. As stopping distance is less than 6 m in such cases, it means that the driver must be drunk, very distracted or extremely slow in detecting a (blind) pedestrian who is suddenly stepping out into the driving lane, normally displaying his white cane. One situation where the problem may be bigger is if the pedestrian stands hidden behind a large object as seen from the driver's position.

For such an accident to be more likely for EV/HEV without extra sound than for ICE vehicles, an additional condition is that the background noise must be low enough not to mask the ICE vehicle's propulsion noise at speeds lower than some 20 km/h. This requires background noise expressed as L_{Aeq} to be lower than approx. 60 dB (which follows from the normal noise levels emitted at such speeds). On a sidewalk in a city, this is rarely the case; one would rather have to be in a suburb or a semi-rural village [26].

Given the conditions mentioned in the previous two paragraphs, it should be obvious that in order for an accident to happen more frequently or more likely for EV/HEVs without extra sound than for similar ICE vehicles, quite rare conditions

must coincide. This author believes that occasions outlined above happen, but only extremely rarely, which may explain why this has not yet been identified as a significant type of accident for EV/HEVs in particular.

ACCIDENTS AT LOW SPEED

Despite the quite unlikely case of a car-pedestrian collision at speeds below 20 km/h there will be cases when it happens. How serious would such collisions be? In an international literature review about fatality risk as a function of impact speed, it appeared that below 20 km/h the risk of a fatality is close to 0 % [27]; see Figure 5.

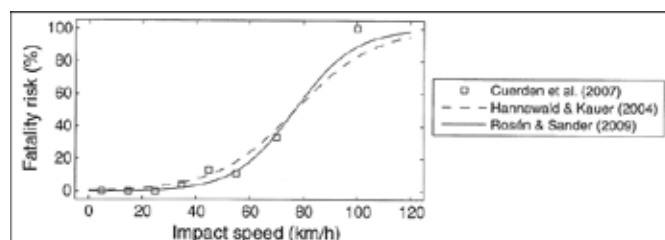


Figure 5. Fatality risk in pedestrian-to-vehicle collisions as a function of impact speed, as determined in three different studies [28]

When looking at risks of severe injury, at an impact speed of 20 km/h, the risk is < 5 %. If risks for a light injury as well as a severe injury are added, the risk is < 25 % [28].

Consequently, making EV and HEV vehicles equally noisy as ICE vehicles, at speeds below about 20 km/h, would have no measurable effect on fatalities and a very limited effect on severe injuries, when a collision happens.

PERCEPTION OF NOISE FROM VEHICLES

There have been numerous studies of how people perceive the noise from EV and HEV versus ICE vehicles. Generally, such studies have been made using a jury of observers who are asked to react when they can hear an approaching vehicle, while the distance to this vehicle is measured. Some studies have been made in laboratories; some have been made outdoors.

There is no point here in mentioning all the studies, since they give rather consistent results; only two of the better will be mentioned. In a German outdoor study using a jury of 12 visually impaired persons, at an approach speed of 10 km/h a Nissan Leaf was detected at distances of 4-7 m while a Lexus IS 250 was detected at 8-20 m (median values). At a speed of 20 km/h, Nissan Leaf was detected at approximately 20 m, while the Lexus was detected at 16-33 m [29]. Thus at 20 km/h there was no distinct difference between the EV and the ICE car; whereas at 10 km/h there was a significant difference. But remember that at 10 km/h (2.8 m/s), stopping distance (reaction time and braking) should be close to the closest detection distance for the EV, and a pedestrian should normally be able to step away from the approaching car before a collision occurs during the 1.5-2.5 s between detection and collision. Rather similar procedures were used in a Japanese study, except that they used more EVs and HEVs as test objects (including AVAS

systems), and results were rather similar too [30].

Others have checked whether the use of AVAS will aid in early detection of vehicles running in electric mode. The answer is “yes”, provided background noise is rather low and speeds are below 20 km/h [30, 31].

However, it has also been admitted that perception of quiet vehicles was poor already before the EVs and HEVs became common [32]. Thus, it is indeed a problem we have been facing for a long time and without concerns for safety until Americans started to react against the quietness of Japanese HEVs.

Consequently, AVAS will have a positive effect on the detection. But is it really needed and what are the consequences?

ADDING ARTIFICIAL SOUND

So, what is the problem with adding some extra sound in forward driving at speeds below 20 km/h and when reversing? The answer is, in summary, that it neutralises a substantial part of the noise reduction or annoyance reduction that may follow from the increasing use of EVs and HEVs.

To begin with reversing: this would hardly be a significant environmental nuisance if the sound is not of an intrusive kind (such as beeps, see below), since reversing is only a very short driving operation. However, the problem is that the driver may be tempted to rely on such sound and refrain from the discomfort of looking backwards carefully, and vision- and hearing-impaired people as well as young children may then be hit. Some kind of radar would be better.

The safety effect of AVAS may not be as expected. The existence of warning sounds will make some drivers feel more confident that they will not hit a pedestrian or bicyclist, and the attention to this potential danger might be lower than if they would be aware of the danger. Even if only relatively few drivers will react in this way it might be enough to offset the positive effect of the warning sound.

If heavy vehicles (trucks and busses) are exchanged from ICE types to EV/HEVs, there will be a substantial improvement in the acoustic environment since at low speeds tyre noise is much lower than propulsion noise. For example, a potential noise reduction of 1 to 8 dB has been measured when comparing an electric to a medium-sized European ICE truck [33]. If compared to the noisier North American trucks, the potential noise reduction is even more dramatic. This would significantly reduce the background noise level in urban areas, and also the maximum levels, and consequently reduce the masking effects (see below).

The conclusions above for light vehicles would, therefore, not hold for heavy EV/HEVs. If these are equipped with extra sounds, they will most probably compensate for a big part of the much lower propulsion noise of these vehicles at low speeds, and thus mean a substantial extra load to the acoustic environment, compared to if extra sound is not generated.

Exchanging ICE types of heavy vehicles with EV/HEV types (without extra sound) in urban settings with average speeds at 50 km/h or lower, will substantially improve the overall noise exposure in the area. It will mean a global breakthrough in noise control; especially in countries having noisy trucks and busses today. This would be much needed in view of the recent WHO report about serious health effects of

noise [34]. A couple of decibels of reduced noise exposure may lead to more saved healthy “life-years” than the few injuries from accidents which may perhaps occur due to the loss of sound cues at low speeds for the EV/HEVs. Adding AVAS sound may then cost more lives than it saves.

IMPORTANCE OF MASKING NOISE

The problem of perception of EV/HEVs at speeds in the range of 5-20 km/h is that background noise is masking the tyre noise. If background noise can be reduced by (say) 6 dB, the perception of 6 dB lower (tyre) noise levels from EV/HEVs will be possible. Six dB corresponds to a doubling of distance for a point source, such as an approaching car, to give the same level as without the 6 dB reduction. That would also improve the health situation and reduce general noise annoyance in all areas of this type.

Therefore, it is strange that the focus of the worldwide work on this subject is only to add noise to the lower levels instead of reducing the higher levels of noise. This author thinks that it would be much better to reduce the higher noise levels, in order to reduce the masking effect, than to add extra noise to the low levels.

One way of achieving this is to encourage the introduction at a fairly large scale of heavy EV/HEVs in the urban areas; i.e. to use EV/HEV busses and distribution trucks which are run in electric mode preferably when they are close to pedestrians, bus stops and residential areas.

Another way is to reduce the maximum noise levels allowed at type approval for the vehicles that contribute the most to the general background noise; this would often but not always be caused by the heavy trucks and busses. The European Parliament is currently reviewing and modifying a proposal from the European Commission which will require reduced vehicle noise limits in a few years [35]. In USA such maximum limit changes for heavy vehicles could be especially effective, as the US heavy vehicle standards are approx. 6 dB weaker than corresponding ones in Europe and East Asia, and they have not been changed since the 1980's.

PRESENT STATUS OF QUIET VEHICLES RULEMAKING (JULY 2012)

Work has been and is going on in psychoacoustics at several places in the world to design suitable sounds. The subject quickly became a favorite subject in acoustical departments at many universities.

With the passage in the United States of the 2010 Pedestrian Safety Enhancement Act [3], and the endorsement of the President in January 2011, the US vehicle safety authority is required to issue a formal regulation on this topic no later than January 2014. Before that they should collect comments and explore the consequences in an Environmental Impact Assessment, which is probably what goes on at this moment. The Act requires EVs and HEVs to use AVAS, without the possibility to switch them off. No later than January 2015 the Secretary shall complete a study and report to Congress as to whether there exists a safety need to apply the motor vehicle safety standard also to conventional (ICE) motor vehicles.

The MLIT in Japan, following consultation with the industry

and representatives of the blind, in 2010 issued guidelines for audible pedestrian warning systems, already in-force early in 2011 [36]. A summary of the Japanese guidelines appear in [12].

As reported above, the informal working group QRTV operated under the GRB and had nine meetings in 2010-2011. At the GRB, the subject has now advanced to a level when a proposal for a Global Technical Regulation (GTR) is available, as developed by the QRTV [6] which was discussed at the September 2012 meeting of GRB. This proposal is partly based on the previous Japanese guidelines that had already been submitted to GRB [36], but is substantially less specific in its performance specifications; yet contains quite exhaustive explanations and discussions.

To summarise the guidelines [6], the main issues are listed in Table 1. It is recommended that the UN GTR be written to apply, in principle, to all quiet vehicles regardless of their type of propulsion. However, due to limited performance information for other vehicles than EV/HEV it is recommended that initial regulatory specifications be limited to EVs and HEVs, operating in their electric mode.

In the proposal to the European Parliament from the Commission in 2011, it is stated that taking into account the

discussions and the information provided in the UN ECE it is proposed to amend the current noise legislation with a new Annex harmonizing the performance of 'Approaching Vehicle Audible Systems' if they are fitted to a vehicle. The fitting of such systems, however, shall be voluntary and remain an option under the discretion of the vehicle manufacturers [35]. The current intention is just to harmonize the AVAS.

SOME AVAS IN USE

Most EV/HEV vehicles available on the market already have AVAS mounted; in some cases these are retrofit systems. Here are but a few notes about this.

For the Toyota Prius, the AVAS is an optional speaker setup in the front of the car that makes a “futuristic” humming sound equivalent to that of a standard petrol-driven vehicle. The cost is reported to be approx USD 170, excluding installation. The speaker is activated when the car starts up but can be turned off at the touch of a button if the driver so desires [37]. A synthesised electric motor sound is emitted at speeds up to 25 km/h and rises and falls in pitch based on the vehicle’s speed.

In the Nissan Leaf, the sound system includes a speaker under the hood and a synthesizer in the dash. The driver will be able to turn it off, but it comes on by default at start up. At

Table 1: The most essential recommendations from QRTV to be part of a Global Technical Regulation (GTR) (not a complete list, major items selected by the author)

The GTR shall currently be applicable to all EVs and HEVs in electric mode, but at some later stage also to quiet vehicles with other motion systems than electric.
 GTR audibility requirements shall address at least the following "at risk" issues:

- a. Vehicles approaching at right angles to the direction of pedestrians intended movement
- b. Vehicles initiating movement from a driveway or in a parking lot
- c. Vehicle travelling at low speed in quiet areas.

A specific alerting signal sound pressure level is not recommended.
 A specific crossover speed, at which the system shall be switched on and off is not specified.
 The alerting system should be automatically activated when the vehicle slows to or below the crossover speed.
 The alerting system will automatically deactivate at vehicle speeds in excess of the crossover speed.
 It is recommended that the sound generated by the alert device monotonically increase or decrease in frequency as a function of vehicle speed. Further, it is recommended that during acceleration or deceleration an increase or decrease of at least 8 % be demonstrated between 10 and 20 km/h.
 It is recommended that the alerting system is operated during temporary stops of the vehicle.
 It is further recommended that the sound level be automatically attenuated during these periods to a level that is adequate to be heard by a pedestrian who is at the curb, immediately adjacent to the vehicle.

It is recommended that the acoustic performance requirements give careful attention to their potential adverse environmental impact, particularly with respect to loudness and frequency content.
 The development of the AVAS shall give consideration to the overall community noise impact.
 The following operating frequency specifications should be considered:

- a. Frequency range of audible signal: between 50 Hz and 5 kHz
- b. The frequency content should include at least two 1/3 octave bands within that range
- c. In case the AVAS produces only two frequencies, these should differ by $\geq 15\%$
- d. An alerting signal’s mid-frequencies (0.5-2 kHz), higher frequencies (2-5 kHz) support audibility and directional cues. Low frequencies (< 500 Hz) support earlier detection but in an urban environment are at risk of being masked.

The following sounds should be prohibited:

- a. Siren, horn, chime, bell and emergency vehicle sounds
- b. Alarm sounds e.g. fire, theft, smoke alarms
- c. Intermittent sound
- d. Melodious sounds, animal and insect sounds
- e. Sounds that confuse the identification of a vehicle and/or its operation (e.g. acceleration, deceleration etc.)

speeds above 30 km/h, the system turns off. The sound is a sine wave sweeping from 2.5 kHz to 600 Hz. At start-up, the sound comes on at its loudest to warn the visually impaired and other pedestrians that a car is about to enter their vicinity. When the Leaf is reversing, the system produces an intermittent “beeping” sound, similar to the back-up warning systems on trucks [39].

The Chevrolet Volt EV has an AVAS that GM calls “pedestrian friendly alert” or “courtesy signal”, which is manually activated by pushing a button on the blinker control stick. It is reported to sound like a soft horn [39].

NON-ACOUSTICAL SOLUTIONS

The author thinks that the acoustic solution in the form of a soft horn applied by GM Volt could be a reasonable compromise, to be applied only when the driver thinks that there is a danger ahead (but it must not be abused by telling pedestrians “keep out of the road, here I come”). Apart from this, non-acoustical solutions are preferred.

In the author's previous paper, several non-acoustical systems for alerting pedestrians or drivers about a potential risk of collision are described [10]. This is not repeated here; nevertheless, a few potential solutions will be mentioned.

Professor Jim Kutsch, President of The Seeing Eye, Inc. (<http://www.seeingeye.org/>), blind himself (as his family) and an expert on seeing-eye dogs, has expressed in an interview that “We’ve added hybrid cars to our training program. You can’t hear them when they are at a full stop. We now teach dogs that a car is a car, whether it’s making a noise or not” [40].

One may also consider making the white cane sticks more hi-tech with special warning indications, such as a blinking lamp when the cane is pointed straight out or when activated by the user.

Several modern cars are already equipped with Autonomous Emergency Braking (AEB) systems; often in combination with pedestrian detection systems. EuroNCAP describes AEB Pedestrian systems which can detect pedestrians and other vulnerable road users like cyclists [41]. They invariably employ a camera combined with a radar – something called sensor fusion. New technologies are appearing on the market that use infrared which can also operate in very low light conditions. EuroNCAP lists two car manufacturers who have such systems fitted: Lexus and Volvo, where Volvo has it as standard equipment on most of its new models [41].

The latest BMW 3-Series has been commended for its pedestrian protection measures following a crash test in Europe, while Volvo has developed an airbag designed to save pedestrians [42]. Volvo's newest pedestrian detection system with AEB is presented in [43]; reading “If the driver does not react to the warning and a collision is imminent, full braking power is automatically applied”.

TRANSFER OF RESPONSIBILITY

The traditional view is that it is the driver who has the main responsibility to avoid a collision with a pedestrian; probably also with a bicyclist. This is natural since the driver has a reasonable protection against injuries in his vehicle while the former are totally unprotected.

A driver being aware of that his vehicle emits dedicated sound that has the expressed intention to inform pedestrians that the vehicle is coming may be tempted to think that this moves some of the responsibility from him over to the pedestrian. This may create a situation which is even worse than with no warning signal, where it is obvious that the driver has the full responsibility. Especially, a vehicle backing out of a parking lot, where it is inconvenient and uncomfortable to look behind, may be an example of this.

CONCLUSIONS

The occurrence of electric driven vehicles on the market promises a unique breakthrough in reduction of urban community noise. The very low noise emission from electric motors means that power unit noise is almost totally absent for such vehicles and that only tyre noise remains. The effect will be that at low vehicle speeds (approximately up to 20 km/h for cars and up to 50-70 km/h for heavy vehicles) the acoustic environment will improve substantially.

However, the supposed problem of quietness of vehicles operating in electric mode has resulted in concerted actions by a number of organisations at a pace which is unique within the subject of traffic noise; the justification for which is questionable. Firstly, the actions have not been based on robust evidence of serious traffic accidents; secondly, the problem (if any) seems to be potentially greater for other types of vehicles than for the cars which have been in focus so far and, thirdly, correspondingly quiet vehicles have been used for decades already without noticing a specific accident problem due to the quietness.

It is suggested in this article that the quietness of cars driven in electric mode may not be a major safety problem. There is simply no robust and consistent traffic accident data that says that quietness of vehicles is a significant cause of accidents.

Nevertheless, for the blind community the quietness of vehicles driven in electric mode must be recognised as a psychological problem, making the blind feel unsafe and experiencing more serious restrictions when the sound cues have been reduced. However, it must also be noted that this situation has existed for a long time due to several types of quiet vehicles operating in our traffic, and did not occur only due to HEVs becoming common on the market.

It is suggested in the article that reducing maximum noise level limits is a much better way for promoting health and safety than adding extra sound to the quietest vehicles. The problem is not that vehicles are getting too quiet; the problem is that background noise masks the noise of the quiet vehicles.

The addition of AVAS to EVs and HEVs, or even to quiet ICE cars, may be directly counter-productive, as it is likely to provide only a marginal safety improvement (if any at all), which may easily be balanced-out by an increased feeling of safety for both pedestrians and drivers, transformation from responsible driving to a belief in AVAS, as well as the impaired health issues due to missing an opportunity to efficiently reduce noise exposure.

The perceived unsafety of the blind due to vehicle quietness should be addressed primarily by reducing the masking of sound cues by noisy vehicles, which would have other

substantial benefits, and by other measures than the acoustical. Training of seeing-eye dogs to care about vehicles in the same way irrespective of sound level may be one; another one may be the collision-preventing systems rapidly being introduced on the market.

When it comes to sound cues in traffic, the most effective measures for accident prevention would probably be to reduce distraction of pedestrians and bicyclists by limiting the use of portable audio systems and cell phone talking as well as texting in traffic environments.

The author suggests discontinuing the work with AVAS, limiting rather than requiring the use of such systems, and instead focusing on limitation of the worst masking noise emissions in urban areas. It may not be as exciting and fashionable to work with noise reduction as with sound production, but it would have more benefits to the safety and health of society.

REFERENCES

All links have been accessed in December 2012. Please note that all the ECE/GRB and QRTV documents are publicly available and can be downloaded via the website:

http://live.unece.org/trans/main/wp29/meeting_docs_grb.html

- [1] The New York Times, *Anti-noise activists oppose sounds for electric cars*, Article in the 21 June 2010, issue of The New York Times
- [2] California Legislative Information, *Senate Joint Resolution No. 6, Chapter 60, Relative to pedestrian safety*, SJR-6, Legislative Counsel's Digest, 30 June 2009. http://leginfo.legislature.ca.gov/faces/billNavClient.xhtml?bill_id=2009201005JR6
- [3] *Pedestrian Safety Enhancement Act of 2010*, S.841 of the 111th Congress of the USA at the second session. <http://www.govtrack.us/congress/billtext.xpd?bill=s111-841>
- [4] JASIC, *A study on approach audible system for hybrid vehicles and electric vehicles - Second report*, Informal document No. GRB-50-08, GRB, WP29, ECE, Geneva, Switzerland, 2009
- [5] QRTV, *Terms of reference and rules of procedure for the grb informal group on quiet road transport vehicles (QRTV)*, Document QRTV-01-02-e, ECE/WP29/GRB, Geneva, Switzerland, 2010
- [6] QRTV, *Draft recommendations for a global technical regulation regarding audible vehicle alerting systems for quiet road transport vehicles - Submitted by the Informal Working Group on Quiet Road Transport Vehicles*, Document ECE/TRANS/WP.29/GRB/2012/6, Geneva, Switzerland, 2012
- [7] EU Commission, *Proposal for a regulation of the european parliament and of the council on the sound level of motor vehicles*, COM(2011) 856 final, 2011/0409 (COD), 9.12.2011, European Commission, Brussels, Belgium, 2011
- [8] SAE J2889/1, *Measurement of minimum noise emitted by road vehicles*, SAE International, Warrendale, PA, USA, 2012
- [9] Transport & Environment, *MEPs could be voting to make vehicles louder*, Press Release 23 June 2012, Brussels, Belgium <http://www.transportenvironment.org/news/meps-could-be-voting-make-vehicles-louder>
- [10] U. Sandberg, L. Goubert and P. Mioduszewski, "Are vehicles driven in electric mode so quiet that they need acoustic warning signals?", *Proceedings of the 20th International Congress on Acoustics*, Sydney, Australia, 23-27 August 2010
- [11] U. Sandberg, "Are quiet vehicles a bigger threat than noisy vehicles?", *Proceedings of Noise-Con 2011*, Portland, USA, 25-27 July 2011
- [12] U. Sandberg, "Adding noise to quiet electric and hybrid vehicles: An electric issue", *Noise/News International (NNI)*, **20**(2), 51-67 (June 2012)
- [13] JASIC, *A study on approach warning systems for hybrid vehicle in motor mode*, Informal document No. GRB-49-10, GRB, WP29, ECE, Geneva, Switzerland, 2009
- [14] NHTSA, *Incidence of pedestrian and bicyclist crashes by hybrid electric passenger vehicles*, NHTSA Technical Report DOT HS 811 204, 2009
- [15] E.N.G. Verheijen and J. Jabben, "Effect of electric cars on traffic noise and safety", RIVM Letter Report Number 680300009/2010, *National Institute for Public Health and the Environment (RIVM)*, Bilthoven, The Netherlands, 2010
- [16] J. Wu, R. Austin and C-L. Chen, "Incidence rates of pedestrian and bicyclist crashes by hybrid electric passenger vehicles: An update", DOT HS 811 526, *National Highway Traffic Safety Administration (NHTSA)*, Washington, DC, USA, 2011
- [17] C. Hogan, "Analysis of blind pedestrian deaths and injuries from motor vehicle crashes, 2002-2006", *Article from Direct Research*, VA, USA, 2008
- [18] P.A. Morgan, L. Morris, M. Muirhead, L.K. Walter and J. Martin, "Assessing the perceived safety risk from quiet electric and hybrid vehicles to vision-impaired pedestrians", Published Project Report PPR525, *Transport Research Laboratory (TRL)*, Crowthorne, UK, 2011
- [19] NFB, *Key stakeholders agree on measures to protect blind pedestrians from silent cars - Urge passage as part of motor vehicle safety act*, National Federation of the Blind, 2010
- [20] WBU, *World Blind Union comments on Japanese guidelines*, World Blind Union, Document QRTV-04-03e, ECE/WP29/GRB, Geneva, Switzerland, 2010
- [21] K. Hara, S. Nakano, K. Sato, K. Ashihara, S. Kiryu and N. Miura, "Perceptibility of environmental sounds by earphone wearers listening to pop and rock music", *Acoustical Science and Technology* **31**(6), 387-393 (2010)
- [22] J. Nasar, P. Hecht and R. Wener, "Mobile telephones, distracted attention, and pedestrian safety", *Accident Analysis and Prevention* **40**(1), 69-75 (2008)
- [23] K. Danks, *iPods & mobile phones are killing people*, Article May 26, 2012 in Sydney Daily Telegraph, NSW, Australia, view at <http://s3blogspot.net/dl/Homework/Term2/Wk8/iPods.pdf>
- [24] Anon, *Distracted walking laws, legislation*, Article on a webpage of Hands-Free Info, 2012, view at <http://handsfreeinfo.com/distracted-walking-pedestrians-law>
- [25] U. Sandberg and J.A. Ejsmont, *Tyre/road noise reference book*, publisher Informex, Kisa, Sweden, 2002
- [26] DELTA, *Note: Comparison of background noise spectra*, AV 1069/11, Denmark, 2011
- [27] E. Rosén, H. Stigson and U. Sander, "Literature review of pedestrian fatality risk as a function of car impact speed", *Accident Analysis and Prevention* **43**(1), 25-33 (2011)
- [28] E. Rosén, H. Stigson and A. Kullgren, *Pedestrian risks in traffic*, Seminar at the Swedish National Road and Transport Research Institute (VTI), Linköping, Sweden, February 2012
- [29] K-P. Glaeser, T. Marx and E. Schmidt, "Sound detection of electric vehicles by blind or visually impaired persons", *Proceedings of Inter-Noise 2012*, New York, USA, 19-22 August 2012

- [30] I. Sakamoto, H. Houzu, M. Sekine, T. Tanaka and K. Morita, "Report on basic research for standardization of measures for quiet vehicles in Japan (Intermit report)", *Proceedings of Inter-Noise 2012*, New York, USA, 19-22 August 2012
- [31] R.W. Emerson, D.S. Kim, K. Naghshineh and K. Myers, "Blind pedestrians and quieter vehicles: how adding artificial sounds impacts travel decisions", *Proceedings of Inter-Noise 2012*, New York, USA, 19-22 August 2012
- [32] K. Yamauchi, Y. Sakabe and S. Iwamiya, "Questionnaire survey on the sound of quiet vehicles", *Proceedings of Inter-Noise 2012*, New York, USA, 19-22 August 2012
- [33] M-A. Pallas, R. Chatagnon and J. Lelong, "Acoustic assessment of a passing-by hybrid distribution truck", *Proceedings of Inter-Noise 2012*, New York, USA, 19-22 August 2012
- [34] WHO, *Burden of disease from environmental noise - Quantification of healthy life years lost in Europe*, World Health Organization, Copenhagen, Denmark, 2011 May be downloaded from:
- [35] EU Commission, *Proposal for a regulation of the European Parliament and of the Council on the sound level of motor vehicles*, 2011/0409 (COD), COM(2011) 856 final, 9.12.2011, Brussels, Belgium, 2011
- [36] UN Economic and Social Council, *Proposal for guidelines on measures ensuring the audibility of hybrid and electric vehicles*, Document ECE/TRANS/WP.29/GRB/2011/6, 2011
- [37] T. Beissmann, *Toyota Prius available with approaching vehicle audible system in Japan*, Toyota car news article, 2010, view at www.caradvice.com.au: <http://www.caradvice.com.au/80718/toyota-prius-available-with-approaching-vehicle-audible-system-in-japan/>
- [38] S. Gutierrez, *Nissan LEAF equipped with warning sounds for pedestrians*, Blog article in Seattle Traffic and Transportation News, Seattle PI, 2010
- [39] K. Sandberg, *Personal communication with the author's son living in Colorado, USA, and proud owner of a GM Volt car*, 2012
- [40] K. Kelly, *The first seeing eye dog is used in America in 1929*, 2012, view at <http://americacomesalive.com/2012/06/25/how-a-dog-breeder-a-blind-man-and-a-german-shepherd-changed-the-world-in-1929/>
- [41] EuroNCAP, *AEB pedestrian system*, European New Car Assessment Programme (EuroNCAP), 2012 <http://www.euroncap.com/results/aeb/pedestrian.aspx>
- [42] Volvo, *Volvo Car Corporation's pedestrian airbag: here's how it works*, Press release from Volvo Car Corporation, 2012
- [43] Volvo, *The all-new Volvo V40 – Pedestrian detection with full auto brake*, Press release from Volvo Car Corporation, 2012

NSW Road Noise Policy: Application Notes

The *NSW Road Noise Policy* (RNP) was published by the former NSW Department of Environment, Climate Change and Water and replaced the *Environmental Criteria for Road Traffic Noise* from 1 July 2011. The RNP contains strategies to address the issue of road traffic noise from existing roads, new road projects, road redevelopment projects and traffic-generating developments. The policy defines criteria to be used when assessing the impact of road traffic noise.

The NSW Environment Protection Authority (EPA) has been asked to clarify the intent of some sections of the policy and has published Application Notes to explain the intended meaning. Application Notes prepared to date cover:

- Relative increase criteria
- Applying the assessment criteria to additional traffic on existing roads generated by land use developments.

The Application Notes can be accessed at <http://www.environment.nsw.gov.au/noise/roadnoiseappnotes.htm>

Discover new heights
in acoustics design



Room Acoustics Software

www.odeon.dk

ACOUSTICAL IMPACTS OF FUTURE GENERATION ROAD VEHICLES

Matthew Stead, Adrian White and Deb James

Resonate Acoustics, Australia

matthew.stead@resonateacoustics.com

Future generation transportation has inherently lower noise emissions which are driven by changes to regulation, improved technology and because of consumer expectations. Lower noise emissions will have an impact on infrastructure projects in terms of reduced capital costs and also improved amenity for the communities surrounding the infrastructure. It has been found that hybrid and electric vehicles will have the greatest impact on lower speed roads (80 km/hr or less) and only marginal impact for 100 km/r roads because tyre noise is the dominant source rather than propulsion noise at this speed. Results of these findings for major road infrastructure routes are presented for consideration by authorities, designers and contractors.

INTRODUCTION

With a resource constrained future, the viability of hybrid and electric vehicles is likely to increase. Hybrid vehicles combine a combustion engine with an electric motor. Propulsion is a mix of combustion and electric motor dependent on vehicle speed and load. Electric propulsion is inherently quieter than combustion propulsion vehicles as observed in current hybrid vehicles when in electric mode. There is even concern that electric vehicles are so quiet at low speeds that they pose a safety hazard to pedestrians and in particular blind pedestrians, as demonstrated by U.S. federal legislation which recently required an assessment of minimum noise levels [1].

Current traffic noise mitigation design for infrastructure projects is either based on noise models which have been calibrated to the current vehicle fleet and mix or on noise models based on historical vehicle noise emissions. There is an inherent assumption that the future vehicle fleet will have similar noise emissions to the existing or past fleet.

The allocation of capital on infrastructure is scrutinised and there is hence benefit in questioning the predicted future noise emissions from vehicles which is the basis for noise models. Anecdotal evidence from projects such as Eastlink in Victoria suggest that a 1 dB(A) increase in noise source level is approximately equal to 0.8 m higher noise walls. At current budgets for concrete noise walls this could equal up to \$2 million for noise walls on both sides of Eastlink. This is a significant proportion of an infrastructure budget and hence it is critical that the accuracy of future traffic noise models be assessed.

This article reviews the sources of noise from road vehicles and makes an informed prediction of future road vehicle noise emissions.

SOURCES OF ROAD VEHICLE NOISE AND NOISE EMISSIONS

The sources of road vehicle noise have been studied in numerous technical publications [2, 3]. The primary sources of noise can be categorised as:

- Road / tyre interaction
- Propulsion
- Aerodynamic
- Other miscellaneous sources such as brakes, suspension, rattle, etc.

At different speeds and under vehicle acceleration or deceleration modes the relative contribution of the sources change. In some cases the propulsion is the main source (generally low speed or under acceleration) and in other cases the road/tyre interaction is the dominant noise source (generally at higher speeds). The study by Lelong [2] found that for passenger cars at lower speeds (<60 km/hr) the propulsion system was the dominant noise source and at higher speed (≥ 60 km/hr) the tyre/road interaction noise was the dominant noise source. This suggests that hybrid or electric vehicles may have similar noise emissions to traditional propulsion vehicles at higher speeds.

A previous study [4] measured vehicle noise emissions on a rural Australian highway. The different vehicle noise emissions (for class Austroads Vehicle Classifications) were then compared with the standardised Traffic Noise Model (TNM) [5] and Calculation of Road Traffic Noise (CORTN) [6] noise models. The findings of the study are repeated in Figure 1. This study showed that the current fleet of Australian vehicles does not have the same emissions characteristics as the TNM or CORTN models. The result of this study is used as the basis for predicting overall noise emissions for Australia in this study.

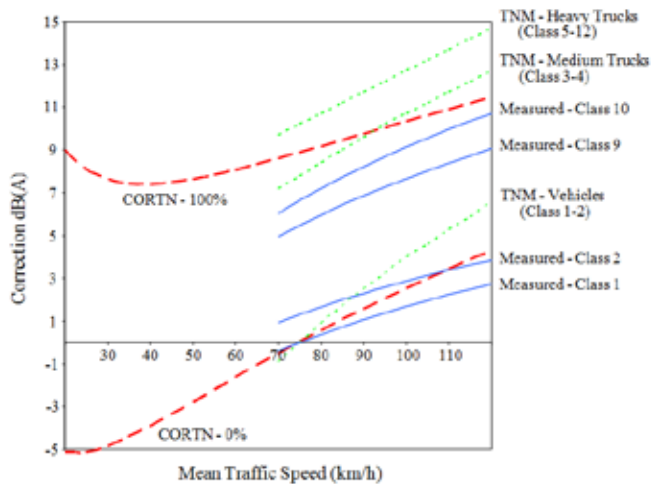


Figure 1. Correction to traffic noise emissions levels using TNM, CORTN and measured by Jurevicius et al. [7] with varying percentage commercial vehicles (normalised to 75 km/hr and 0% commercial vehicles)

HISTORICAL ROAD VEHICLE NOISE EMISSION REDUCTIONS

The regulations associated with vehicle noise emissions have gradually been reducing the noise emission limits over the past 45 years [7]. The development of overall vehicle noise emission limits in the EU, Japan and USA from [7] is shown in Figure 2. The effect of noise emission regulations on received noise levels at residences vary significantly depending on the study being assessed in Sandberg 2001. The overall conclusion of the [7] study was that regulations have not been effective and only small reduction in noise levels at residences have been achieved over the studied 30 year time period. This primarily is related to the regulation of propulsion noise the when the dominant tyre/road interface noise has not been regulated to the same degree.

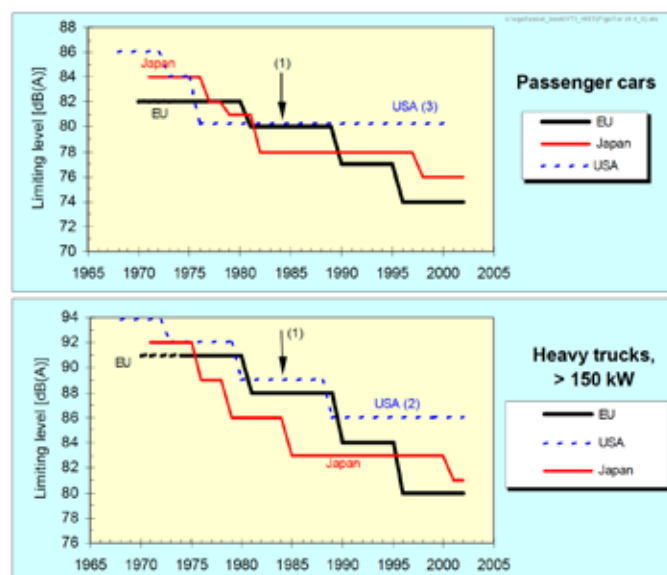


Figure 2. Examples of the development of individual vehicle noise emission limits over the years including some projected limits [7]

PROJECTED FUTURE FLEET MIX

Projections on the future vehicle fleet mix are difficult to make. There is a trend towards more hybrid vehicles as demonstrated by the number of models available. The current percentage of hybrid vehicles being sold in the USA is around 3% [8]. This is expected to increase but at an unknown rate.

In this article, a low (<10%), medium (50%) and high (90%) mix of passenger hybrid / electric vehicles has been assumed. Commercial vehicles are likely to have a slower adoption of hybrid vehicle technology due to the additional range and loads they carry. As such it is assumed that the noise emission for commercial vehicles is likely to remain similar to existing levels given the restricted choice of hybrid commercial vehicles.

ASSESSMENT OF ELECTRIC/HYBRID AND COMBUSTION VEHICLE PASS-BY NOISE EMISSION

To assist in the analysis of noise from hybrid/electric vehicles compared with a combustion engine vehicle, a back-to-back test was carried out with a hybrid and a manual 4 cylinder combustion engine passenger vehicle. A Toyota Camry was selected for the testing and two vehicles with similar tyre wear and the same model chassis were sourced. The test vehicles both had the same tyre make and model (Dunlop Supersport 300E) and similar wear. This model vehicle was selected as it is a mid-size vehicle and currently in production as both a hybrid and non-hybrid version.

A section of test road (Boundary Road, Truganina, Victoria, Australia) was selected which had a surface equivalent to dense graded asphalt, was flat, straight and in a rural setting without other traffic. The road was a single lane and there were no significant reflecting surfaces or road imperfections where the measurements were taken. The test road was used for vehicle pass by noise measurements. The surrounding area was grassed and flat. The tests consisted of a number of pass-bys with varying constant speed and engine load. At the time of the testing the conditions were minimal wind, 10 deg C, clear skies and 86 % relative humidity.

A calibrated Class 1 Bruel and Kjaer 2250 hand-held analyser and sound level meter with audio recording was used to take measurements of the vehicle pass by. The sound level meter was located 7.0 m from the centre line of the vehicle and was mounted on a tripod 1.2 m above the ground level. The overall averaged results of the testing is summarised in Table 1.

The coasting noise levels at 100 km/hr per hour were 0.4 dB(A) lower for the 4 cylinder vehicle and 1.2 dB(A) lower for the hybrid vehicle with constant speed and engine load. At lower speeds the propulsion noise was more significant compared to tyre/road interface noise. The difference between the engine loaded and unloaded noise levels show the engine / motor is not the dominant noise source at 100 km/hr and there was a greater difference with the hybrid vehicle.

Table 1. Vehicle maximum pass-by relative noise levels

Test Condition	Average individual vehicle maximum pass-by noise level		Difference between 4 Cylinder and Hybrid Camry maximum pass-by noise level (positive number where 4 cylinder has a higher noise level)
	Hybrid Camry	4 Cylinder Combustion Camry	
60 km/hr constant speed and engine load	70.6 dB(A)	72.9 dB(A)	2.3 dB(A)
80 km/hr constant speed and engine load	75.0 dB(A)	78.3 dB(A)	3.3 dB(A)
100 km/hr constant speed and engine load	79.4 dB(A)	80.1 dB(A)	0.7 dB(A)
100 km/hr coasting (engine unloaded)	78.2 dB(A)	79.7 dB(A)	1.5 dB(A)

Table 2. Predicted change on overall noise emissions

Percentage Commercial Vehicle Low (5%) Medium (10%) High (20%)	Hybrid Vehicle Fleet Percentage			
	Speed	Low (10%)	Medium (50%)	High (90%)
60 km/hr				
Low CV%		0.2 dB(A)	1.1 dB(A)	1.7 dB(A)
Medium CV%		0.2 dB(A)	0.9 dB(A)	1.4 dB(A)
High CV%		0.2 dB(A)	0.7 dB(A)	1.0 dB(A)
80 km/hr				
Low CV%		0.4 dB(A)	1.6 dB(A)	2.4 dB(A)
Medium CV%		0.3 dB(A)	1.3 dB(A)	2.0 dB(A)
High CV%		0.2 dB(A)	0.9 dB(A)	1.4 dB(A)
100 km/hr				
Low CV%		0.1 dB(A)	0.3 dB(A)	0.5 dB(A)
Medium CV%		0 dB(A)	0.2 dB(A)	0.4 dB(A)
High CV%		0 dB(A)	0.2 dB(A)	0.3 dB(A)

ASSESSMENT OF ROAD/TYRE INTERACTION NOISE EMISSION

The noise emissions from the road / tyre interaction could reduce with future advances in tyre and road technology with between 4 and 6 dB(A) theoretically possible with current reported technologies [9]. The current Australian Design Rule for passenger car tyres [10] however does not provide noise limits and hence without a regulatory driver there is unlikely to be significant change in Australia. While tyres may be imported from Europe (where there are noise limits) the impact on reducing noise on Australian road noise emission is questionable in the absence of a regulatory driver. For the purposes of this paper it is hence assumed that there will be no significant reduction in tyre noise emission levels in Australia.

ANALYSIS

Changes to future vehicle emission levels have been calculated for the low (<10%), medium (50%) and high (90%) mix of passenger hybrid / electric vehicles using measured

results from Table 1 and vehicle emission levels from Figure 1. The percentage of commercial vehicles is assumed to be low (5%), medium (10%) and high (20%) with no change in commercial vehicle noise emissions and no change due to tyre/road interaction noise levels.

From Table 2 it can be seen that significant noise reduction (> 0.5 dB(A)) is only achieved at lower speeds (less than 80 km/hr) and with medium to high hybrid vehicle fleet mix. In limited cases the difference is greater than 1 dB(A). Hybrid vehicles are not likely to have a significant impact for freeway / expressway infrastructure projects operating at 100 km/hr.

CONCLUSIONS

The simplistic assumption that hybrid or electric vehicles will significantly reduce the scale of noise walls on urban freeways is not shown by the research in this paper. While over time the propulsion noise levels have reduced, the overall noise levels have not significantly reduced mainly to the slower improvements in tyre technology. While this is not likely to change rapidly in the future because of a lack of regulation

around tyre noise in Australia, there is still the potential for reductions in vehicle noise emissions with hybrid or electric vehicles. Should there be a change to tyre noise regulations the reductions could be much more significant. Pressure should be placed on the reduction of tyre noise emissions. The impact on the reduction in noise is greatest at low speeds and with greater than 50% of the vehicle fleet being hybrid or electric. The results from this research have found that for a low percentage of hybrid vehicles there is unlikely to be any significant changes to vehicle noise emissions.

REFERENCES

[1] United States Federal Congress, *Bill S. 841 (111th) Pedestrian Safety Enhancement Act of 2010*, <http://www.govtrack.us/congress/bills/111/s841> (last accessed November 2012)

[2] J. Lelong, "Vehicle noise emission; Evaluation of tyre/road and motor noise contributions," *Proceedings of InterNoise 99*, Florida, USA, 6-8 December 1999

[3] C. Hansen and D. Bies, *Engineering noise control, Theory and practice*, 4th edition, London, New York, Spon Press, 2009

[4] D. Jurevicius, P. Agnew and M. Stead, "Correlation of rural highway road traffic noise with vehicle speed and commercial vehicle percentage for the day and night time periods", *Proceedings of the 14th International Congress of Sound and Vibration*, Cairns, Australia, 9-12 July 2007

[5] G.G. Fleming, A.S. Rapoza and C.S.Y. Lee. *Development of National Reference Energy Mean Emission Levels for FHWA Traffic Noise Model (FHWA TNM®)*, Version 1.0, Report No. FHWA-PD-96-008/DOT-VNTSC-FHWA-96-2, U.S. Department of Transportation, Research and Special Programs Administration, November 1995

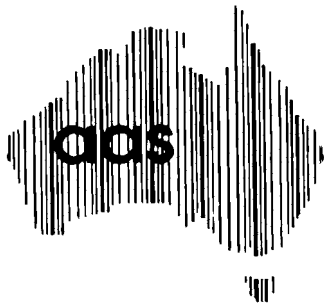
[6] UK Department of Transport, Welsh Office, *Calculation of Road Traffic Noise*, 1998, http://www.noiseni.co.uk/calculation_of_road_traffic_noise.pdf

[7] U. Sandberg, "Noise emissions of road vehicles, Effect of regulations", Final Report 01-1, *International Institute of Noise Control Engineering*, 2001

[8] Hybrid Cars, April 2012 Dashboard, <http://www.hybridcars.com/news/april-2012-dashboard-45388.html> (last accessed November 2012)

[9] Forum of European National Highway Research Laboratories (FEHRL), Study S12.408210 *Tyre/Road Noise*, Volume 1, Final Report, 2006

[10] Vehicle Standard, Australian Design Rule 23/02 *Passenger Car Tyres*, Federal Register of Legislative Instruments F2007C00769, Australian Government, 2007



Update Your Records

The AAS will be increasing the use of the on-line records with an update of the web page in the near future. The decision has been made on the model layout for this new improved website which will greatly increase the navigation and value for the website.

It is important that the records held in the membership base are up to date. It is the responsibility of each member to log on, check the current listing and update your company, address, preferred email, etc. So please check out your records now. If you have forgotten your username and/or password, you can retrieve them with the forgot username / forgot password options and then you can check and amend your AAS records.



NATAcoustic

National Acoustic Calibration Laboratory

NATA Calibration of

- Sound Level Meters
- Loggers
- Analyzers
- Calibrators



We Calibrate All SLMs & Calibrators

- B & K
- Norsonics
- Rion
- NTI
- ARL
- RTA Technology
- Svantek
- Larson Davis
- Cesva
- CEL
- 01dB
- Pulsar
- Sinus



National Acoustic Calibration Laboratory
 A Division Of
 Renzo Tonin & Associates (NSW) Pty Ltd
 ABN 29 117 462 861
 1/418A Elizabeth St, Surry Hills, NSW 2010
 PO Box 877 STRAWBERRY HILLS, NSW 2012
 Ph (02) 8218 0570
 Email: service@natacoustic.com.au
 Web: natacoustic.com.au

NEWS

Recent Actions on Human Vibration

Safe Work Australia (SWA) has developed fact sheets to raise awareness of exposure to whole-body and hand-arm vibration and give guidance on how to reduce the exposure of workers to vibration. The fact sheets provide information on the health effects resulting from exposure to vibration from common sources in the workplace. Information is included on the levels of exposure which are known to cause health effects, and suggested control measures which can be put in place. These fact sheets are the initial stages of work examining the feasibility of developing a model code of practice on controlling the risks of vibration at work. Since awareness and knowledge on the health effects and available hazard controls is relatively low in Australia, these fact sheets are being made available to business as a first step. These sheets are available from

<http://www.safeworkaustralia.gov.au/sites/SWA/AboutSafeWorkAustralia/WhatWeDo/Publications/Pages/Hand--arm-vibration-fact-sheet.aspx>

and

<http://www.safeworkaustralia.gov.au/sites/SWA/AboutSafeWorkAustralia/WhatWeDo/Publications/Pages/Whole-body-vibration-fact-sheet.aspx>

SWA is currently examining the development of guidance and the feasibility of a model code of practice on controlling the risks of vibration at work. The report Implementation and effectiveness of the European Directive relating to vibration in the workplace examines the requirements and effectiveness of the European Machinery Directive (2006/42/EC) and the Directive on Vibration (2002/44/EC) as implemented in the UK. It considers whether adoption of similar regulatory framework could be appropriate for Australia. It also provides a summary of the evidence for the health effects resulting from exposure to vibration and the identified gaps in vibration health effects knowledge.

The AAS has been the proponent to Standards Australia to initiate a project for a direct text adoption as an Australian Standard of the ISO standard on the measurement of Hand-Arm Vibration. This project has been approved to be undertaken but there is still some work to be done before the document appears as an Australian Standard.

The UK Health and Safety Executive (HSE) has published a new research report on Uptake and quality of health surveillance for hand-arm vibration and noise exposure. As well as surveying the uptake, quality and use of results of health surveillance, it has some interesting statistics on risk assessments and training completed.

See: <http://www.hse.gov.uk/research/rrhtm/rr948.htm?eban=govdel-noise&cr=08-Oct-2012>

Noise Induced Hearing Loss Priority

Safe Work Australia has published the Australian Work Health and Safety Strategy 2012-2022 to provide a 10 year framework to continue to drive improvements in workplace health and safety in this country. The strategy sets out four outcomes and seven action areas, seven priority industries and six priority work-related disorders. The latter includes Noise-induced Hearing Loss. The strategy is available at www.safeworkaustralia.gov.au

ISVR turns 50

2013 will mark the 50th anniversary of the foundation of the Institute of Sound and Vibration Research (ISVR) at the University of Southampton, UK. To celebrate the achievements of its people, past and present, ISVR will be hosting a two-day symposium on 11-12 July 2013. The symposium will feature talks from key speakers having an association with the ISVR. The celebrations will culminate in a social function with a buffet supper and entertainment.

The event will include presentations by Julie Brinton (South of England Cochlear Implant Centre), Tim Leighton (ISVR), Goran Pavić (Institut National des Sciences Appliquées, Lyon), Mike Griffin (ISVR), Stuart Bolton (Purdue University), Colin Smith CBE (Rolls-Royce), John Shelton (AcSoft), John Dixon (ISVR Consulting) Paul White (ISVR), Steve Elliott (ISVR), Stefan Bleleck (ISVR).

The EJ Richards Lecture titled *Thirty Years of Auditorium Design* will be given by Mr Rob Harris, Global Acoustic Leader, Arup.

The tickets for the event are £50 for full attendance, with a reduced cost for partial attendance. Details of the event are available online at <http://www.isvr.co.uk/ISVR-50th-anniversary>

Science Media Assistance

The Australian Science Media Centre has developed a new free online tool, ScienceMediaSavvy.org, to help scientists work with the media and better inform public debate on the major issues of the day. ScienceMediaSavvy.org has been developed with support from CSIRO, and provides tips and advice for understanding and dealing with the news media. ScienceMediaSavvy.org is not intended to replace hands-on media training workshops but will help those of you who are unable to take the time or foot the cost of attending an in-depth media training course or for those who need a refresher. The instant online availability of ScienceMediaSavvy.org will help fill a gap in terms of what is currently available, giving advice on dealing with the media as needed, from any internet-enabled computer, smartphone or tablet.

A short video explaining what ScienceMediaSavvy.org is all about is available on YouTube at www.youtube.com/watch?v=zkh98pwCUG

Acoustic Excellence Award for AECOM

AECOM secured the Engineers Australia Excellence Award in the South Australia Buildings and Structures category for their acoustic engineering services on the new Adelaide Film and Screen Studio. AECOM acoustic engineers provided a solution to the South Australian Film Corporation (SAFC) that will support the growth of film, television, audio visual and media industries in South Australia. The team, led by Dr Peter Swift, worked closely with the SAFC to identify their needs around acoustically sensitive spaces and meet Dolby Premier Mixing Studio requirements. The studios incorporate two soundstages, the Dolby Premier studio, various post-production areas including edit rooms, an additional dialogue recording room (ADR) and Foley (sound effects) room, and the 96-seat screening theatre. The world-class studios enable South Australia's screen industry to remain at the forefront of the Australian film production

ASA honours to Neville Fletcher

At its October meeting in Kansas City, the Acoustical Society of America held a session to honour the important contributions of Neville Fletcher in diverse areas of acoustics. Recovering from some surgery, Neville was unable to attend in person, so the ASA was persuaded to hold its first intercontinental electronic session. The audiences in Kansas City and Sydney each saw a screen showing the presentation slides, plus two small video screens showing the audiences in both cities. After the session, the Kansas City participants retired to the buffet social, while their Australian colleagues enjoyed breakfast.

Ex-students and other close collaborators of Neville's spoke on birdsong and a variety of musical instruments; Tom Rossing summarised Neville's huge contribution to acoustics as well his important contributions in several other areas of physics.

Neville Fletcher is a fellow of the Australian Academy of Science, the Australian Academy of Technological Sciences and Engineering, the Australian Acoustical Society, the Acoustical Society of America, the Institute of Physics (London) and the Australian Institute of Physics. His awards include the Edgeworth David Medal (Royal Society of NSW), the Thomas Ranken Lyle Medal (Australian Academy of Science), the Silver Medal in Musical Acoustics (Acoustical Society of America) and the Australian Government's Centenary Medal. He is a Member of the Order of Australia (AM). Neville has written 7 books, about 200 research papers, 6 patents, 5 reports and 4 booklets for schools.

Rossing Prize for Excellence in Education to Joe Wolfe

In October 2012, Joe Wolfe was presented with the Rossing Prize for Excellence in Education from the Acoustical Society of America. Joe and his UNSW team are internationally recognised for their educational web sites. These began last century when the acoustics lab presented its research for a general audience, and then expanded to include a broad range of introductory materials in acoustics (see www.phys.unsw.edu.au/music).

Recently, with George Hatsidimitris and John Smith, Joe has made Physclips, envisaged as a multi-level multi-media introduction to physics. The volumes on Mechanics, Waves and Sound are now finished and the team is working on Light. Physclips is available at www.animations.physics.unsw.edu.au



Acoustical Society of America president David Bradley presents Joe Wolfe with the Rossing prize for education.

Acoustica's 'Green' Production Line

At the production plant of Acoustica, in NSW, Australia, the world's first water based viscoelastic acoustic noise barrier production line has been opened. These noise barriers herald a shift away from petrochemical based barriers and in particular what until now has been the industry standard, loaded vinyl barriers which include harmful plasticisers. QuietWave® is the culmination of the adoption by Acoustica of the principles of green chemistry and seven years of research and development. Green chemistry, also called sustainable chemistry, is a philosophy of chemical research and engineering that encourages the design of products and processes that minimize the use and generation of hazardous substances. The result is the world's first water based mass loaded Acoustic NoiseBarrier. In September 2012, the NSW Minister for Primary Industries and Small Business, the Honourable Katrina Hodgkinson, officially opened the production line today at the St Mary's NSW production plant of Acoustica Pty Ltd. This natural organic barrier is the beginning of a move away from mass loaded PVC and thermoplastic barriers towards environmentally acceptable alternatives.

More information from www.acoustica.com.au, info@acoustica.com.au

Colin G Speakman Travel Bursary

During 2012, the Queensland Division established the Colin G Speakman Travel Bursaries. The bursaries were established in honour of Colin's contribution to the Society and Division over many years. Two (2) bursaries of up to \$1200 are provided to assist with travel and registration costs associated with attendance at the annual conference of the Australian Acoustical Society, or in years when Australia hosts or co-hosts an international acoustical conference, the relevant international conference (and associated satellite conferences). To be eligible for these awards, prospective applicants must have had a paper accepted at a designated conference for that year.

The 2012 bursaries were made available for student travel to *Acoustics 2012, Acoustics, Development and the Environment* at Fremantle. No applications were received for the 2012 award. Applications are sought for the 2013 bursaries. These will support student travel to *Acoustics 2013, Science, Technology and Amenity*, to be held at Victor Harbor, South Australia on 17-19 November 2013. Submissions close 5.00 pm Friday 30th August 2013.

The Queensland Division conducts an educational awards program to encourage and support acoustical education and research at institutions of learning in Queensland. Awards are granted on an annual basis in two divisions, a schools division (Division I) and a tertiary division (Division II).

More information on the QLD Division education and travel awards can be found at www.acoustics.asn.au/joomla/notices.html

NEW PRODUCTS

VibraScout USB DC Triaxial Vibration Measurement System

Dytran Instruments, Inc. is an industry leader in the design and manufacture of piezoelectric and DC MEMS sensors to support a variety of vibration testing applications, including NVH, component durability, modal and structural analysis, flight vibration testing, seismic monitoring, road load data acquisition, transmission testing, ride quality and real time monitoring of plant & equipment, vehicles, sea going vessels and aircraft. Included among the new Dytran DC MEMS sensors is the VibraScout Vibration Measurement System now available through Kingdom Pty Ltd, which includes a USB digital triaxial accelerometer combining a MEMS accelerometer with a microcontroller to create an intelligent sensor.

The VibraScout Vibration Measurement System consists of a USB triaxial DC response accelerometer, 15-foot 4-pin to USB cable assembly, VibraScout Data Acquisition Software, and VibraScout Windows

compatible Post Processor software on CD (no license required). In addition to the vibration measurement system, the only required hardware is a personal computer with a USB port.

The accelerometer model features power from a PC bus, and as a result no additional external power supply is required. The software package supplied with each system allows for real time, three directional acceleration acquisition (including Static Inclination) along with real-time temperature monitoring. The VibraScout Post Processor software is designed to provide a user with the tools to apply non-linear interpolation to resample raw data recorded with VibraScout software to higher frequencies, thus improving signal resolution. The VibraScout USB Vibration Measurement System was designed for a variety of low-to-medium frequency vibration applications where portability is critical including quick, easy in-field data collection; Noise, Vibration and Harshness (NVH); static angular measurements; ride quality; vibration measurement and diagnosis at rotating machinery; and simplified field data testing. The system is also ideal for calibration of sensors where qualification is required in the low range down to DC (0 Hz)

For further information kingdom9@kingdom.com.au, www.kingdom.com.au

300 m Range Wireless Transmitters

SAVTEK have conducted testing with 9dBa aeriels on the SINUS 'Virtual Wire' Type 1 wireless transmitter and receiver. The new aeriels achieved a line-of-sight range of 300m between the transmitter and receiver while conducting acoustic measurements. This means it is possible to transmit type 1 acoustic or vibration signals up to 300m away and across roads, rivers or train lines. The wireless transmitter system can also be used through walls for transmission loss testing or when you need to place a transducer in a sealed space. The units are available for rent or sale and as 1 or 2 channels. They have an internal 6 hour rechargeable battery and are able to power 200V polarised or ICP transducers.

Further information from Darryl Watkins at SAVTEK, (07) 3300 0363 or dwatkins@savtek.com.au, www.savtek.com.au

MEETING REPORTS

NSW Division

On 25th September, Colin Tickell of Hatch Associates gave a technical talk titled *Assessing environmental noise compliance of upgrade projects within long-term existing industrial sites*. His talk described how noise objectives were established for new projects at two sites - BlueScope Steel Port Kembla

steelworks and Boral Berrima Cement Plant. Both companies have operations that have continued at the same sites since the 1930s and have many older items of plant. Colin's talk described how noise objectives were established for the new projects whilst existing plant on the sites were operating 24-hours / 7-days per week, how objectives for new plant items were set, and how compliance with the contribution objectives was demonstrated.

The NSW Division held their AGM on 30th October at the National Acoustics Laboratory, Chatswood. Immediately following the AGM was a technical meeting with a talk presented by Marion Burgess of UNSW Canberra, Chris Schulten of Railcorp NSW, and Barry Murray of Wilkinson Murray. They each gave short presentations related to *Application of broadband reversing alarms*. Their presentations were followed by a panel discussion.

The NSW Division held their 2012 Christmas Breakfast on 4th December at AECOM. During the breakfast a presentation was given by Len Wallis titled *Why don't consumers consider acoustics?* Following the presentation there was a presentation by GRAS including their new ANSI head.

VIC Division

On 1st November, the Victoria Division had a successful visit to and viewing of the recently refurbished Hamer Hall in the Victorian Arts Complex. The attendees were broken up into two groups and were taken around the venue and shown items of interest architecturally and historically. The acoustic impact of the changes was explained by Amanda Robinson of Marshall Day Acoustics, who was part of the team who worked on the project with Kirkegaard Associates from the US. The major changes of the refurbishment included redesign of the stage and surrounding area, partial removal of balcony 'arms', new air-conditioning system, addition of high frequency absorption over heritage elements, new retractable over-stage reflector and new sound system. The tour was followed by drinks and finger food in the Amcor Room and Amanda fielded some further technical questions impromptu. The AGM was held and positions ratified. Simon DeLisle is stepping down as Division Secretary and was thanked by Norm Broner.

The Victoria Division held its annual End of Year Dinner at the Malvern Valley Golf Club. 29 members came to hear the guest speaker, Andrew Stephenson, Partner at Clayton Utz, talk on the topic *Expert witnesses - tips and traps for engineers*. Andrew Stephenson heads the Clayton Utz Construction Group and the International Arbitration Group in Melbourne. Andrew explained that the role of an expert is to give factual evidence, to be independent and impartially assist the court but not to be an advocate for the client! Experts need to provide an objective unbiased opinion, state clearly the facts upon which your opinion was based, where necessary make clear when

the field of interest is outside their expertise and not to play inappropriate expertise. It is a mistake for an expert to try and win the case on behalf of the client, that is, the role of counsel. Andrew interspersed his talks with amusing anecdotes and transcripts from his wide experience which illustrated some of the points that he had made.

QLD Division

The second half of 2012 was a busy period for the Queensland Division. On 22nd August, Ben Hoddinott, Manager of Clinics for Neurosensory, presented a talk titled *Audiology for the non-audiologist*. In his talk Ben described the mechanisms behind hearing loss, the types of hearing tests conducted to determine the extent of any loss and how hearing can be restored using hearing aids and cochlear implants. The talk was well received with everyone who attended learning something new.

A joint technical meeting was hosted by Poly-Tek and Pyrotek on the 18th September. Neil Allen, General Manager of Poly-Tek, presented the development history of their new composite panel noise barrier system which has just been approved for use to reduce rail and road traffic noise by the Queensland Department of Transport and Main Roads. Richard Latimer, Marketing Manager of Pyrotek Noise Control, presented information about their product range and introduced their new absorptive product Reapor, which is made from recycled glass granules fused together to form a homogenous panel.

The Queensland AGM and a technical talk titled *Modelling and control of railway dynamic and acoustic phenomena* were held on 31st October. The required quorum for the AGM was easily achieved, with Ian Hillock and Claire Richardson choosing to reprise their roles on the Committee. Matthew Fishburn of Alpha Acoustics and David Borgeaud of Savery and Associates nominated to join the Committee, increasing the total Queensland Committee membership to nine. The technical talk was presented by Associate Professor Paul Meehan from the School of Mechanical Engineering at the University of Queensland.

On 5th December, the 2012 Christmas party was held at the Queensland Cricketers Club overlooking the Gabba Cricket Ground. There was a good turn out with many Society members encouraged to bring their partners to enable them to have an insight into the operations of the Society. Dr Rebecca Dunlop from the Cetacean Ecology and Acoustics Laboratory at the University of Queensland presented an interesting talk on whale noise that was well received by everyone present.

Planning has commenced for 2013 with the technical talk program anticipated to commence late February. Notice of these events will be placed on the AAS website, with the Queensland Division welcoming members from other states to participate in the technical talk program.

SA Division

The South Australian division held a dinner at Enzo's Ristorante on 14 June 2012 to honour the many years of contributions to the SA division from Peter Teague and Byron Martin, who have recently departed the state. We wish them all the best with their future endeavours.

The Annual General Meeting (AGM) was held on 4 September 2012 at the University of Adelaide. The SA Division Committee would like to thank Dr Carl Howard, who stepped down from his position of chairperson at this meeting, for the time and effort that he has put in both as chairperson of our division, and as an active committee member for many years prior to that. We congratulate Jonathan Cooper, who has since been elected as our new chairperson.

Following the AGM, Federal Council President Peter Heinze presented a talk entitled *Insul prediction software: A review and what is new in version 7*. Insul is a program developed by Marshall Day Acoustics for predicting the sound insulation of building elements and constructions. Peter demonstrated the latest version, describing the software's new features including prediction of triple panel constructions, new materials editor, auralisation of sound level differences, free field incidence, new frame types and users own maintenance of database of materials.

The SA Division provided partial sponsorship of \$750 to assist undergraduate students from the University of Adelaide, Wei Shern Wong and Nicholas Cheng, to attend and present a paper entitled *Frequency shifting listening device* at Acoustics 2012 Fremantle. The paper, outlining their Honours project work, describes the design, construction and performance of a device that shifts frequency in real time and amplifies low frequency noise into the audible frequency range.

The SA Division are now busy organising Acoustics 2013 *Science, Technology and Amenity*, the annual conference of the Australian Acoustical Society, which will be held at McCracken Country Club, in the beautiful seaside region of Victor Harbor, South Australia, 17-19 November 2013. In the meantime, the SA Division are looking forward to our upcoming annual Christmas function, which will be held at Panacea Restaurant on 7 December 2012.

WA Division

In the last few months the WA Division of the AAS was busy preparing for the annual acoustics conference. As such, there was no time for technical meetings or society functions. With the conference now being over, the WA division looks forward to 2013 and will no doubt be organising some events to get members together again.

The Acoustics 2012 conference was held in late November at the Esplanade Hotel in Fremantle. The conference was well attended by sponsors/exhibitors and delegates. A

successful conference is only possible with the help of several committed people. A special thanks goes out to Luke Zoontjens, Alec Duncan, Norm Broner, Kingsley Hearne, Terry McMinn, Ben Farrell, John Macpherson, Pam Gunn, Sasha Gavrilov and Gareth Forbes.

FUTURE CONFERENCES

ICA 2013 Montréal, Canada

The 21st International Congress on Acoustics, ICA2013, will be held 2-7 June 2013 at the Palais des Congrès in downtown Montréal, Canada. This meeting is hosted by the Acoustical Society of America (ASA) and the Canadian Acoustical Association (CAA). The high standard technical program will include plenary, distinguished, invited, contributed and poster papers covering all aspects of acoustics. There will be an extensive technical exposition highlighting the latest advances in acoustical products.

Several satellite meetings on specialised topics will be held in conjunction with ICA2013. The International Symposium on Room Acoustics (ISRA) will be held 9-11 June 2013 in Toronto, immediately following the ICA. More information on ISRA can be found at www.ISRA2013.com.

More information on ICA2013 can be found at www.ica2013montreal.org

International Symposium on Room Acoustics

The International Symposium on Room Acoustics, ISRA 2013, will be held in Toronto, Canada, June 9-11, 2013 immediately following the ICA congress in Montreal.

ISRA 2013 will be a single stream conference on acoustical issues related to performance spaces. ISRA 2013 will include presentations by 4 internationally acclaimed keynote speakers and a number of special sessions. Sessions will include both invited and contributed papers presented in either lecture or poster format. There will also be technical tours of performance spaces and an extended tutorial session.

More information at www.isra2013.com

ICSV20 Bangkok, Thailand

The 20th International Congress on Sound and Vibration (ICSV20) will be held from 7-11 July 2013 in Bangkok, Thailand. The conference will be held at the Imperial Queen's Park Hotel which is strategically located in the city centre and the important commercial district, with direct access to a lush public park. Theoretical and experimental research papers in the fields of acoustics, noise, sound, and vibration are invited for presentation. Important dates: Abstracts are due 15 February 2013 and full papers 1 April 2013

More information at www.icsv20.org

Inter-Noise 2013 Innsbruck, Austria

The 42nd International Congress and Exposition on Noise Control Engineering will be held in Innsbruck, Austria from 15-18 September 2013. The Congress is being organized by the Austrian Noise Abatement Association for the International Institute of Noise Control Engineering (I-INCE). Innsbruck, the capital of the Tyrol, is located in the Alpine region of Austria, in the valley of the river Inn, at 580 metres above sea level. It is surrounded by mountain ranges and numerous peaks which reach an altitude of 2700 metres above sea level. The city has

140,000 inhabitants and hosts one of the oldest universities in Europe, founded in the year 1562. The conference will be held at the award winning Innsbruck Congress Centre. More information at www.internoise2013.com

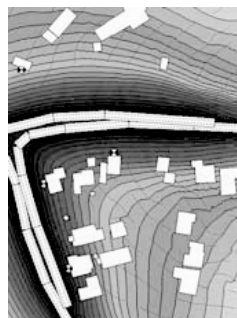
Wind Turbine Noise 2013 Denver, USA

The 5th International conference on Wind Turbine Noise (2013) is organised by INCE/Europe in cooperation with INCE-USA. WTN13 will be held in Denver, Colorado from 28-30 August 2013. The conference is relevant to those with an interest in wind turbine noise and its effect on people. Abstracts are due by 15 April 2013.

More information at www.windturbinenoise2013.org

PRUAC 2013

The 4th Pacific Rim Underwater Acoustics Conference (PRUAC 2013) will be held from 9-11 October 2013 at the Jinxi hotel in Hangzhou, China. PRUAC 2013 will be held with the conference theme of Underwater Acoustics and Ocean Dynamics. Topics include internal wave observation and prediction, environmental uncertainty and coupling to sound propagation, environmental noise and ocean dynamics, dynamic modelling in acoustic field, acoustic tomography and ocean parameters estimation, time reversal and matched field processing, underwater acoustic localization and communication, and measurement instrumentation and platform. More information at <http://pruac.zju.edu.cn/index.htm>



Cadna A[®]

State-of-the-art
noise prediction software

CadnaA is the premier software for the calculation, presentation, assessment and prediction of noise exposure and air pollutant impact. It is the most advanced, powerful and successful noise calculation and noise mapping software available in the world.

- . One button calculation
- . Presentation quality outputs
- . Expert support



Renzo Tonin & Associates is now the distributor for CadnaA in Australia & NZ.

Contact us for a quote!

RENZO TONIN & ASSOCIATES
Inspired to achieve

p 02 8218 0500

f 02 8218 0501

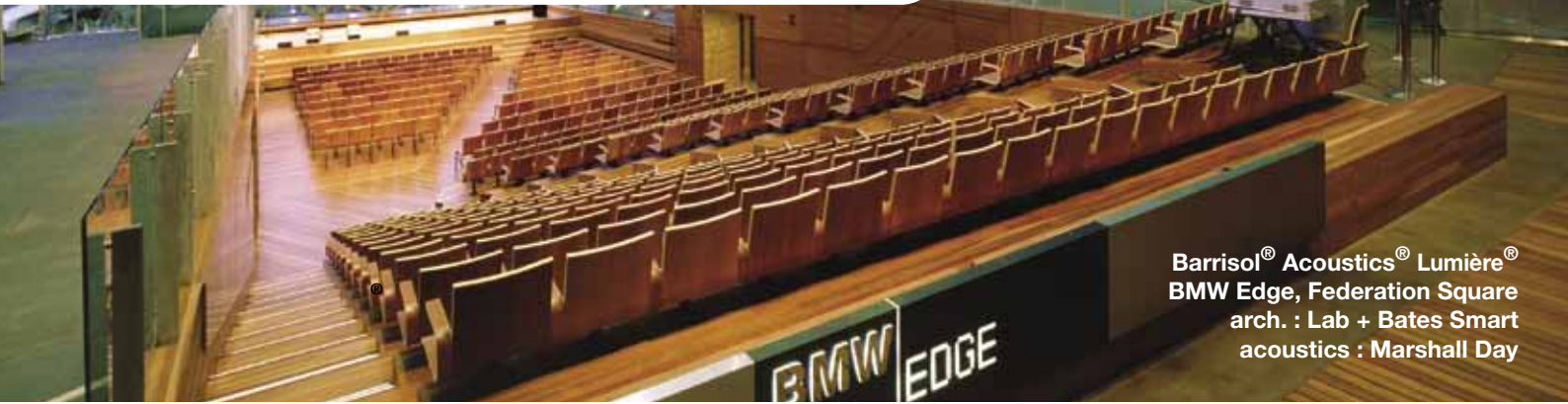
e sydney@renzotonin.com.au

www.renzotonin.com.au



BARRISOL®

Les Acoustics® - Microperforated Stretch Ceilings



Barrisol® Acoustics® Lumière®
BMW Edge, Federation Square
 arch. : Lab + Bates Smart
 acoustics : Marshall Day

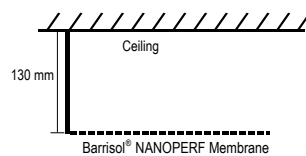
Barrisol ceilings with invisible microperforations provide exceptional acoustic performance without compromising your design.

Each perforation is just 0.1mm diameter, with up to 500,000 microperforations per square meter. Ceiling panels are not restricted to fixed panel sizes or shapes, with single custom ceiling panels up to 50 square meters in size.

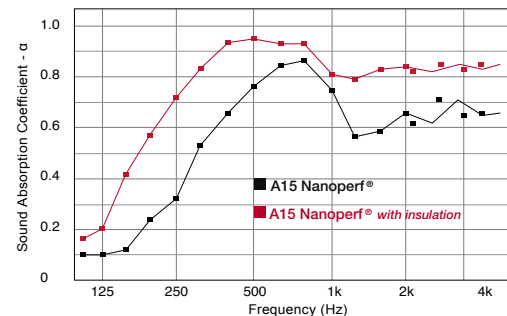
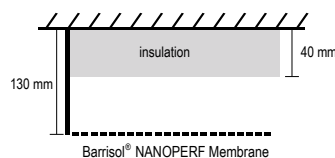
The sound absorption works by converting sound energy into thermal energy through friction with the microperforations. The friction is increased by the resonance of air within the cavity between the microperforated membrane and ceiling.

Barrisol microperforated acoustic solutions are available across the entire Barrisol range of 230 colours and 18 finishes, including gloss, satin, matt, translucent and recycled.

■ A15 NANOPERF® without insulation



■ A15 NANOPERF® with insulation

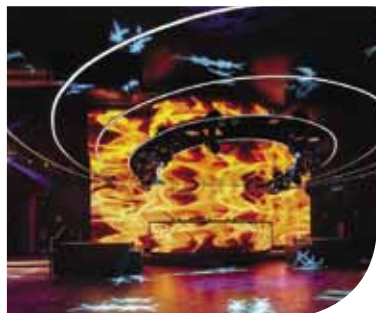


A15 Nanoperf®
NRC : 0.62

A15 Nanoperf® with insulation
NRC : 0.83



Barrisol® Acoustics - A20 Acoperf®
 Oslo Opera House
 4000m², matt white ceiling panels (60m²/panel)
 architect : Snohetta Architects
 acoustics : Arup
 2009 European Award for Contemporary Architecture



Barrisol® Acoustics - A15 Nanoperf®
 Marquee Nightclub, The Star, Sydney
 High gloss black acoustic curved ceilings
 architect : Squillace Nicholas Architects
 acoustics : AECOM



Barrisol® Lumière® Acoustics - A30 Microacoustic®
 London Aquatics Centre
 139 backlit translucent acoustic petal shaped panels
 architect : Zaha Hadid
 acoustics : Arup



Barrisol® Acoustics - A15 Nanoperf®
 Bucharest Sunplaza - Romania
 10,000m² Barrisol rectangular ceiling panels
 finish: gloss, matt, satin
 architect : Chapman Talyor

www.barrisol.com.au

melbourne 03 98790628

sydney 02 96606044

brisbane 07 38510055

adelaide 08 82926600

perth 08 92482245

nz +64 9 525 6575

DIARY

2013

2 - 5 May, Singapore

International Congress on Ultrasonics (ICU 2013)
<http://www.icu2013.com.sg/>

26 - 31 May, Vancouver, Canada

IEEE International Conference on Acoustics, Speech, and Signal Processing (ICASSP)
<http://www.icassp2013.com>

2 - 7 June, Montréal, Canada

21st International Congress on Acoustics (ICA 2013)
<http://www.ica2013montreal.org>

9 - 11 June, Toronto, Canada

International Symposium on Room Acoustics (ISRA 2013)
<http://www.isra2013.com>

7 - 11 July, Bangkok, Thailand

20th International Congress on Sound and Vibration (ICSV20)
<http://www.icsv20.org>

23 - 26 July, Glasgow, UK

Invertebrate Sound and Vibration (ISV 2013)
<http://www.isv2013.org>

26 - 28 August, Denver, USA

Noise-Con 2013
<http://www.inceusa.org/nc13>

27 - 30 August, Denver, USA

Wind Turbine Noise 2013
<http://www.windturbine2013.org>

15 - 18 September, Innsbruck, Austria

Inter-Noise 2013
<http://www.internoise2013.com>

9 - 11 October, Hangzhou, China

4th Pacific Rim Underwater Acoustics Conference
<http://pruac.zju.edu.cn/index.htm>

2014

6 - 10 July, Beijing, China

21st International Congress on Sound and Vibration (ICSV21)
<http://www.iiav.org/index.php?va=congresses>

7 - 12 September, Krakow, Poland

Forum Acusticum 2014
<http://www.fa2014.pl/>

17 - 19 November, Melbourne, Australia

Inter-Noise 2014
<http://www.internoise2014.org/>

2015

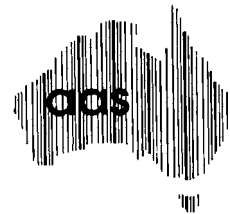
10 - 15 May, Metz, France

International Congress on Ultrasonics (2015 ICU)
<http://www.me.gatech.edu/2015-ICU-Metz/>

2016

5-9 September, Buenos Aires, Argentina

22nd International Congress on Acoustics (ICA 2016)
<http://www.ica2016.org.ar/>



Meeting dates can change so please ensure you check the conference website: <http://www.icacommission.org/calendar.html>



**Acoustic
Research
Labs Pty Ltd**

Level 7 Building 2 423 Pennant Hills Rd
Pennant Hills NSW AUSTRALIA 2120
Ph: +61 2 9484 0800 A.B.N. 65 160 399 119
www.acousticresearch.com.au

Sales

SALES

- ◆ Sound Level Meters
- ◆ Octave Analysers
- ◆ Vibration Meters
- ◆ Logging Kits
- ◆ Data Recorders
- ◆ Amplifiers



Hire



Ngara Noise Logger

Full audio and $\frac{1}{10}$ th second data recording

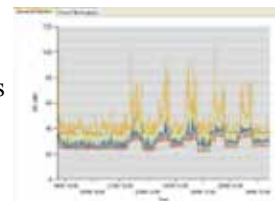
HIRE

- ◆ Loggers
- ◆ Sound Level Meters
- ◆ Octave Analysers
- ◆ Acoustic Calibrators
- ◆ Vibration Loggers



FIREFLY

- ◆ Ngara post-processing software
- ◆ Creates $\frac{1}{1}$ and $\frac{1}{3}$ octave statistics
- ◆ Data in graphical format.
- ◆ Play audio
- ◆ Export WAV to MP3



NATA CALIBRATION

- ◆ Sound Level Meters
- ◆ Noise Loggers
- ◆ Octave Band Filters
- ◆ Acoustic Calibrators
- ◆ Conditioning Amplifiers



FROM THE COMPANY WHO BROUGHT YOU A QUIET ENVIRONMENT

PYROTEK

NOISE CONTROL



www.pyroteknc.com



a new website with

MORE VIDEOS MORE CASE STUDIES MORE PRODUCT INFORMATION
MORE PRODUCT NEWS MORE NEW APPLICATIONS

SUSTAINING MEMBERS

The following are Sustaining Members of the Australian Acoustical Society.
Full contact details are available from <http://www.acoustics.asn.au/sql/sustaining.php>

3M AUSTRALIA

www.3m.com

EMBELTON

www.vibrationisolation.com.au

ACOUSTIC RESEARCH LABORATORIES

www.acousticresearch.com.au

HOWDEN AUSTRALIA

www.howden.com.au

ACRAN

www.acran.com.au

IAC COLPRO

industrialacoustics.com/australia

ACU-VIB ELECTRONICS

www.acu-vib.com.au

NSW DEPT OF ENVIRONMENT &

CLIMATE CHANGE

www.environment.nsw.gov.au

ADAMSSON ENGINEERING

www.adamsson.com.au

PEACE ENGINEERING

www.peaceengineering.com

AERISON PTY LTD

www.aerison.com

PYROTEK NOISE CONTROL

www.pyroteknc.com

ASSOCIATION OF AUSTRALIAN

ACOUSTICAL CONSULTANTS

www.aaac.org.au

SINCLAIR KNIGHT MERZ

www.globalskm.com

BARRISOL AUSTRALIA

www.barrisol.com.au

SOUND CONTROL

www.soundcontrol.com.au

BORAL PLASTERBOARD

www.boral.com.au/plasterboard

SOUNDSCIENCE

www.soundscience.com.au

BRUEL & KJAER AUSTRALIA

www.bksv.com.au

VIPAC ENGINEERS AND SCIENTISTS

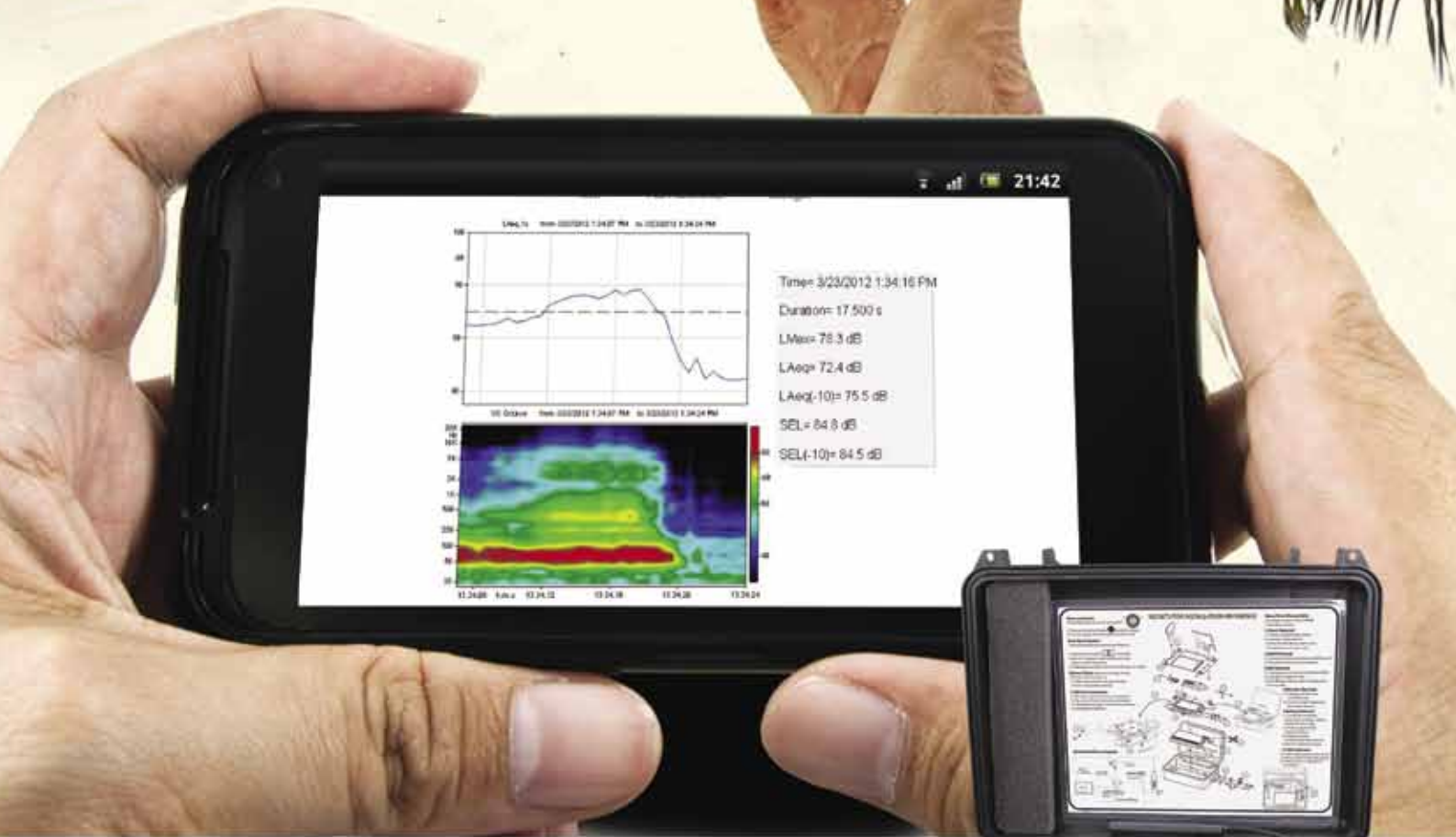
www.vipac.com.au

CSR BRADFORD INSULATION

www.bradfordinsulation.com.au

 **LARSON DAVIS**
A PCB PIEZOTRONICS DIV.

Announcing the
NEW! NoiseTutor



Noise Monitoring Made Easy

- Rapid deployment, no complex installations required
- Eliminate frequent visits to remote locations
- Easily share data among customers, consultants and project leads

Learn more at

www.thermofisher.com.au/noisetutor



ThermoFisher
SCIENTIFIC

For customer service, call 1300-735-295
Email: InfoIndustrialAU@thermofisher.com
Visit us online: www.thermofisher.com.au

AUSTRALIAN ACOUSTICAL SOCIETY ENQUIRIES

NATIONAL MATTERS

- * Notification of change of address
- * Payment of annual subscription
- * Proceedings of annual conferences

Richard Booker - General Secretary
 Australian Acoustical Society
 PO Box 1843 Toowong DC QLD 4066
 Tel: (07) 3122 2605
 email: GeneralSecretary@acoustics.asn.au
 www.acoustics.asn.au

SOCIETY SUBSCRIPTION RATES

For 2012/13 Financial Year:

Fellow and Member \$130.00
 Graduate, Associate and Subscriber . . \$100.00
 Retired \$40.00
 Student \$30.00

Including GST

DIVISIONAL MATTERS

Enquiries regarding membership and sustaining membership should be directed to the appropriate State Division Secretary

AAS - NSW Division

Laura Allison
 c/- AECOM
 Level 21, 420 George Street
 Sydney, NSW 2000
 Tel: (02) 8934 0035
 Fax: (02) 8934 0001
 Laura.Allison@aecom.com

AAS - Queensland Division

PO Box 760
 Spring Hill Qld 4004
 Sec: Richard Devereux
 Tel: (07) 3217 0055
 Fax: (07) 3217 0066
 rdevereux@acran.com.au

AAS - SA Division

AECOM,
 Level 28, 91 King William St
 ADELAIDE S.A. 5005
 Sec: Darren Jurevicius
 Tel: (08) 7100 6400
 Fax: (08) 7100 6499
 darren.jurevicius@aecom.com

AAS - Victoria Division

c/- Simon de Lisle
 Arup Acoustics
 Level 17, 1 Nicholson Street
 Melbourne VIC 3000
 Tel: (03) 9668 5580
 Fax: (03) 9663 1546
 simon.delisle@arup.com.au

AAS-WA Division

Unit 3
 2 Hardy Street,
 SOUTH PERTH 6151
 Sec: Norbert Gabriels
 Tel (08) 9474 5966
 Fax (08) 9474 5977
 gabriels@iinet.net.au

ACOUSTICS AUSTRALIA INFORMATION

GENERAL BUSINESS

Advertising Subscriptions

Mrs Leigh Wallbank
 PO Box 70, OYSTER BAY 2225
 Tel (02) 9528 4362
 Fax (02) 9589 0547
 wallbank@zipworld.com.au

PRINTING, ARTWORK

Cliff Lewis Printing

91-93 Parraweena Road
 CARINGBAH NSW 222
 Tel (02) 9525 6588 Fax (02) 9524 8712
 email: matthew@clp.com.au

ADVERTISING RATES

B&W	Non-members	Sus Mem
1/1 Page	\$784.00	\$699.15
1/2 Page	\$509.40	\$457.40
1/3 Page	\$392.00	\$352.90
1/4 Page	\$326.70	\$294.00

Spot colour: available
 Prepared insert: \$424.70 Conditions apply
 Column rate: \$26.40 per cm (1/3 p 5.5cm width)
 All rates include GST

Discounted rates for 3 consecutive ads in advance

Special rates available for 4-colour printing

All enquiries to: Mrs Leigh Wallbank
 Tel (02) 9528 4362 Fax (02) 9589 0547
 wallbank@zipworld.com.au

ARTICLES & REPORTS

NEWS, BOOK REVIEWS

NEW PRODUCTS

The Editor, Acoustics Australia
 c/o Nicole Kessissoglou
 School of Mechanical & Manufacturing Engineering
 University of New South Wales
 NSW 2052 Australia
 Mobile: +61 401 070 843
 acousticsaustralia@acoustics.asn.au

SUBSCRIPTION RATES

	Aust	Overseas
1 year	A\$77.20	A\$88.33
2 year	A\$133.10	A\$157.30
3 year	A\$189.00	A\$227.27

Australian rates include GST.
 Overseas subscriptions go by airmail
Discounted for new subscriptions
 20% Discount for extra copies
 Agents rates are discounted.

ACOUSTICS AUSTRALIA ADVERTISER INDEX - VOL 40 No 3

Kingdom Inside front cover	Peace Engineering 202	ARL 230
Bruel & Kjaer 164	Odeon 220	Pyrotek 231
Cliff Lewis Printing 164	(NATA) Renzo Tonin & Associates . . 224	Thermo Fisher Scientific 233
Matrix 164	Renzo Tonin & Associates 228	ACU-VIB inside back cover
SAVTek 166	Barrisol 229	Bruel & Kjaer back cover

SVAN 971 SLM & ANALYSER

Low-cost type 1 SLM

An extremely small SLM (pocket-size & light weight) with options for 1/1 & 1/3 octave analysis. Simple Start/Stop operation mode. Intended for general acoustic measurements, occupational health and environmental noise measurements

- ✓ Class 1 SLM meeting IEC 61672:2002
- ✓ Easy to use predefined setups
- ✓ Three parallel independent profiles
- ✓ 1/1 or 1/3 octave real-time analysis
- ✓ Advanced time-history logging
- ✓ Acoustic dose measurements
- ✓ Voice comments recording
- ✓ Audio events recording
- ✓ MicroSD memory card
- ✓ Self-vibration monitoring



More info: www.acu-vib.com.au

NATA Calibrations



Acoustic and vibration instrument calibration laboratory servicing the whole of Australia and Asia Pacific region. FAST turnaround. NATA registered. All brands

Sales & Service



We supply instruments from several manufacturers, giving you a wider selection to choose from. We also service ALL brands and makes.

Instrument Hire



We have a wide range of acoustic and vibration instruments for hire. Daily, weekly or monthly rental periods available. Call for advice on the best instrument to suit you

70 years. Driving innovation.



The **roar** of a car's engine and the **feel** of the ride; the **clear** audio of a hearing aid; the **drone** of planes from a busy airport; the **quality** of a mobile phone. **Sound and vibration** is all around us and constantly affects our lives.

70 years. Driving innovation.



www.bksv.com/70

Helping solve sound and vibration challenges is in the DNA of **Brüel & Kjær** – just like our iconic green instruments and red shakers.

For **70 years** we have built our reputation on partnerships with customers and a dedication to excellence in sound and vibration.

From the world's first acoustic analyzer to the flyover beamforming systems of today, when people need solutions in sound and vibration, they turn to us for the answers.

But we are not standing still. Our commitment and innovation remain as we evolve to meet the future challenges of our customers.

www.bksv.com/70

HEADQUARTERS: DK-2850 Naerum · Denmark · Telephone: +45 4580 0500
Fax: +45 4580 1405 · www.bksv.com · info@bksv.com

Brüel & Kjær Australia

Suite 2, 6-10 Talavera Road, PO Box 349, North Ryde NSW 2113 Sydney
Tel: +61 2 9889 8888 · Fax: +61 2 9889 8866 · www.bksv.com.au · auinfo@bksv.com

MELBOURNE: Suite 22, Building 4, 195 Wellington Road, Clayton VIC 3170
Tel: +61 3 9560 7555 Fax: +61 3 9561 6700 · www.bksv.com.au · auinfo@bksv.com

Local representatives and service organisations worldwide.

Brüel & Kjær 
creating sustainable value